การสังเคราะห์ท่อนาโนคาร์บอนจากตัวเร่งปฏิกิริยาโลหะนิเกิลที่เตรียมด้วยวิธีการเคลือบด้วยไฟฟ้าและการใช้งานด้านตัวเก็บประจุยิ่งยวด

SYNTHESIS OF CARBON NANOTUBES BY ELECTROPLATED NICKEL CATALYST AND ITS SUPERCAPACITOR APPLICATION

วิศิษฏพงศ์ ยอดศรี
VISITTAPONG YORDSRI

วิทยานิพนธ์นี้เป็นส่วนหนึ่งของการศึกษาตามหลักสูตรปริญญาวิทยาศาสตรมหาบัณฑิต
สาขาวิชานาโนวิทยาและนาโนเทคโนโลยี
วิทยาลัยนาโนเทคโนโลยีพระจอมเกล้าลาดกระบัง
สถาบันเทคโนโลยีพระจอมเกล้าเจ้าคุณทหารลาดกระบัง
พ.ศ. 2559
KMITL-2016-NT-M-001-002

การสังเคราะห์ท่อนาโนคาร์บอนจากตัวเร่งปฏิกิริยาโลหะนิเกิลที่เตรียมด้วยวิธีการเคลือบด้วยไฟฟ้าและการใช้งานด้านตัวเก็บประจุยิ่งยวด

SYNTHESIS OF CARBON NANOTUBES BY ELECTROPLATED NICKEL CATALYST AND ITS SUPERCAPACITOR APPLICATION

วิศิษฏพงศ์ ยอดศรี
VISITTAPONG YORDSRI

วิทยานิพนธ์นี้เป็นส่วนหนึ่งของการศึกษาตามหลักสูตรปริญญาวิทยาศาสตรมหาบัณฑิต
สาขาวิชานาโนวิทยาและนาโนเทคโนโลยี
วิทยาลัยนาโนเทคโนโลยีพระจอมเกล้าลาดกระบัง
สถาบันเทคโนโลยีพระจอมเกล้าเจ้าคุณทหารลาดกระบัง
พ.ศ. 2559
KMITL-2016-NT-M-001-002

SYNTHESIS OF CARBON NANOTUBES BY ELECTROPLATED NICKEL CATALYST AND ITS SUPERCAPACITOR APPLICATION

VISITTAPONG YORDSRI

A THESIS SUBMITTED IN PARTIAL FULFILLMENT
OF THE REQUIREMENT FOR THE DEGREE OF
MASTER OF SCIENCE IN NANOSCIENCE AND NANOTECHNOLOGY
COLLEGE OF NANOTECHNOLOGY
KINGMONGKUT'S INSTITUTE OF TECHNOLOGY LADKRABANT
2016
KMITL-2016-NT-M-001-002

หัวข้อวิทยานิพนธ์	การสังเคราะห์ท่อนาโนคาร์บอนจากตัวเร่งปฏิกิริยาโลหะนิกเกิลที่เตรียม ด้วยวิธีการเคลือบด้วยไฟฟ้าและการใช้งานด้านตัวเก็บประจุยิ่งยวด
นักศึกษา	นายวิศิษฏพงศ์ ยอดศรี
รหัสประจำตัว	56607003
ปริญญา	วิทยาศาสตรมหาบัณฑิต
สาขาวิชา	นาโนวิทยาและนาโนเทคโนโลยี
พ.ศ.	2559
อาจารย์ที่ปรึกษาวิทยานิพนธ์	ผศ.ดร.วินัดดา วงศ์วิริยะพันธ์
อาจารย์ที่ปรึกษาวิทยานิพนธ์ร่วม	ดร.ชัญชณา ธนชยานนท์

บทคัดย่อ

การวิจัยนี้ได้ศึกษาการสังเคราะห์ท่อนาโนคาร์บอนอย่างง่ายบนแผ่นทองแดงด้วยเทคนิคการเคลือบผิวด้วยไอเคมีเพื่อนำไปประยุกต์ใช้งานด้านอุปกรณ์กักเก็บพลังงานโดยเป็นขั้วของตัวเก็บประจุยิ่งยวด ในกระบวนการเคลือบผิวด้วยไอเคมี โลหะคะตะลิสต์เป็นส่วนประกอบที่สำคัญสำหรับการสังเคราะห์ท่อนาโนคาร์บอน ในงานวิจัยนี้จึงเลือกใช้นิกเกิลเป็นคะตะลิสต์ อนุภาคนาโนของนิกเกิลถูกปลูกลงบนแผ่นทองแดง ด้วยวิธีการเคลือบผิวด้วยไฟฟ้ากระแสตรง เนื่องด้วยเป็นกระบวนการที่ง่าย ค่าใช้จ่ายน้อย ทำได้อย่างรวดเร็ว สามารถเลือกพื้นที่สำหรับการปลูกได้ และไม่ต้องใช้ระบบสุญญากาศ โดยในงานวิจัยได้ศึกษาผลของแรงดันไฟฟ้าต่อสัณฐานวิทยาของคะตะลิสต์ และโครงสร้างของท่อนาโนคาร์บอน ในขั้นตอนการปลูกคะตะลิสต์กำหนดให้แรงดันไฟฟ้าที่จ่ายในระบบการเคลือบผิวด้วยไฟฟ้ากระแสตรงมีค่า 1.0, 1.5 และ 2.0 โวลต์ โดยตัวแปรอื่นมีค่าคงที่ได้แก่ อุณหภูมิ 45 องศาเซลเซียส ระยะห่างระหว่างขั้ว 100 มิลลิเมตร และเวลาในการปลูก 5 นาที สำหรับกระบวนการสังเคราะห์ท่อนาโนคาร์บอนด้วยเทคนิคการเคลือบผิวด้วยไอเคมี สังเคราะห์ในเตาท่อที่อุณหภูมิ 800 องศาเซลเซียสเป็นเวลา 20 นาที และใช้เอทานอลเป็นแหล่งกำเนินคาร์บอน ทำการวิเคราะห์ลักษณะทางด้านสัณฐานวิทยาของอนุภาคนาโนนิกเกิลด้วยเทคนิคกล้องจุลทรรศน์แรงอะตอม ทำการวิเคราะห์ลักษณะทางด้านสัณฐานวิทยาและลักษณะโครงสร้างของชั้นกราไฟต์ของท่อนาโนคาร์บอนด้วยเทคนิคกล้องจุลทรรศน์อิเล็กตรอนแบบส่องกราด กล้องจุลทรรศน์อิเล็กตรอนแบบส่องผ่าน และรามานสเปกโทรสโกปี นอกจากนี้ท่อนาโนคาร์บอนที่สังเคราะห์ลงบนแผ่นทองแดงที่เคลือบด้วยอนุภาคนาโนนิกเกิล ถูกนำไปประยุกต์ใช้เป็นขั้วสำหรับตัวเก็บประจุยิ่งยวด โดยทำการทดสอบสมบัติทางไฟฟ้าเคมีด้วยเทคนิคไซคลิกโวลแทมเมทรีและกัลวานอสแตติกชาร์จดิสชาร์จ จากผลการวิจัย พบว่าเงื่อนไขแรงดันไฟฟ้า 1.5 โวลต์เป็นเงื่อนไขที่ดีที่สุด คือได้ขนาดอนุภาคนาโนนิกเกิลเฉลี่ยประมาณ 55$\pm$3 นาโนเมตร และได้ท่อนาโนคาร์บอนที่มีผนังท่อซึ่งเป็นชั้นของกราไฟต์ขนานกับแนวแกนยาวของท่อนาโนคาร์บอน ในขณะที่เงื่อนไขแรงดันไฟฟ้าที่ 1.0 โวลต์ เกิดท่อนาโนคาร์บอนที่มีผนังท่อทำมุมทแยงกับแนวแกนยาวของท่อนาโนคาร์บอน ส่วนในเงื่อนไขแรงดันไฟฟ้าที่ 2.0 โวลต์ สิ่งที่ได้คือท่อนาโนคาร์บอนที่เป็นเกลียวใหญ่และมีขนาดไม่คงที่ จากผลวิจัยดังกล่าวชี้ให้เห็นว่า เงื่อนไขแรงดันไฟฟ้าที่จ่ายในระบบการเคลือบผิวด้วยกระแสไฟฟ้ากระแสตรงมีผลโดยตรงกับขนาดและการกระจายตัวของขนาดของอนุภาคนาโนนิกเกิล โดยอนุภาคนาโนนิกเกิลที่มี

ขนาดเล็กและมีการกระจายตัวของขนาดที่แคบเป็นปัจจัยสำคัญสำหรับการสังเคราะห์ท่อนาโนคาร์บอนที่มีลักษณะคงที่ นอกจากนี้ จากการวิเคราะห์สมบัติทางไฟฟ้าเคมีพบว่า ขั้วท่อนาโนคาร์บอนที่สังเคราะห์ได้ มีสมบัติทางด้านการเก็บประจุด้วยค่าสัมประสิทธ์การเก็บประจุที่ 53 ฟารัดต่อกรัม จากผลการวิจัยเบื้องต้นนี้แสดงให้เห็นว่าสามารถสังเคราะห์ท่อนาโนคาร์บอนอย่างง่ายโดยใช้อนุภาคนาโนนิกเกิลที่เตรียมด้วยเทคนิคการเคลือบด้วยไฟฟ้ากระแสตรง และสามารถพัฒนาสมบัติทางไฟฟ้าเคมีของขั้วท่อนาโนคาร์บอนได้ด้วยการศึกษาเงื่อนไขโครงสร้างของอนุภาคนาโนนิกเกิลและท่อนาโนคาร์บอนที่เหมาะสมที่สุด

คำสำคัญ : การเคลือบด้วยไฟฟ้ากระแสตรง ท่อนาโนคาร์บอน การเคลือบผิวด้วยไอเคมี ซุปเปอร์คาปาซิเตอร์

Thesis Title	Synthesis of Carbon Nanotubes by Electroplated Metal Catalyst and its Supercapacitor Application
Student	Mr. Visittapong Yordsri
Student ID	56607003
Degree	Master of Science
Program	Nanoscience and Nanotechnology
Year	2016
Thesis advisor	Assit. Prof. Dr. Winadda Wongwiriyapan
Thesis Co-advisor	Dr. Chanchana Thanachayanont

ABSTRACT

This research studies facile synthesis of carbon nanotube (CNT) on copper sheets by chemical vapor deposition (CVD) and its energy storage application as an electrode in supercapacitor. In CVD process, metal catalyst is an essential ingredient in the synthesis of CNT. In this work, nickel (Ni) was chosen as a catalyst. Ni nanoparticles were deposited on the copper sheet by the direct current (DC) electroplating technique. The DC electroplating is simple to set up, low cost, fast, can deposit to a selected area and does not need vacuum system. The effects of DC-electroplating voltage on the morphology and structure of the CNTs was investigated. The applied voltage was varied from 1.0, 1.5 to 2.0 V, while the electroplating temperature, time and distance between electrodes were fixed at 45°C, 5 min and 100 mm, respectively. The CNTs synthesis by CVD was carried out in the tube furnace at 800 °C using ethanol as carbon source for 20 min. The morphology of the electroplated Ni was characterized by atomic force microscopy (AFM). The morphology, diameter and structure of the graphitic layer, and the crystallinity of the synthesized CNTs were characterized by field emission scanning electron microscopy (FESEM), transmission electron microscopy (TEM) and Raman spectroscopy, respectively. Furthermore, the CNTs synthesized on Ni-electroplated Cu sheet was used as a supercapacitor electrode. The electrochemical measurements were carried out in a three-electrode setup connected to an electrochemical work station. Electrochemical properties were characterized by cyclic voltammetry (CV) and galvanostatic charge/discharge (CD) technique. The results show that at the applied voltage of 1.5 V, Ni nanoparticles with a narrow distribution of sizes were formed with an average size of 55±3 nm, which in turn, yielded synthesized CNTs with a uniform diameter of approximately 60±5 nm with graphitic layers parallel to the CNTs axis. On the other hand, the electroplated Ni at 1.0 V produced CNTs with graphitic layers with an angle to the CNTs axis, while the

electroplated Ni at 2.0 V produced curly CNTs with a wide diameters distribution. These results show that the Ni nanoparticle size distribution could be controlled by electroplated voltage. Our observation was that the Ni nanoparticles with a narrow distribution of sizes and a uniform diameter was a key for uniform CNTs synthesis. The synthesized CNTs showed a specific capacitance of 53 $F.g^{-1}$. All these results signified that facile growth of CNTs by Ni NPs catalyst, deposited using DC electroplating method was fully achieved. Further optimization of structures of Ni catalyst and CNTs should improve the supercapacitor performance.

Keywords : Electroplating, Carbon nanotube**,** Chemical vapor deposition, Supercapacitor

ACKNOWLEDGEMENTS

First, I would like to express my deep and sincere gratitude to my advisor, Asst. Prof. Dr. Winadda Wongwiriyapan (College of Nanotechnology, King Mongkut's Institute of Technology Ladkrabang, KMITL) and co-advisor, Dr. Chanchana Thanachayanont (National Metal and Materials Technology Center, MTEC) for their encouragement, helpful suggestions, remarkable patience, and kind support.

I am deeply grateful to Asst. Prof. Dr. Benchapol Tunhoo, Asst. Prof. Dr. Apiluck Eiad-ua, Dr. Mayuree Phonyium (College of Nanotechnology, KMITL), Dr. Supanit Porntheeraphat (National Electronics and Computer Technology Center, NECTEC) and Prof. Dr. Supapan Seraphin (The University of Arizona) for their comments and suggestions on this dissertation.

Finally, I would like to thank all the colleagues and friends, especially those who are the members of Nanocarbon Materials Research Laboratory, College of Nanotechnology, KMITL for their supports and kindnesses.

Visittapong Yordsri

CONTENTS

CONTENTS (Cont.)

LIST OF FIGURES

Page

LIST OF FIGURES (Cont.)

Page

LIST OF TABLES

Page

CHAPTER 1
INTRODUCTION

1.1 Background and Problem

Carbon nanotube (CNTs) is one of the most promising materials in nanotechnology due to its great properties such as large effective surface area, excellent mechanical properties and electrical properties. In recent researches, CNTs show many great potentials for improving the performance of electronics devices, energy storage devices and sensors. For future application, the method of synthesis with a large-scale production and a simple synthesis method is very important. Chemical vapor deposition (CVD) is one of the presently available methods that matched for CNTs synthesis requirement. Metal catalyst is an essential ingredient for the CVD process. As for catalyst preparation, evaporation and sputtering techniques are normally utilized, but these techniques are time-consuming, high cost with vacuum system and limited in size. For practical application, the simple catalyst preparation is absolutely required. Electroplating, a proposed technique for such catalyst preparation, is simple to set up, low cost, fast and does not need vacuum.

In this study, facile growth of CNTs was made possible by using direct-current (DC) electroplating for Ni nanoparticles (NPs) catalyst preparation; with the Ni-deposited catalyst, CNTs was synthesized by using CVD with ethanol vapor as carbon source. The effects of DC-electroplating voltage on the morphology and structure of the CNTs were investigated. Furthermore, for demonstration of a potential application, supercapacitors based on the synthesized CNTs were fabricated and their electrochemical properties were determined.

1.2 Objectives of the study

1.2.1 To fabricate Ni nanoparticles by direct-current electroplating technique for CNTs synthesis.

1.2.2 To optimize the synthesis of CNTs by chemical vapor deposition technique using electroplated Ni nanoparticles as catalyst.

1.2.3 To demonstrate the potential application of the synthesized CNTs as supercapacitor.

1.3 Scope of the study

1.3.1 Deposition of Ni nanoparticles on the substrate by electroplating technique and characterization by atomic force microscopy and X-ray photoelectron spectroscopy.

1.3.2 Synthesis of CNTs by CVD and characterization by scanning electron microscopy, transmission electron microscopy and Raman spectroscopy.

1.3.3 Characterization the electrochemical properties of the synthesized CNTs (such as cyclic voltammetry and galvanostatic charge-discharge).

1.4 Expected Results

1.4.1 Deposition of the Ni nanoparticle on the substrate with a narrow size distribution by electroplating technique.

1.4.2 Growth of CNTs from the electroplated Ni nanoparticle with a uniform size and high quality.

1.4.3 Demonstration of the CNTs electrode as supercapacitor.

CHAPTER 2
THEORETICAL BACKGROUND

2.1 Carbon nanotube

Normally, the sp^2 hybridization of carbon is the basis for the well-known graphite structure. Besides this, carbon can form other structures, such as the closed cages with honeycomb carbon arrangement, C_{60}, which was discovered by H.R. Kroto *et al*. in 1985 [1]. From this, various structures of carbon cages were discovered. In 1991, Iijima first observed the tubular carbon structure as "a new type of finite carbon structure consisting of needle-like tubes" [2]. The observed carbon structure consists of few graphitic shells with the spacing between shell of 0.34 nm. Two years later (1993), Iijima and Ichihashi [3] and Bethune *et al*. [4] achieved the synthesis of single-wall carbon nanotube (SWNT).

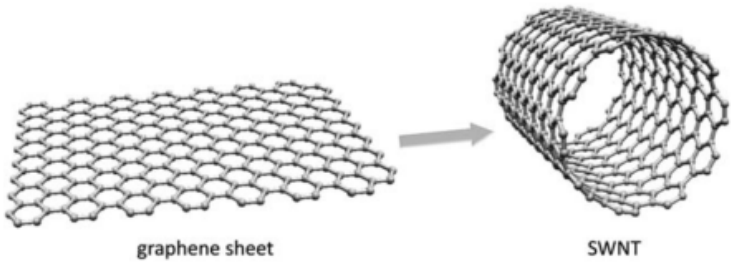

Figure 2.1 Wrapping of graphene sheet to form SWCNT [5].

Structurally, SWCNT can be compared to ''rolled up'' one- atom-thick sheets of graphite called graphene as shown in Figure 2.1. The way the graphene is wrapped along the honeycomb graphene structure is given by chiral vector *C* which is a result of a pair *(n,m)* of integers that corresponds to graphene vectors a_1 and a_2. The principle of SWNT construction from a graphene sheet along the chiral vector *C* is shown in Figure 2.2. There are two standard types of SWNT constructions from a single graphene sheet according to integers *(n,m)*. The *(n,0)* structure is called ''zigzag'' and the structure where *n=m (n,n)* is called ''armchair''. The third non-standard type of CNTs construction, which can be characterized by the equation where $n > m > 0$, is called ''chiral'' [5]. These different structures lead to the different properties of SWNT such as metallic or semiconducting [6].

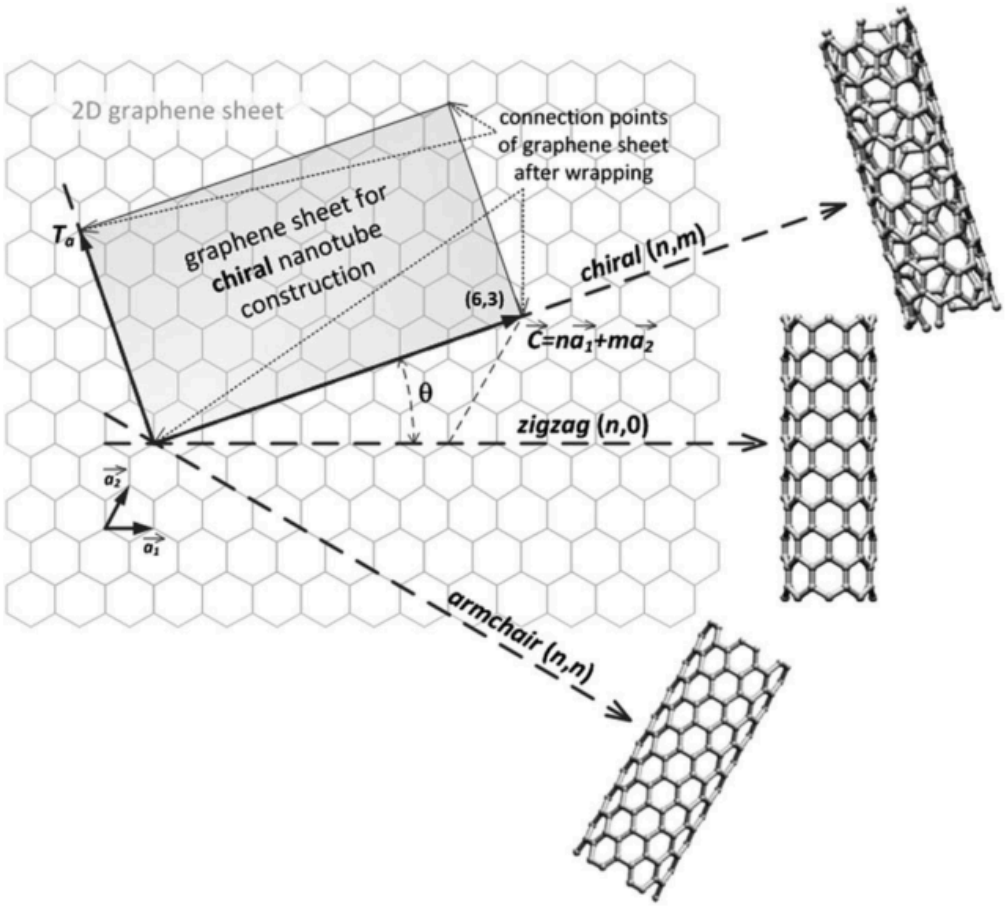

Figure 2.2 The principle of CNTs construction from graphene sheet along the chiral vector C [6].

CNTs can be either SWNT, the only one layer of graphene layer roll into tube structure, or multi-wall carbon nanotube (MWNT), the tubular that consists of many layers of graphene with the layer spacing of around 0.34 nm. For the MWNT, it can be few layers or more up to 100 layers.

CNTs have great properties with high surface area per unit weight, good mechanical properties (100 times stronger than steel, but 6 times lighter), high electrical conductivity, high thermal conductivity. Their unique properties are suitable for utilizing in composite materials for improvement of mechanical-properties and as additives to various structural materials. Some of the extraordinary properties of CNTs are shown in Table 2.1.

Table 2.1 The extra ordinary properties of CNTs.

	SWCNT	MWCNT
High surface area per unit weight	very broad scale from 50 - 1315 $m^2.g^{-1}$	10 - 500 $m^2.g^{-1}$
Good mechanical properties :		
Young's modulus	~ 1 TPa	~ 1.2 TPa
Tensile strength	~ 60 GPa (ropes)	~ 0.15 TPa
Thermal properties @ room temperature*	~ 1750-5800 $W.m^{-1}.K^{-1}$	> 3000 $W.m^{-1}.K^{-1}$
Electrical properties		
Typical resistivity	~ 10^{-4} ohm.cm	n/a
Typical current density	10^7-10^9 $A.cm^{-2}$	n/a
Electronic properties	• Metallic (bandgap=0 eV) if (n-m) is divisible by 3 • Semiconducting (bndgap=0.4-2 eV) if (n-m) is not divisible by 3	Non-semiconducting (bandgap ~0 eV)

2.2 Synthesis of carbon nanotube

Generally, MWNT and SWNT are normally produced by three main techniques, arc-discharge technique, laser-ablation technique and chemical vapor deposition (CVD).

2.2.1 Arc-discharge

Arc-discharge is a technique that normally used for synthesis of carbon fibers and fullerenes. However, Iijima used this technique to synthesize the MWNT in 1991 [2] and also SWCNTs [3] in 1993. For arc-discharge technique, a direct-current arc voltage is applied across two high-purity graphite electrodes as anode and cathode. The electrodes are vaporized by the direct-current through the separation of two graphite electrodes with around 1-2 mm in 400 mbar of helium atmosphere. The schematic experimental setup of arc-discharge is shown in

Figure **2.3**. From the process, if the anode and cathode are pure graphite, MWNTs are deposited on the cathode side. In the case of the graphite containing a metal catalyst (such as Fe, Co, Ni, Y or Mo), the SWNT can be produced either on anode or cathode side. The quality and quantity of CNTs such as lengths, diameters, purity are dependent on varied parameters and conditions such as inert gas pressure, gas type, current, system geometry, and metal concentration.

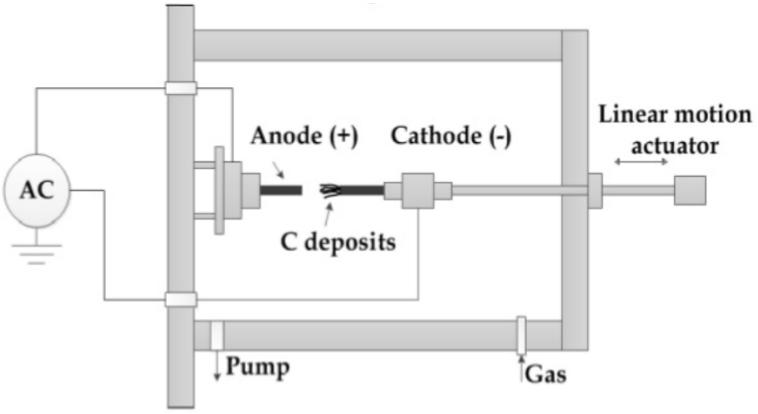

Figure 2.3 The schematic of arc-discharge technique [7].

Transmission electron microscopy (TEM) study of carbon nanotube morphology grown by arc-discharge revealed that there were many varieties in shape especially near the tube tips. Ebbesen and Ajayan [8] reported the large-scale synthesis of MWNTs by variant of standard arc-discharge technique. Two thin graphite rods were used and applied with direct-current potential of 18 V in helium atmosphere. With helium pressure at 500 Torr, the nanotubes give the maximum yield up to 75% relative to the starting graphitic material. The characterization by TEM revealed that the sample consisted of nanotubes with two or more carbon shells. The tube diameters are between 2 and 20 nm with length of several micrometers. The tube tips were capped with a combination of hexagons and pentagons.

In 1993, Iijima and Ichihashi [3] and Bethune *et al*. [4] almost simultaneously reported about arc-discharge and the SWNTs synthesis with catalyst-assisted process. Iijima used arc-discharge chamber filled with mixed gas of 10 Torr of methane and 40 Torr of argon. Two vertical thin electrodes were placed at the center of chamber. The lower electrode, cathode, had the thin layer of iron. The arc-discharge condition is running by a direct-current of 200 A at 20 V across both electrodes. The component of argon, iron and methane were the main critical parameters for SWNTs synthesis. The nanotubes obtained were curved and tangled into bundles with each tube having diameters of 1 nm and quite broad distribution from 0.7 to 1.65 nm. Bethune *et al*. reported the used of thin electrodes as anode with bored holes which were filled with mixture of pure powdered metals (Fe, Ni or Co) and graphite. The electrodes were vaporized in arc-discharge with a current of 95-105 A in 100-500 Torr of helium atmosphere. The TEM characterization showed that only cobalt metal catalyst can yield the nanotubes with single atomic layer walls with uniform diameter of 1.2 ± 0.1 nm.

Large scale synthesis of SWNTs by arc-discharge was reported by Journet *et al*. [9]. The two graphite electrodes were used with 600 mbar of helium atmosphere. The anode had a hole drilled at the end which was filled with a mixture of metallic catalyst (such as Ni-Co, Co-Y or Ni-Y) and graphite powder. The arc-discharge was processed by a current of 100 A and a constant voltage of 30 V. From scanning electron microscopy (SEM), the obtained product consists of a large amount (80%) of entangled carbon ropes. The high-resolution TEM images indicated that the ropes obtained had diameters from 5 to 20 nm and each rope consisted of bundle of tubes. Each tube diameters were around 1.4 with the separation of 1.7 nm. The spectra from X-ray diffraction (XRD) showed the period arrangement of tubes in the ropes. This pattern of XRD spectra of Journet et al. [9] is similar to the XRD data report from Thess *et al.* [10] (using laser-ablation technique) that obtained in 70-90% yield and tube diameter around 1.4 nm. The nanotubes also form into bundle of a few tens of nanotubes. Both reports lead to the nanotubes growth mechanism that does not depend on the method conditions. It depends much more on the kinetics of carbon condensation in a non-equilibrium situation. Furthermore, between the two methods, the arc-discharge technique is much cheaper than the laser-ablation technique.

2.2.2 Laser-ablation

Laser-ablation is a technique that the laser is focused on the graphite target under high temperature with argon atmosphere (around 500 Torr). The carbon that was vaporized by laser will be flowed with argon gas carrier to the outer heating zone and form CNTs at the collector (cooler zone behind heating zone), Figure 2.4. In case of SWNTs synthesis, the graphite target contained with metal particles is needed. The CNTs produced by laser-ablation technique are much more purified and have smaller size distribution than the previous technique, i.e. the arc-discharge technique.

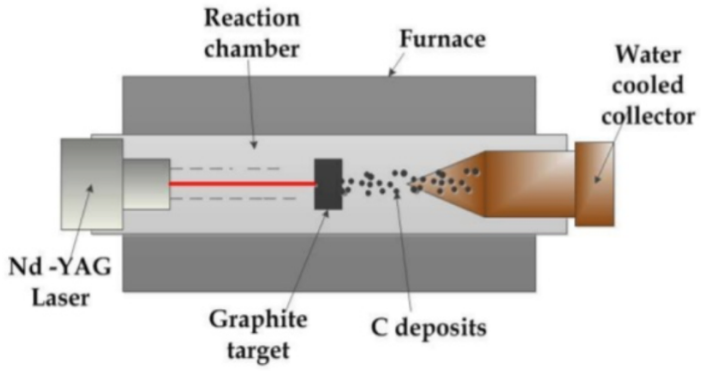

Figure 2.4 The schematic of Laser-ablation technique [7].

Smalley *et al.* (1996) reported the high yield (>70%) production of SWNTs using laser-ablation technique by vaporizing the graphite rods that contained small amounts of Ni and Co at 1200 °C [10]. By TEM and XRD characterization, the obtained SWNTs were uniform in diameters and formed as bundles with micrometer length. The bundles show the triangular lattice with a lattice constant, a = 1.7 nm (van der Waals bonding). The nanotubes represent as metallic structure with a main tube *(10,10)* structure. Therefore, both MWNTs and SWNTs can be obtained by this technique. The metal particles added in the graphite rod as catalysts were important factor for SWNTs forming.

2.2.3 Chemical vapor deposition

Chemical vapor deposition (CVD) is the technique that is widely used for CNTs synthesis, due to its advantage above the others that have less complicate setup, low cost due to do not need vacuum, variety of carbon source and can scale up for mass production.

For CVD process, catalyst is an essential parameter for CNTs growth. The substrates with catalyst deposited have been placed in the reactor that is heated up to 600 – 1000 °C and the hydrocarbon source is supplied to react in a reaction over surface of catalyst for 15-60 min. Then, CNTs grown on catalyst in reactor are collected after cooling the system to room temperature, Figure 2.5.

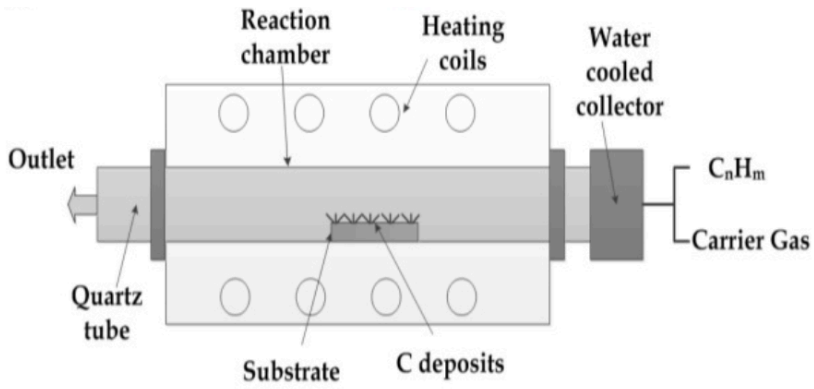

Figure 2.5 The schematic of chemical vapor deposition [7].

Carbon fibers and filaments have been produced by chemical vapor deposition, CVD, technique using the hydrocarbon source with catalyst added since 1960. Yacaman *et al*. (1993) [11] and Ivanov *et al* (1994) [12,13] were the first group that reported the growth of MWNTs by CVD technique. The CVD technique normally used with the catalyst-assisted for carbon nanotube forming and has been improved and optimized. Generally, ethylene or acetylene were used for the carbon source in a

tube reactor at temperature around 550 to 750 °C. The catalyst used for CNTs is metal. The best results obtained for catalyst chosen are Fe, Ni or Co nanoparticles. These are the same optimal catalysts with the previous arc-discharge and laser-ablation techniques, implying the common nanotube growth mechanism.

Li *et al*. [14] reported the large-scale synthesis of aligned CNTs by CVD technique. The mesoporous silica with iron nanoparticles catalyst was used as substrate. The carbon source was mixture of 9% acetylene in nitrogen gas that flown into the reactor with 110 cm^3/min flow rate. The carbon atoms from acetylene that decomposed at 700˚C were formed on the substrate as the carbon nanotube. SEM and the energy-dispersive X-ray spectroscopy (EDX) used for the obtained CNTs characterization. The SEM image showed that the nanotubes continuously grew from bottom to the top as thin film with length of around 50 to 100 mm. The nanotubes structure was multi-wall that had the diameters around 30 nm (40 shells) and formed arrays with each tube spacing of around 100 nm, equal to the spacing of pores on mesoporous silica substrate.

For the average yield of SWNTs, both arc-discharge and laser-ablation technique can be more than 70% yields. But the big disadvantage of these techniques are the carbon solid source temperature that needs to be high up to 3000 °C and the nanotubes structure that usually form in tangle. The tangled CNTs obtained is difficult in purification and the applications. In the other hand, CVD is the technique that the CNTs obtained can be controlled by the catalyst with additional low cost and high yield. Table 2.2 below shows the comparison of CVD with other synthesis techniques.

Table 2.2 Comparison of CVD with other popular CNTs synthesis techniques [6].

Parameter	Chemical vapor deposition	Arc discharge	Lase ablation
Process	Place substrate in oven, heat to high temperature, and slowly add a carbon source. A decomposed source frees up carbon atoms, which recombine in the form of CNTs	Connect two graphite rods to a power supply, place them a few millimeters apart. At 100 amps, carbon vaporizes and forms hot Plasma	Blast graphite with intense laser pulses; use laser pulses rather than electricity to generate carbon gas from which the CNTs form, try various conditions until hit on one that produces amounts of SWNTs
Condition	Low-pressure inert gas (argon)	Argon or nitrogen gas at 500 Torr	High temperatures within 500-1000 C at atmospheric pressure
Yield	High	Low	Low
Operating temperature	500-1200	~4000	Room temperature to 1000
Product	SWCNT : long tubes with diameter ranging from 0.6 to 4 nm. MWCNT : long tubes with diameter ranging from 10 to 240 nm.	SWCNT : short tubes with diameter of 0.6-1.4 nm. MWCNT : short tube with inner diameter of 1-3 nm and outer diameter of approximately 10 nm.	SWCNT : long bundles of tubes (5-20 um), with individual diameter from 1 to 2 nm. MWCNT : not vary much interest in this technique, as it is too expensive, but MWNT synthesis is possible.
Carbon source	Fossil-based hydrocarbon and botanical hydrocarbon	Pure graphite	Graphite
Purity	Medium to high	Medium	Low
Cost	Low	High	High
Average	Easiest to scale up to industrial production, long length, simple process, SWNT diameter controllable, and quite pure	Can easily produce SWCNT, MWNTs. SWNTs have few structural defects, MWNTs without catalyst, not too expensive, open air synthesis possible	Good quality, higher yield, and narrower distribution of SWNT than arc-discharge

2.3 Carbon nanotube growth mechanisms

The growth mechanisms of CNTs are still being debated since their first explored. Many different models have been proposed [15]. No single growth mechanism has been finalized to explain the CNTs growth mechanism. The most widely accepted model utilizing traditional catalysts of transition metals such as Fe, Ni, Co, is the vapor-liquid-solid (VLS) mechanism [16].

For CNTs growth formation, there are two general cases: (i) tip-growth [17] and (ii) base-growth [18]. In tip-growth model, the interaction between catalyst and substrate is weak where the molten metal catalyst has an acute contact angle with the substrate (Figure 2.6(a)) [19]. The carbon atoms that have decomposed from a hydrocarbon source diffuse into the metal top surface whereas the nanotube precipitates out at the bottom of the catalyst, thus lifting the catalyst above the substrate. Growth ceases when the surface of the particle is covered with excess carbon. In the latter case, the diffusion is similar to the first case, however, due to the strong catalyst-substrate interaction, the catalyst remains on the substrate (Figure 2.6(b)) [19]. The nanotube crystallizes out first as a fullerene hemispherical dome and extending into a hollow carbon cylinder as carbon continues diffuses upward.

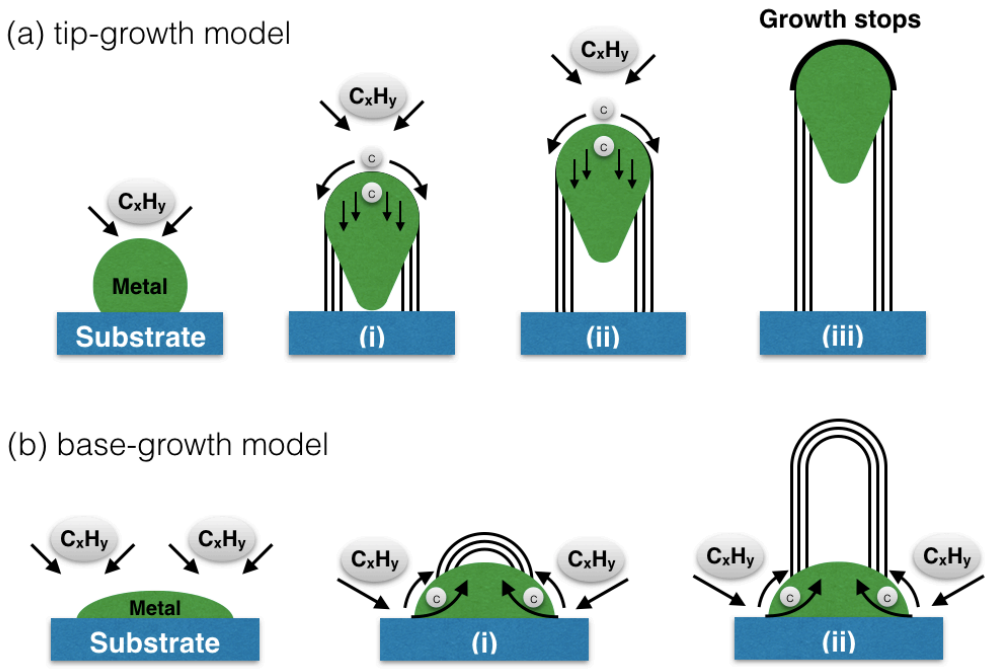

Figure 2.6 Widely-accepted growth mechanisms for CNTs: (a) tip-growth model, (b) base-growth model [19].

2.3.1 Types of catalysts

It is widely accepted that catalysts are essential ingredients for CNTs synthesis by CVD. The synthesis of both SWCNTs and MWNTs using transition metals such as Fe, Ni, Co, and Pd has become a routine process, which sometimes leads to a misconception that these metal catalysts are required for the formation of CNTs. During the past ten years, increasing attention has been made to search for new catalysts for nanotube growth. For instance, it has been shown that different metals such as Au, Ag, Cu, Pt, Rh, Mn, Mo, Sn, Mg, and Al can be used as catalysts [20–26].

2.3.2 Catalyst size

It is often assumed in the CNTs growth model by CVD process that one catalyst seed nucleates one nanotube; hence, the diameters of the nanotubes are determined by the sizes of the catalyst particles. It has been suggested that uniform nanotubes can be achieved if monodisperse catalyst nanoparticles are used. Although researchers have been able to produce a narrow diameter distribution of CNTs [27–31], it is often found that the majority of particles were not nucleating nanotubes. It has been proposed that under a given growth condition where carbon feeding and temperature are fixed, there is an optimal diameter of catalyst particles to nucleate CNTs [32]. According to this hypothesis, particles with a larger than optimal diameter are inactive due to “underfeeding” (Figure 2.7), whereas smaller particles are poisoned due to “overfeeding”. In “overfeeding” excessive carbon feeding creates a graphite shell which inhibits the CNTs nucleation. The “underfeeding” situation requires further investigation because the experimental study showed that large nanoparticles did not nucleate, even after prolonging growth time to allow the particles to collect more carbon.

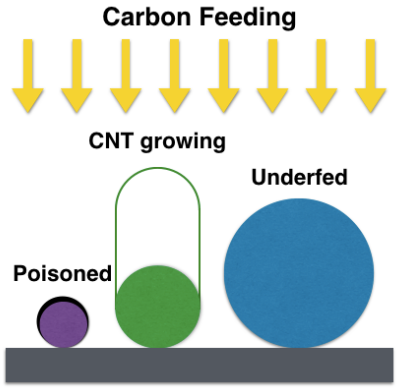

Figure 2.7 Schematic of overfeeding (poison) and underfeeding on various size particles.

Activation of nanoparticles is determined by their diameters under a given carbon feeding rate. Larger particles are underfed and not nucleating growth, while smaller particles are cutoff from carbon supplies by one or more layers of graphene sheet (the black layer in Figure 2.7). Only particles with a moderate and suitable size can nucleate growth.

2.4 Catalyst preparation

For the catalyst preparation, there are many methods such as evaporation, sputtering or chemical vapor deposition (CVD). Among of all, the CVD is the technique that has the advantage of easy setup, large area of substrate and low cost due to its common setup that do not need vacuum.

2.4.1 Evaporation

Thermal evaporation is one of the simplest of the physical vapor deposition (PVD) techniques. Basically, the material is heated in a vacuum chamber until its surface atoms have sufficient energy to leave the surface. At this point, they will traverse the vacuum chamber at thermal energy (less than 1 eV), and coat a substrate positioned above the evaporating material (average working distances are 200 mm to 1 meter). The pressure in the chamber must be below the point where the mean free path is longer than the distance between evaporation source and the substrate. The mean free path is the average distance an atom or molecule can travel in a vacuum chamber before it collides with another particle thereby disturbing its direction to some degree. This is typically 3.0×10^{-4} Torr or lower. The main reason to run at the high end of the pressure range is to allow an ion beam source to be employed simultaneously for film densification or other property modification.

2.4.2 Sputtering

Sputtering is a technique that is used to deposit thin film of material on the substrate. First, the gas plasma is created then accelerated the ions from plasma and bombarded onto the target materials. The target material is eroded by the arriving ions and is ejected in form of neutral particles (may be atoms, clusters of atoms or molecules). The ejected particles will move in a straight direction until they contact with something, other particles or some surface. If the substrate is placed in the path

of the ejected particles direction, it will be coated by the thin film of the target material.

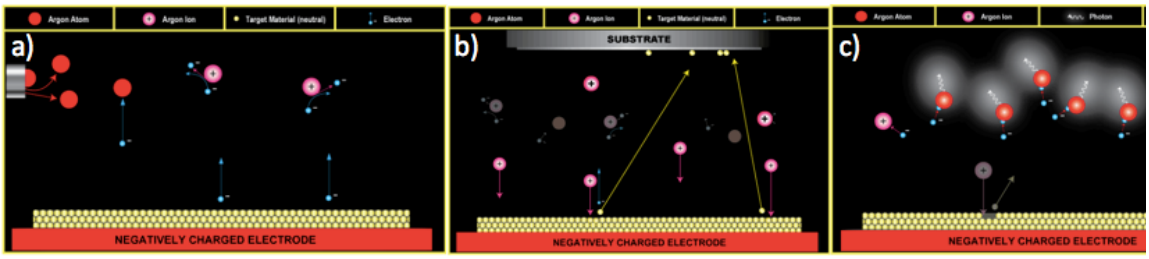

Figure 2.8 The schematic of sputtering process [33].

The sputtering process (Figure 2.8) can be explained as bellows;

a) The "free electrons" will immediately be accelerated away from the negatively charged electrode (cathode). These accelerated electrons will approach the outer shell electrons of neutral gas atoms in their path and, being of a like charge, will drive these electrons off the gas atoms. This leaves the gas atom electrically unbalanced since it will have more positively charged protons than negatively charged electrons (-) thus it is no longer a neutral gas atom but a positively charged "ion" (e.g. Ar^{+}).

b) At this point, the positively charged ions are accelerated into the negatively charged electrode (cathode) striking the surface and "blasting" loose electrode material and more free electrons by energy transfer. The additional free electrons feed the formation of ions and the continuation of the plasma. The blasted out materials move with straight direction than place onto the substrate upward as film coating.

c) All the while, free electrons find their way back into the outer electron shells of the ions thereby changing them back into neutral gas atoms. Due to the laws of conservation of energy, when these electrons return to a ground state, the resultant neutral gas atom gas gained energy and must release that same energy in the form of a photon. The release of these photons is the reason the plasma appears to be glowing.

2.4.3 Electroplating

Electroplating is the technique that passing an electric current through a solution called an electrolyte. The setup is done by immersing two electrodes into the electrolyte and connected both electrodes into circuit with power supply. The electrodes and electrolyte are carefully chosen of elements or compounds. While

current applied, the metal atoms will be generated from electrolyte as metal ion that will be deposited on the surface of one electrode. These called electroplating. All kinds of metals can be plating by this method such as gold, silver, tin, zinc and nickel. The electroplating technique is similar to the electrolysis (using electricity for splitting up the chemical solution), which is the reverse of the process.

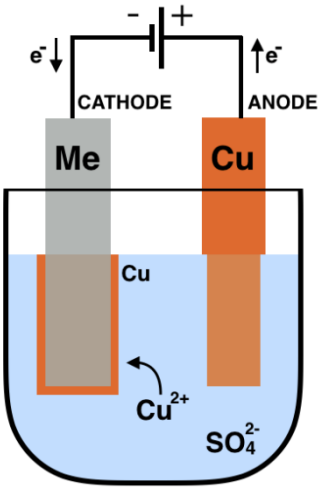

Figure 2.9 Electroplating of a metal (Me) with copper in a copper sulfate bath.

Figure 2.9 is the example process of electroplating, after voltage is applied, the copper anode is oxidized to Cu^{2+} by loss of two electrons. In the electrolyte solution, the Cu^{2+} and the anion SO_4^{2-} are from copper sulfate. At the cathode side, the Cu^{2+} is reduced to metallic copper by gaining two electrons from the current supplied that form the Cu plating on the cathode side. The plating technique is most common for a single metallic element.

2.5 Supercapacitor

Supercapacitor is an electrochemical capacitor that has very high capacitance compared with the conventional capacitor. They can store hundreds or thousands of times more charge then the conventional. However, the energy density of the supercapacitor is still lower in case of compared with batteries and fuel cells. From the Ragone plot in Figure 2.10, supercapacitor is between the conventional capacitor and batteries in term of energy density and power density but cannot give high power, while the conventional capacitors show high power but low energy density.

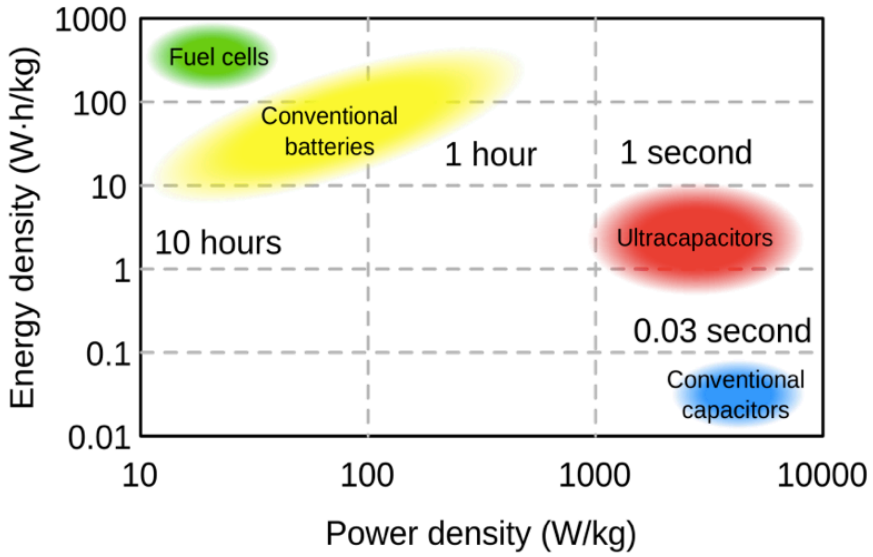

Figure 2.10 Ragone plot showing comparison for various energy storage devices [34].

In additional, from the charge-discharge process, the supercapacitor can be fully charged in seconds or minutes compared to the batteries that require to hours in charging. Supercapacitor also have longer life time (> 100,000 cycle) than batteries (around 3,000 cycle)

2.5.1 Conventional capacitor

Capacitor is an energy storage device, of which two passive metal plates are to store energy electrostatically in an electric field. The two plates with the same area of *A* and separated with dielectric thickness of *d*, were assembled as shown in Figure 2.11.

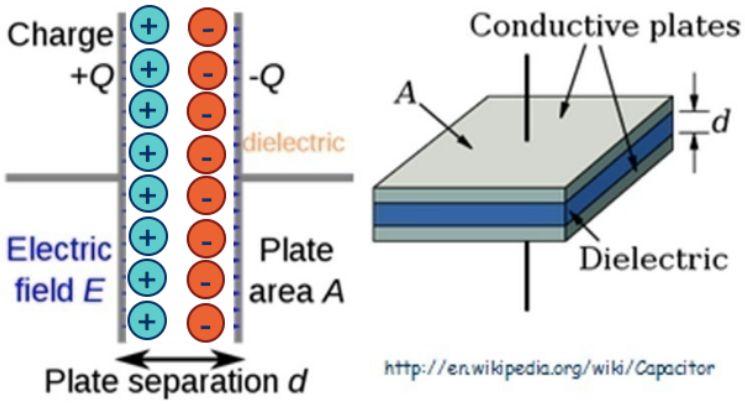

Figure 2.11 Schematic of capacitor with two parallel conductive plates [35].

Then, the capacitance *C* of the capacitor is defined as:

$$C = \frac{Q}{V} \tag{2.1}$$

where *Q* is the accumulated charge on each plate and *V* is the potential difference between the two plates. *C* is determined by the dimension of the capacitor and the property of dielectric between the plates, and can be calculated by:

$$C = \varepsilon_0 \varepsilon_r A/d \tag{2.2}$$

where ε_0 is the permittivity in vacuum and ε_r is the relative dielectric constant of the dielectric between the charged plates.

2.5.2 Supercapacitor

Generally, for the supercapacitor basic energy storage mechanism, it can be classified into two categories; (1) Electrical double layer capacitor (EDLC) and (2) Pseudocapacitor.

2.5.2.1 Electrochemical double layer capacitors (EDLC)

An electrochemical double layer capacitor (EDLC) stores its charge with electrostatic and consists of two layers of opposite charges that form at the interface of the electrode and electrolyte, separated by a distance at the atomic scale. For EDLC, the electrolyte can be either aqueous or non-aqueous liquid, or solid material as conducting polymer.

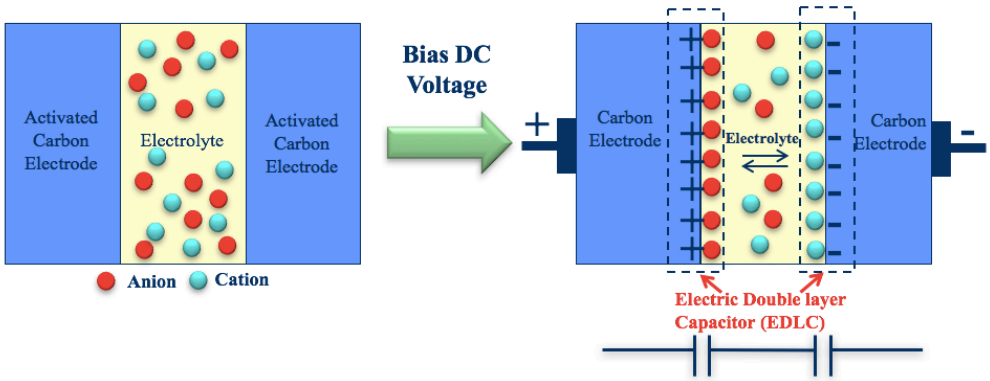

Figure 2.12 The schematic show the mechanism of electrochemical double layer capacitors (EDLC).

Figure 2.12 shows the schematic view of EDLC while charging by applying voltage. The process details are as follows;

- Before charging, in electrolyte, positive and negative ions are uniformly dispersed and there is no electric field at the electrode surface
- When a voltage is applied, the ions are attracted to the electrode with the opposite charge
- Energy is stored as a charge separation in double layers formed at the interface between the surface of electrode material and the electrolyte

2.5.2.2 Pseudocapacitor

Pseudocapacitor is a part of electrochemical capacitor, usually used together with the EDLC to form the supercapacitor. In pseudocapacitor, electrical energy stores by electron charge transfer between the electrode and electrolyte by reduction-oxidation reaction (redox reaction). A pseudocapacitor has chemical reaction that make electrical charge store faradaically at the electrode while in case of EDLC, the electrical charge is stored electrostatically with no interaction between electrode and ions. Electrochemical pseudocapacitors generally use metal oxide or conductive polymer electrodes with high amount of electrochemical pseudocapacitance.

EDLCs and pseudocapacitors also have different advantages, the EDLSs have higher power output but pseudocapacitors are greater in term of energy density. The comparison between both types shows in Table 2.3. In term of the lifetime usage, the EDLCs have much longer than the pseudocapacitors due to the materials limitation.

Table 2.3 The comparison of EDLCs and psudocapacitors [36].

Types	Mechanisms	Materials	Merits	Demerits
EDLCs	Charge separation at the electrode-electrolyte interface	Carbon materials	High power density, and good cycling behaviors	Low energy density, and low working voltage
Pseudo-capacitors	Reversible surface Faradic redox reactions	Transition metal oxides, conducting polymers	High capacitance and energy density	Poor cycling behavior, and low working voltage

2.5.3 Electrochemical measurement

Electrochemical is the study of the chemical response of a system to an electrical stimulation. This studies the loss of electrons (oxidation) or gain of electrons (reduction) occured during the electrical stimulation. These reduction and oxidation reactions are commonly known as redox reactions [36].

In electrochemical experiment, many parameters can be measured such as potential (*E*), current (*i*), charge (*Q*) and time (*t*), where as

- Potential (*E*) is the amount of electrical force of energy in a system. As the potential increases, more force is available to make a reaction happen. The base unit for potential is the volt (V).
- Current (*i*) is the magnitude of the electron flow in a system. Its base unit is amperes (A), but most electrochemical experiments measure currents on the microampere (10^{-6} A) or nanoampere (10^{-9} A) scale. Cathodic *i* is due to a reduction. Anodic *i* is due to an oxidation.
- Charge (*Q*) is a measure of the number of electrons used per equivalent. Its base unit is the coulomb (C). The charge can be directly measured or calculated by multiplying current and time.

In electrochemical techniques, there are three electrodes, the working electrode, the reference electrode and the counter electrode. The three electrodes are connected to a potentiostat instrument which controls the potential of the working electrode and measures the result current.

2.5.3.1 Cyclic voltammetry

Cyclic voltammetry (CV), is one of the commonly used electrochemical measurement techniques with the advantage of ability to characterize an electrochemical system. In CV measurement, the potentiostat applies a potential to the working electrode with specific scan rate then reverses the scan, returning to the initial potential (see triangular wave from in Figure 2.13).

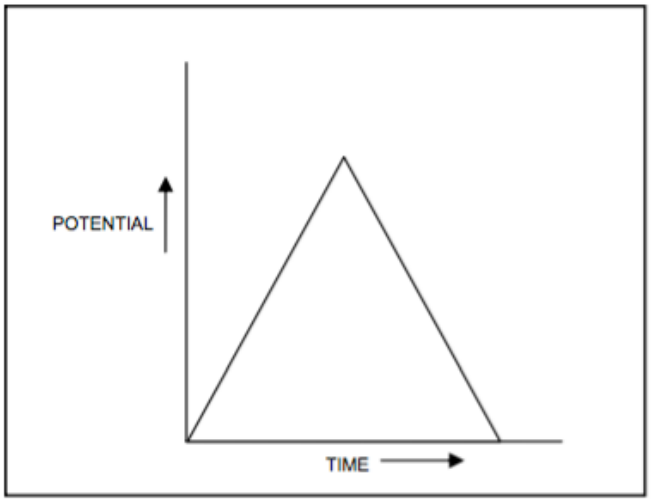

Figure 2.13 Typical excitation waveform for cyclic voltammetry.

During the potential sweep, the potentiostat measures the current result obtained from each applied potential. These values are collected then plot into CV graph of the current versus applied potential. The example of CV graph plot is shown in Figure 2.14.

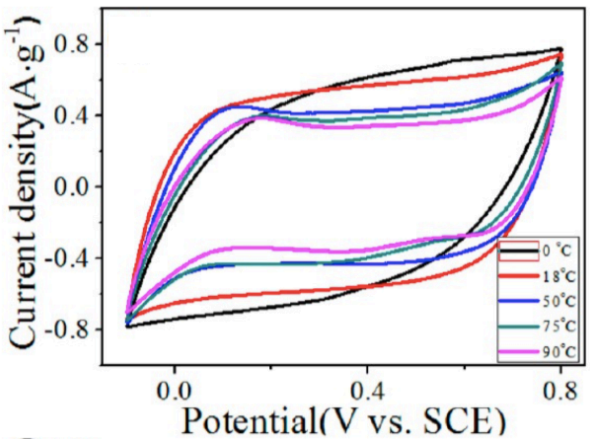

Figure 2.14 The example of cyclic voltammetry graph plot [37].

For the specific capacitance (C_s), can be calculated from the CV curve that obtained from the electrochemical measurement with equation 2.3

$$C_s = \frac{\int_{V_1}^{V_2} i(V)dV}{2(V_2 - V_1)mv} \quad (2.3)$$

where C_s is the specific capacitance ($F \cdot g^{-1}$), m is the mass of the electrode (g), v is the scan rate of CV curves ($V \cdot s^{-1}$), and $(V_2 - V_1)$ represents the potential window (V).

The energy density (E) and power density (P) of the assembled supercapacitor also can be calculated from CV curves by equation 2.4 and equation 2.5

$$E = \frac{1}{2} C V^2 \quad (2.4)$$

$$P = \frac{E}{t} \quad (2.5)$$

where C is the specific capacitance ($F \cdot g^{-1}$), V is the potential drop (V), and t is the discharge time.

2.5.3.2 Galvanostatic charge-discharge

Galvanostatic charge-discharge (CD), is the standard technique used to test the performance and cycle-life of EDLCs and batteries. A loop of charging and discharging is called as one cycle. Charge and discharge are conducted with constant current until reach the set voltage. The loop is repeated in cycle times to observe repeatable and the cycle-life time before performance is drop. The example of CD curve is shown in Figure 2.15.

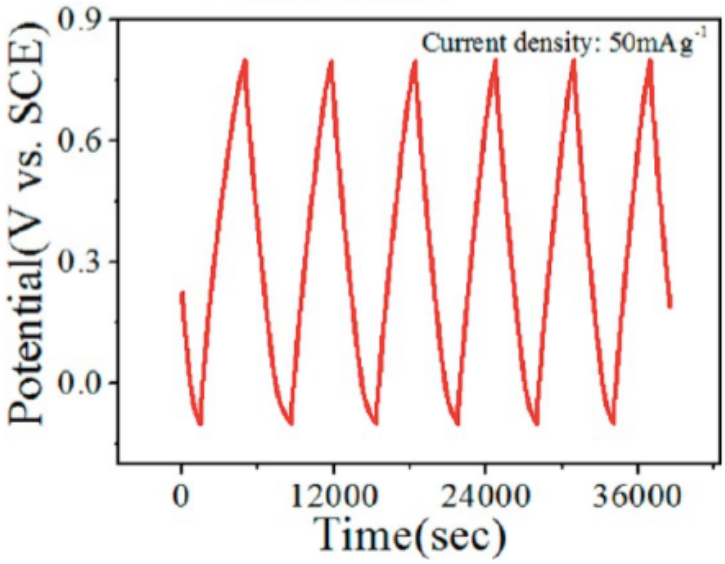

Figure 2.15 The example of galvanostatic charge-discharge curve [37].

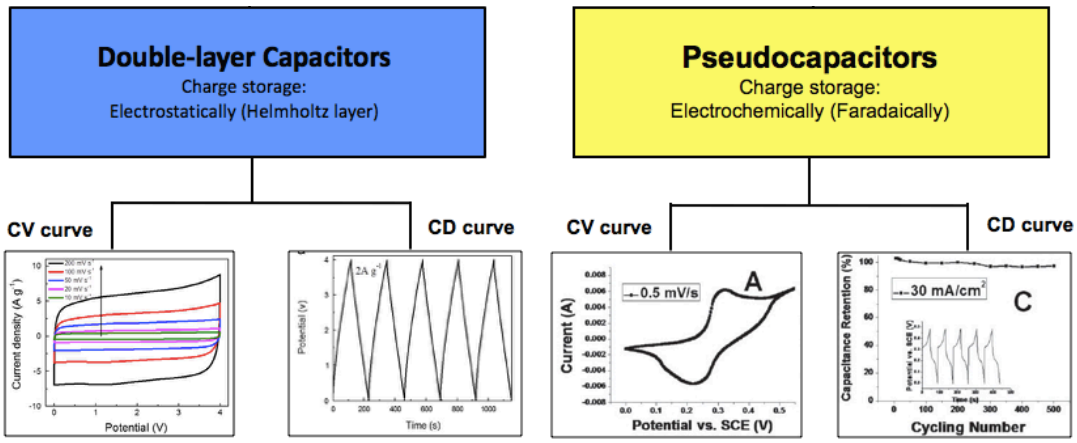

Figure 2.16 Example CV and CD curves from EDLC and pseudocapacitors.

The plot results of electrochemical measurement such as CV curve and CD curve from EDLC and pseudocapacitors are showed in Figure 2.16. The CV curve from EDLC is generally ploted as the rectangular shape while the pseudocapacitor usually generates with the additional redox reaction as oxidation and reduction peaks. In the case of CD curve, the EDLC shows with triangular repeatable charge-discharge curve but the pseudocapacitor shows with quasi-triangular representing the additional discharge time from redox reaction.

CHAPTER 3
RESEARCH METHODOLOGY

This research has focused on facile fabrication of CNTs electrode which is composed of two steps. The first step was to deposit Ni nanoparticles that acted as a catalyst on a copper (Cu) substrate by direct-current (DC) electroplating technique. The second step was to grow the CNTs on the Ni-electroplated Cu substrate by using chemical vapor deposition (CVD) technique. Several characterization techniques were utilized to investigate the optimum conditions for the fabrication of CNTs electrode. Finally, the optimized CNTs electrode was used to demonstrate its potential application as supercapacitor. Figure 3.1 shows a flow chart of the experimental procedure. The following section describes each step in detail.

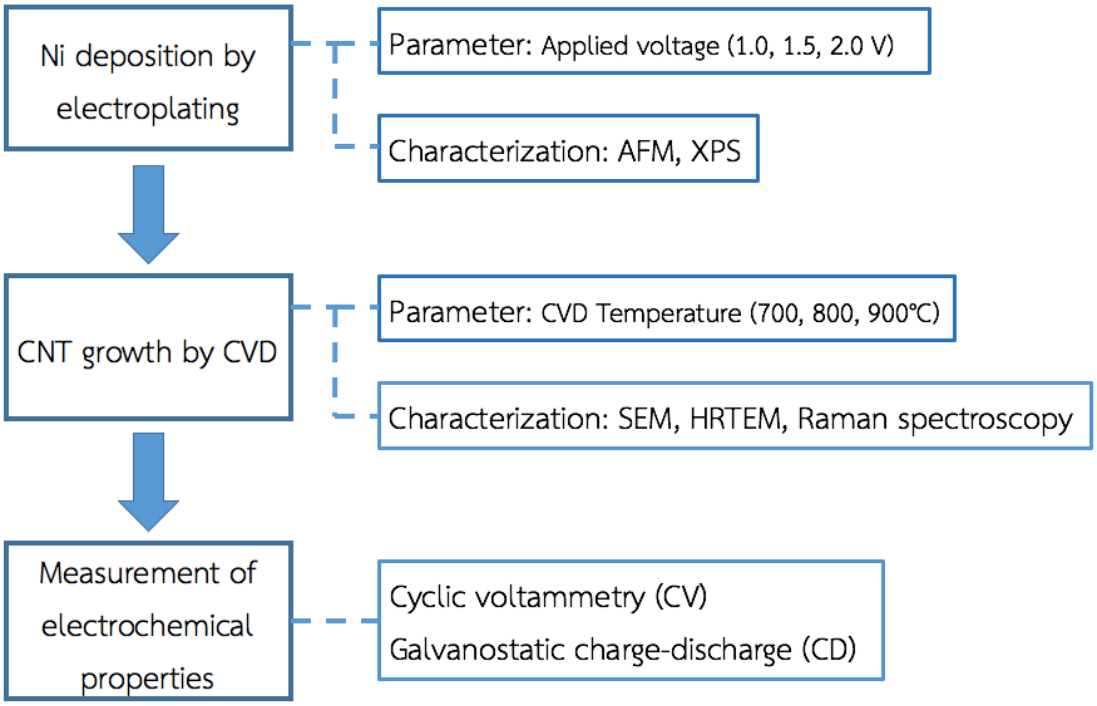

Figure 3.1 A flow of research procedure.

3.1 Deposition of Ni nanoparticles by direct-current electroplating

3.1.1 Materials and equipment

Materials and equipment used in this research for deposition of Ni catalyst are as follows:

(1) Cu sheet (99.9% purity, Nilaco Corporation, Japan)
(2) Ni Ingot (commercial grade)
(3) Ni solution electrolyte (commercial grade)
(4) Ethanol (AR grade, Labscan)
(5) Acetone (AR grade, Labscan)
(6) DC-Power supply
(7) Hot plate

3.1.2 Method of deposition of Ni nanoparticles by direct-current electroplating

99.9% pure Cu sheet (Nilaco Corporation, Japan) was cut to a size of 10 mm x 10 mm and was used as a substrate for Ni nanoparticle preparation by a direct-current (DC) electroplating technique. Prior to electroplating, Cu sheet was ultrasonically cleaned in ethanol, acetone and distilled water for 10 minutes, respectively. In electroplating process, the prepared Cu substrate was placed as an anode and Ni ingot was set to be a cathode with a 100 mm gap distance. Commercial Ni electroplating solution was used as electrolyte. The electrolyte temperature was fixed at 45^{o}C. Electroplating parameter studied in this research was the applied voltage. The applied voltages were varied at 1.0, 1.5 and 2.0 V. A schematic view of the setup and a photo of the setup are shown in Figure 3.2 (a) and (b), respectively.

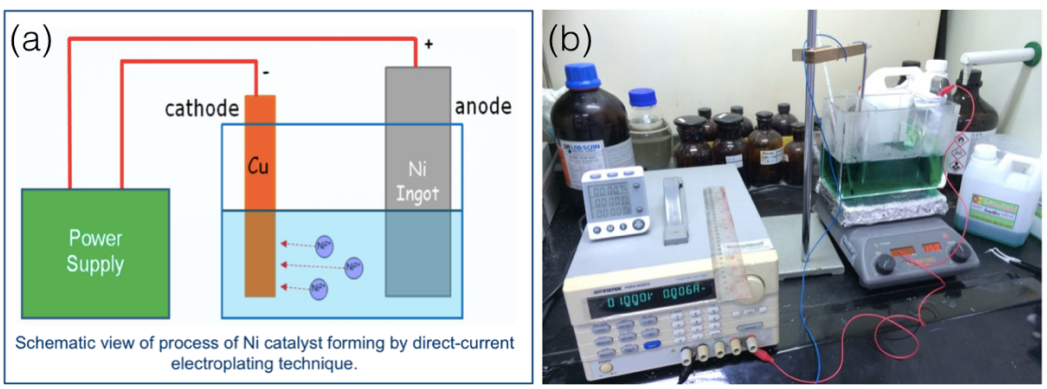

Figure 3.2 (a) Schematic view and (b) photograph of direct-current electroplating.

3.2 Growth of carbon nanotube on Ni-electroplated Cu by chemical vapor deposition

3.2.1 Materials and equipment for growth of carbon nanotube

Materials and equipment used in this research for growth of CNTs are as follows:

(1) Ethanol (AR grade, Labscan)

(2) Argon gas (99.95% purity)

(3) Tube furnace (Maximum temperature 1200 °C)

(4) Quartz tube (Diameter inside 21 mm, Length 120 cm)

(5) Quartz boat

(6) Mantle

(7) Gas control unit

3.2.2 Method of growth of carbon nanotube on Ni-electroplated Cu by chemical vapor deposition

Chemical vapor deposition (CVD) was used to synthesize CNTs on the Ni nanoparticle-electroplated Cu substrate prepared from the previous step (Section 3.1). For the CVD setup, a 120-cm long quartz tube was used as a reactor. The Ni nanoparticle-electroplated Cu substrates were set in the middle of the heating zone of the quartz tube as shown in Figure 3.3. Argon gas was purged in the quartz tube for 30 min at a flow rate of 0.6 LPM to replace oxygen and other gas contents in the reactor. Then, the reactor was heated up to setting temperature (varied with 700, 800 and 900°C) for 1 hr. Ethanol was vaporized and directly carried into the quartz tube by argon bubbling for 20 min to grow the CNTs. After CNTs growth, the reactor was cooled down to room temperature under atmosphere of argon gas flow. The profile of temperature and gas flow is shown in Figure 3.4.

For the CNTs growth by CVD, two parameters were studied (the CVD temperature and the electroplating voltage). First, to optimize CVD temperature, the electroplating voltage was fixed at 1.5 V and CVD temperatures were varied at 700, 800 and 900 °C. The CVD condition is shown in Table 3.1. Second, the CVD temperature was fixed at the optimum temperature and the electroplating voltages were varied at 1.0, 1.5 and 2.0 V.

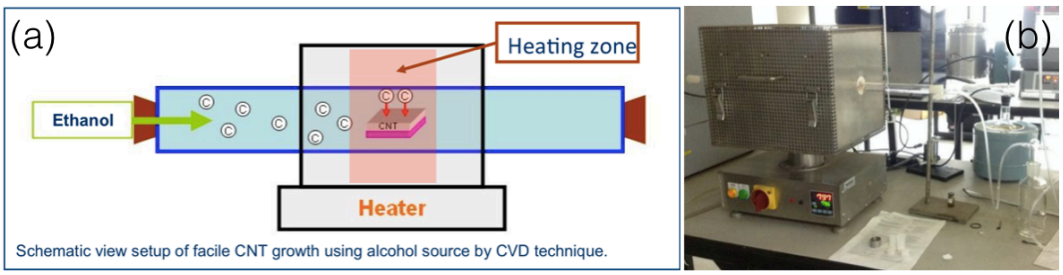

Figure 3.3 (a) Schematic view and (b) photograph of CVD setup.

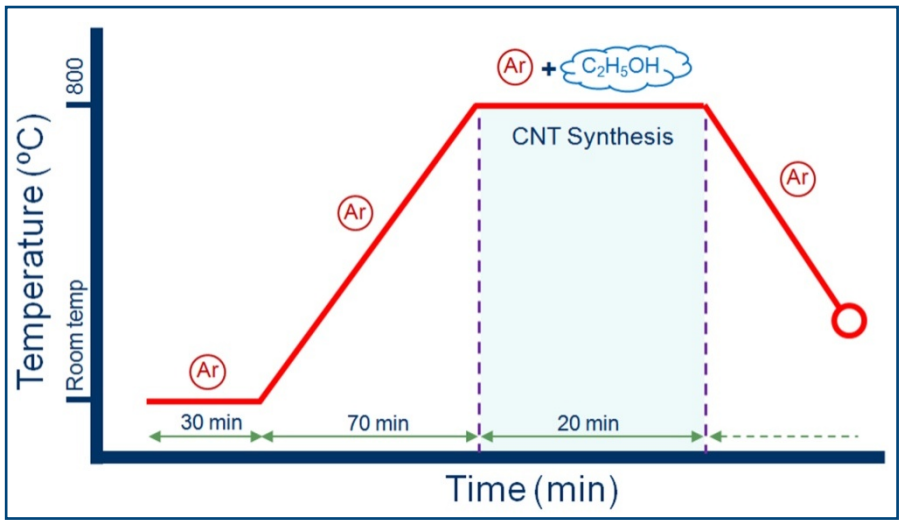

Figure 3.4 Temperature and gas profile for CVD process.

Table 3.1 Chemical vapor deposition conditions.

CVD condition	
Carbon source:	Ethanol (AR grade)
AR flow rate:	0.4 LPM
Ethanol flow rate	0.3 LPM
Pressure:	Atmospheric pressure
Temperature (varied):	700, 800, 900 °C
Time:	20 min

3.3 Characterization of Ni nanoparticles and CNTs

The morphology of the electroplated Ni was characterized by atomic force microscopy (AFM; SEIKO SPA400) with dynamic force mode (DFM) and a polysilicon

tip (NT-MDT; HA_NC ETALON) was used with resonance frequency = 235 kHz. The scan area was 2x2 μm^2. The chemical state of Ni was characterized by X-ray photoelectron spectroscopy (XPS; Kratos Analytical, AXIS Ultra DLD).

The morphology, diameter and structure of the graphitic layer, and the crystallinity of the synthesized CNTs were characterized by field emission scanning electron microscopy (FESEM; Hitachi, SU-8030) with an accelerated voltage at 1kV and a working distance of 10cm, transmission electron microscopy (TEM; JEOL, JEM-2010) using an accelerated voltage at 200 kV with LaB_6 filament and Raman spectroscopy (Thermal Scientific, DXR™ SmartRaman Spectrometer) with a laser wavelength of 532 nm, respectively. Table 3.2 shows a summary of analysis techniques and information that can be obtained from each technique.

Table 3.2 Characterization techniques and their corresponding information.

Techniques	Information
Atomic force microscopy (SEIKO, SPA400)	Ni catalyst size
X-ray photoelectron spectroscopy (Kratos Analytical, AXIS Ultra DLD)	Ni chemical state
Scanning electron microscopy (HITACHI, SU-8030)	CNTs morphology
High resolution transmission electron microscopy (JEOL, JEM-2010)	CNTs diameter and graphitic layer structure
Raman spectroscopy (Thermal Scientific, DXR™ SmartRaman Spectromete)	CNTs crystallinity

3.4 Measurement of electrochemical properties

3.4.1 Materials and equipment for measurement of electrochemical properties

Materials and equipment used in this research for measurement of electrochemical properties are as follows:

(1) 1M Sulfuric acid electrolyte
(2) Pt counter electrode
(3) Ag/AgCl reference electrode
(4) Faraday cage (to block electric field)
(5) Electrochemical instruments (Metrohm, Autolab PGSTAT302)

3.4.2 Method of measurement of electrochemical properties

Electrochemical properties were measured in a three-electrode setup as shown in Figure 3.5. It was connected to an electrochemical workstation (Metrohm, AUTOLAB PGSTAT 302). The CNTs synthesized on Ni-electroplated Cu sheet (an area of 10 mm x 10 mm) was used as a working electrode. Pt and Ag/AgCl electrodes were used as counter and reference electrode, respectively. 1M H_2SO_4 aqueous solution was used as electrolyte. Electrochemical properties were characterized by cyclic voltammetry (CV) and galvanostatic charge/discharge (CD) technique. CV tests were done at a potential range of -0.3 to 0.2 V at a scan rate of 5, 20 and 100 $mV{\cdot}s^{-1}$. CD tests were performed at a current of 5 mA. The specific capacitance (C_s, $F{\cdot}g^{-1}$) was evaluated from CV curves according to the following equation (2.3);

$$C_s = \frac{\int_{V_1}^{V_2} i(V)dV}{2(V_2 - V_1)mv} \tag{2.3}$$

Where $\int_{V_1}^{V_2} i(V)dV$ is a total voltammetric charge obtained by integration of positive and negative sweep in CV curve, V_2 - V_1 is a potential window width (V), m is a total mass of active materials (g) and v is a scan rate ($V{\cdot}s^{-1}$).

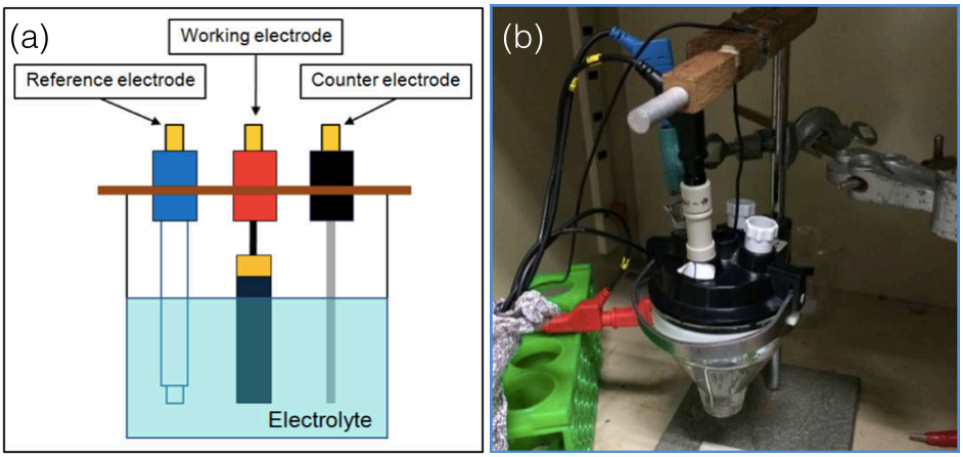

Figure 3.5 (a) Schematic diagram and (b) photograph of three electrode setup for electrochemical analysis.

CHAPTER 4
RESULTS AND DISCUSSIONS

This chapter explains the results of formation of Ni nanoparticles by DC-electroplating method and the synthesis of CNTs from the electroplated Ni by chemical vapor deposition. The effect of electroplated voltage on morphology and chemical states of the electroplated Ni and the quality of the synthesized CNTs were investigated. The DC electroplated Ni nanoparticles (NPs) were characterized the average size and the chemical states by atomic force microscope (AFM) and X-ray photoelectron spectroscopy (XPS) techniques, respectively. The synthesized CNTs by chemical vapor deposition (CVD) were characterized the morphology, internal structure and crystallinity by scanning electron microscopy (SEM), transmission electron microscopy (TEM) and Raman spectroscopy techniques, respectively. Figure 4.1 (a)-(c) shows photographs of Cu sheet before and after DC-electroplating, and after CVD process, respectively. The color of Cu sheet changed to silver color with Ni coating after DC-electroplating. After CVD process for CNTs growth, the obtained sample was obviously changed to black color wholly covered with black powder.

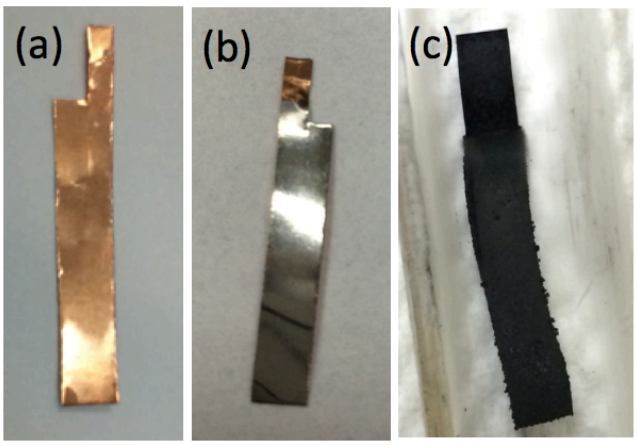

Figure 4.1 (a) Cu substrate, (b) Ni nanoparticles on Cu substrate by DC-electrplating and (c) CNTs synthesis by CVD.

4.1 Formation of Ni nanoparticles by direct-current electroplating

4.1.1 Atomic force microscopy investigation of Ni nanoparticles

After the DC-electroplating process on the Cu foils, the average sizes of the Ni nanoparticles formed by different electroplating voltages (1.0, 1.5 and 2.0 V) were measured by AFM.

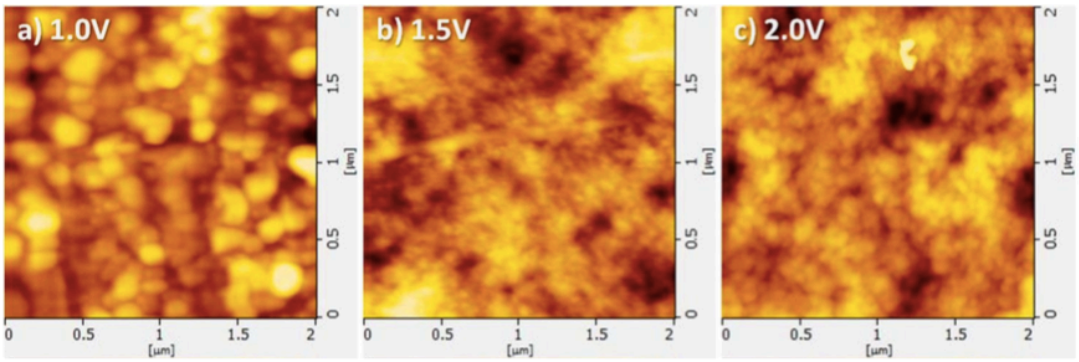

Figure 4.2 AFM images of Ni NPs on Cu foils electroplated at the voltages of (a) 1.0 V, (b) 1.5 V and (c) 2.0 V.

Figure 4.2 (a-c) shows the AFM images of the Ni NPs on Cu foils electroplated at the voltages of 1.0, 1.5 and 2.0 V, respectively. Ni NPs were formed at all of these electroplating voltages. At the applied voltage of 1.0 V, Ni NPs varied in small and larger clusters were formed; their average sizes were 44±7 nm and 120±14 nm, respectively. At the applied voltage of 1.5 V, Ni NPs with a narrow distribution of sizes were formed with an average size of 55±3 nm. When the applied voltage was increased to 2.0 V, the sizes of the formed Ni NPs increased to approximately 103±12 nm. Thus, the size of formed Ni NPs could be controlled by varying electroplating voltages.

The different size of NPs with increasing electroplating voltage can be explained by Faraday's Laws of electrolysis and Ohm's law as follows. Theoretically, Faraday's laws of electrolysis state that the amount of a material deposited on an electrode is proportional to the amount of electricity used. According to Ohm's law, the amount of current flow is proportional to the voltage. The higher the applied voltage, the higher amount and the higher energy of the positively charged Ni ions at the anode to migrate to the cathode, and reduce with the electrons to form Ni metal. The higher amount and the higher energy of the positively charged Ni ions will cause the high growth rate and large aggregation of the Ni metal.

4.1.2 X-ray photoelectron spectroscopy investigation of Ni nanoparticles

Figures 4.3-4.5 show XPS spectra of Ni NPs on Cu foils electroplated at the voltages of 1.0, 1.5 and 2.0 V, respectively.

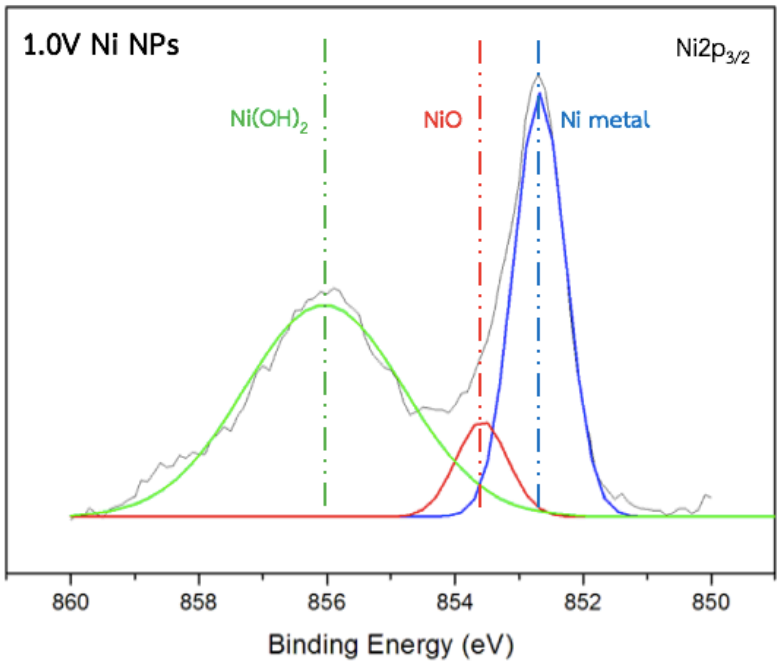

Figure 4.3 XPS spectra of Ni NPs on Cu foils electroplated at the voltages of 1.0 V.

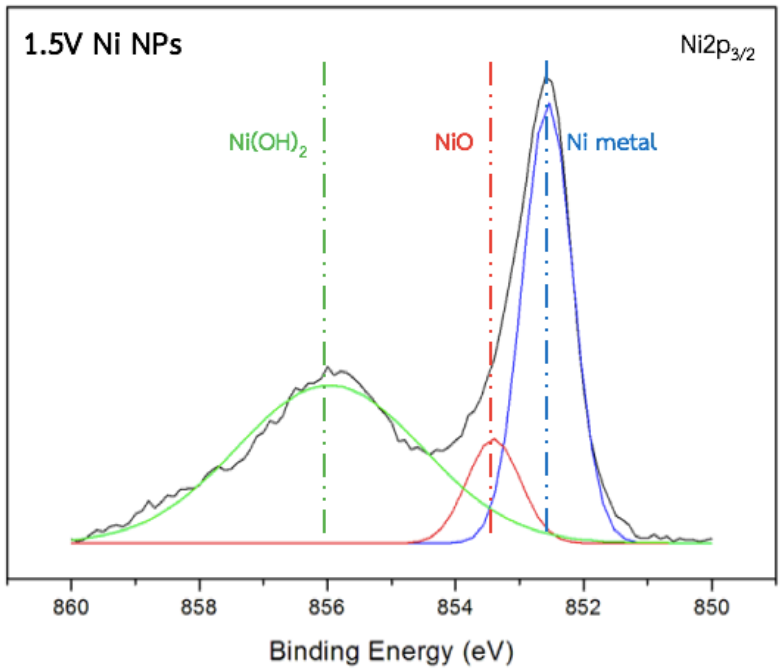

Figure 4.4 XPS spectra of Ni NPs on Cu foils electroplated at the voltages of 1.5 V.

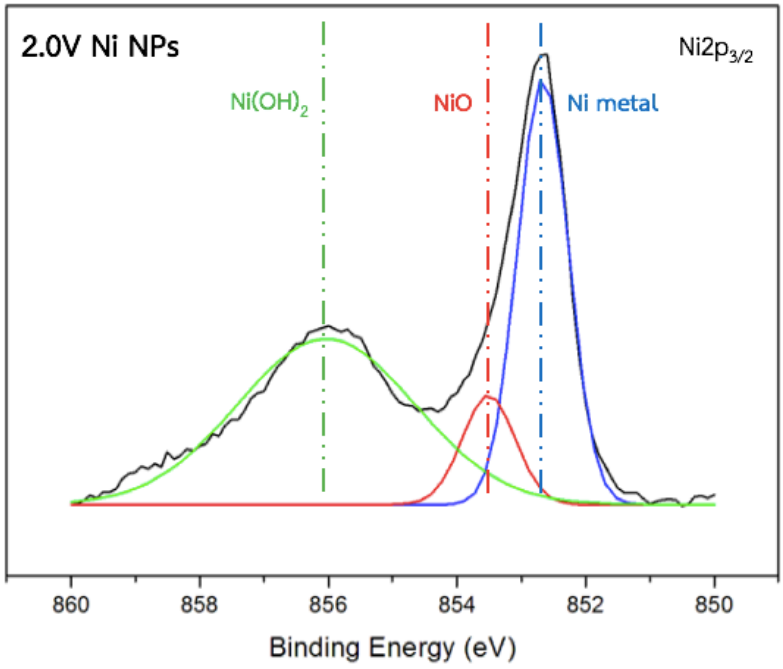

Figure 4.5 XPS spectra of Ni NPs on Cu foils electroplated at the voltages of 2.0 V.

From the XPS characterization of Ni $2p_{3/2}$, two main peaks were found at 852.8 and 856.0 eV. From peak deconvolution, the separated peaks were illustrated and match with binding energy at 852 eV, 853 eV and 856 eV that indicated to the Ni metal, NiO and $Ni(OH)_2$ formation, respectively. The atomic percentage of each oxidation states of Ni was showed in Table 4.1.

Table 4.1 The atomic percentage of each oxidation states of Ni from the electroplating voltages of 1.0, 1.5 and 2.0 V.

	Atomic % of Ni formation		
	Ni metal	NiO	$Ni(OH)_2$
1.0 V NPs	36.26	8.16	55.58
1.5 V NPs	39.13	9.69	51.18
2.0 V NPs	38.18	10.22	51.60

From XPS measurement results, the atomic percentage of each Ni oxidation states from the different electroplating voltages was similar value. The relatively same composition of Ni was formed although use the different electroplating voltages.

4.2 Effect of growth temperature on growth of carbon nanotube

In CNTs synthesis by CVD, temperature is the most important parameter that could affect to the quality of CNTs. In this experimental, the CVD temperatures were varied with 700, 800 and 900°C. The electroplating voltage for Ni NP formation was fixed at 1.5 V. SEM technique was used for characterization of the synthesized CNTs morphology

4.2.1 Scanning electron microscopy investigation of carbon nanotube grown from different growth temperatures

Figures 4.6-4.8 show SEM images of the synthesized CNTs at different temperatures recorded at the magnification of x5,000.

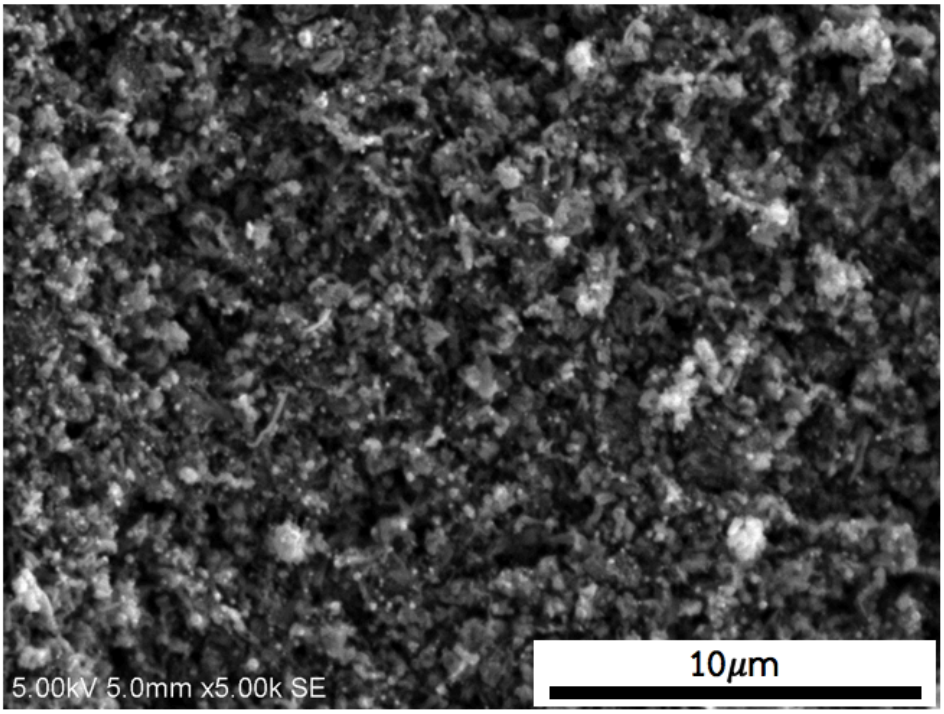

Figure 4.6 SEM image of CNTs from 1.5 V electroplating and CVD at 700°C.

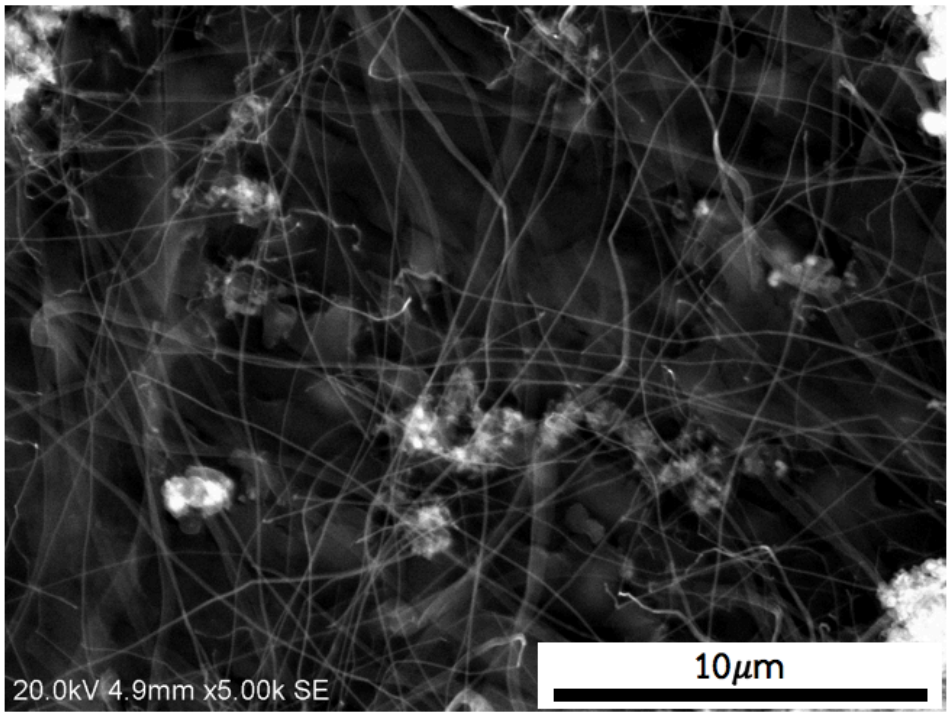

Figure 4.7 SEM image of CNTs from 1.5V electroplating and CVD at 800°C.

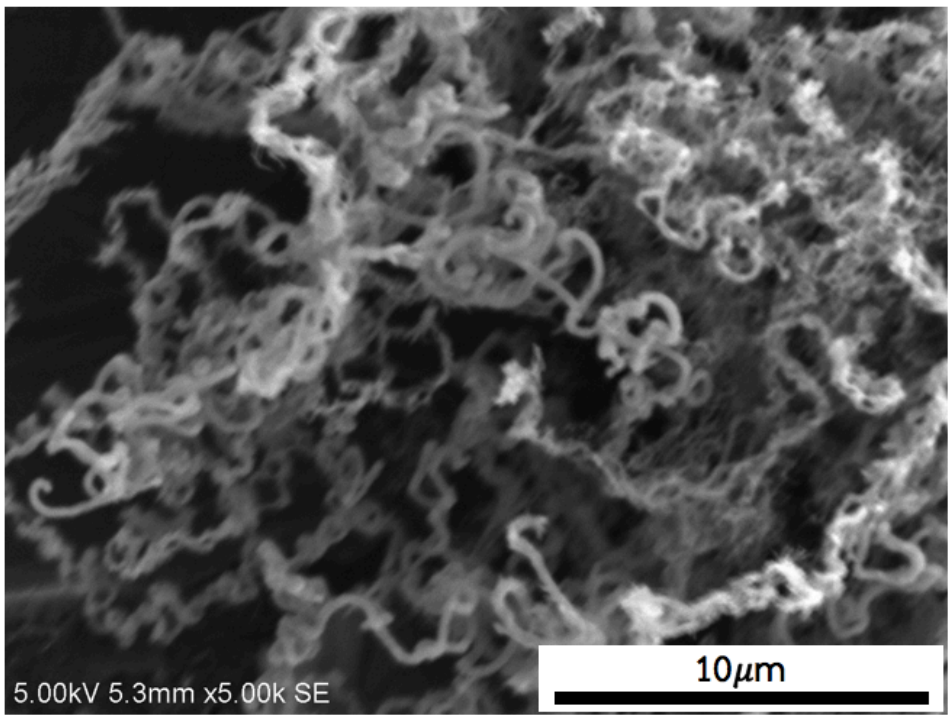

Figure 4.8 SEM image of CNTs from 1.5V electroplating and CVD at 900°C.

From the SEM results (Figure 4.6 – Figure 4.8), the morphology of CNTs grown at different growth temperature were totally different. At growth temperature of 700°C, a very short and curly CNTs were formed. The bright spots, corresponding to metal

NPs were clearly seen on the surface. At growth temperature of 800°C, the CNTs morphology was totally different from that of 700°C. The synthesized CNTs were relatively straight line with a relatively small diameter. At growth temperature of 900°C, the CNTs became curl shape and their diameter were larger compared to that of 800°C. From these results, the growth temperature of 800°C is the optimal condition to obtain the relative straight and small CNT. At low temperature (700°C), the temperature may be not sufficient for carbon diffusion on Ni NPs and saturation to form CNT, thus the nanotube structure cannot be formed. On the other hand, higher temperature (900°C), the diffusion rate of carbon is high and the Ni NPs possibly agglomerated in to a large size, resulting in the non-uniform CNT.

4.3 Effect of Ni electroplating voltage on growth of carbon nanotube

From experiment in section 4.2, it was found that the growth temperature of 800°C was the most appropriate condition for CNTs growth. Next, the effect of electroplating voltages, 1.0, 1.5 and 2.0 V, for Ni nanoparticle formation on CNTs morphology was investigated (hereinafter referred to as Ni1.0-CNTs, Ni1.5-CNTs and Ni2.0-CNTs, respectively). The CNTs growth temperature was fixed at 800°C. The synthesized CNTs were characterized by scanning electron microscopy (SEM), transmission electron microscopy (TEM) and Raman spectroscopy.

4.3.1 Scanning electron microscopy investigation of carbon nanotube grown from different Ni electroplating voltages

Figure 4.9 -Figure **4.11** show SEM images of CNTs synthesized from different Ni electroplating voltages at growth temperature of 800 °C.

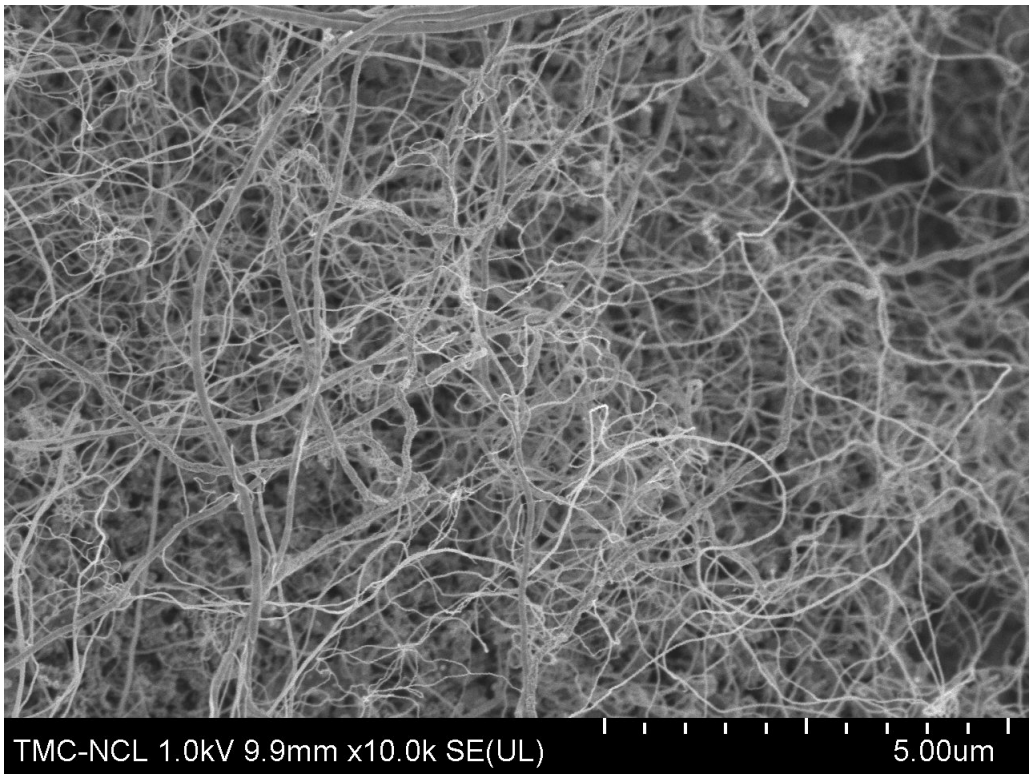

Figure 4.9 SEM image of CNTs from 1.0 V electroplating and CVD at 800 °C.

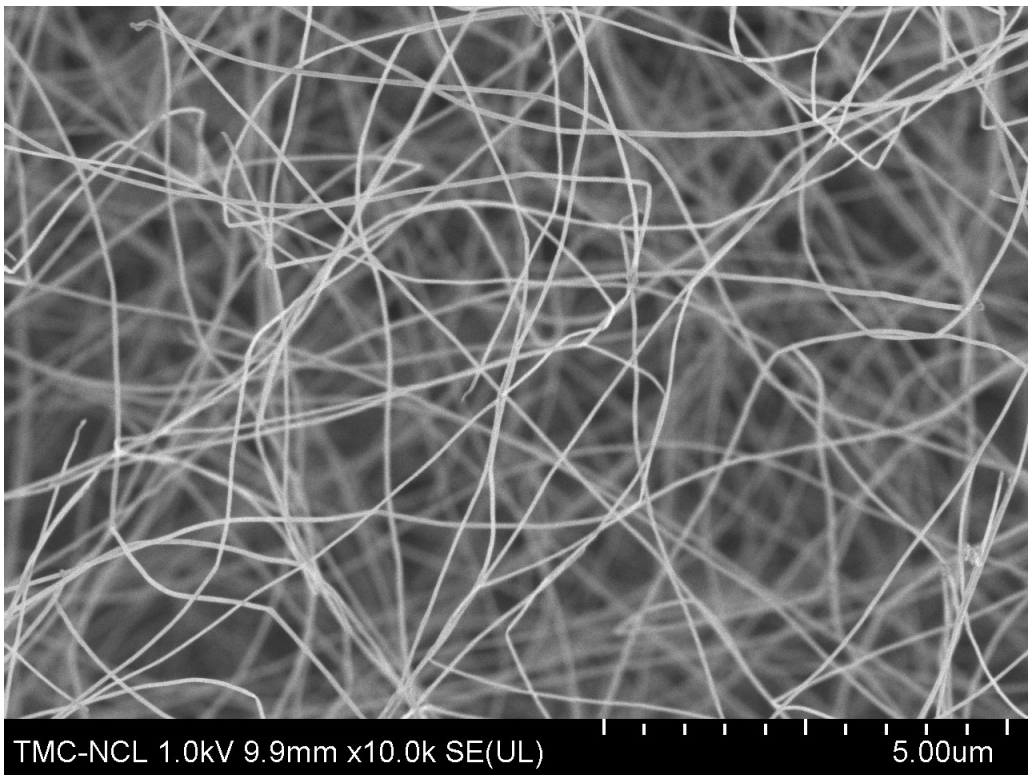

Figure 4.10 SEM image of CNTs from 1.5 V electroplating and CVD at 800 °C.

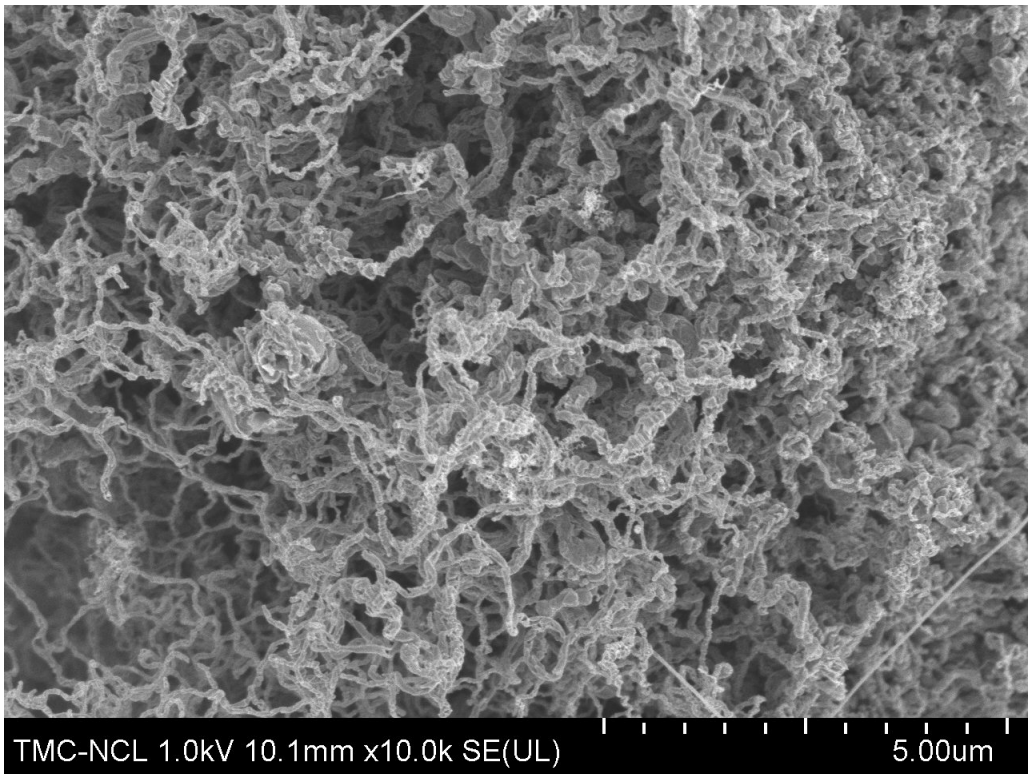

Figure 4.11 SEM image of CNTs from 2.0 V electroplating and CVD at 800 °C.

The overall morphology of the sample surfaces was examined by SEM technique. The SEM analysis was carried out with magnification at x10,000 that could reveal the CNTs in a wide area to confirm the uniformity of the synthesized CNTs. From the SEM images, it was obviously seen in Figure 4.11 that the Ni2.0-CNTs had the agglomerated clusters of curly-shape CNTs. While as seen in Figure 4.9 and Figure 4.10, Ni1.0-CNTs and Ni1.5-CNTs had a similar feature showing the high aspect ratio CNTs and non-agglomerated clusters. CNTs in Figure 4.10 were straighter and appear larger in diameters than those in Figure 4.9. For more details of the CNTs having diameters in a nanometer scale (less than 100 nanometers), TEM technique was a suitable technique that can provide sufficient resolution and internal structures of the CNTs.

4.3.2 Transmission electron microscopy investigation of carbon nanotube grown from different Ni electroplating voltages

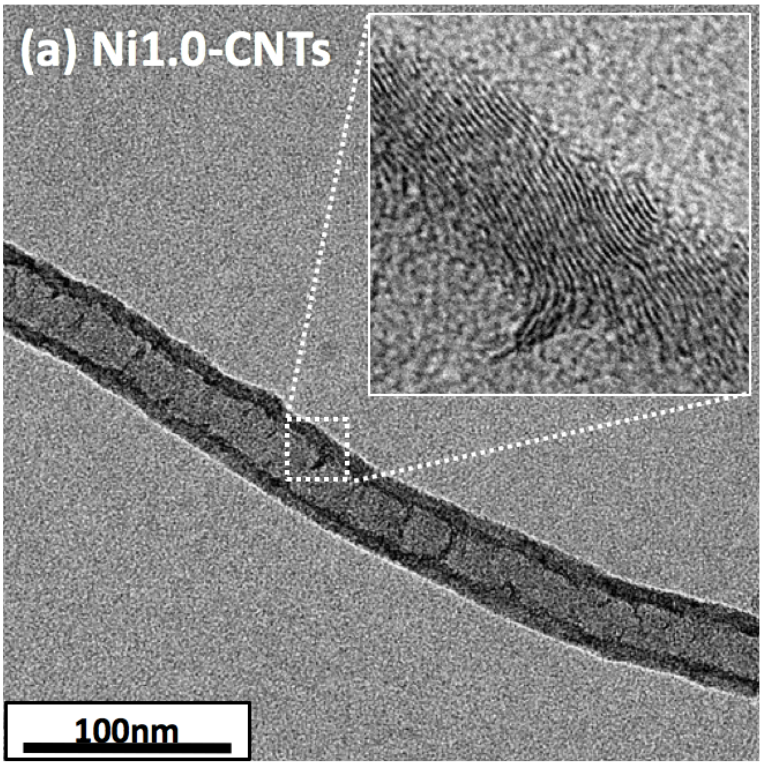

Figure 4.12 TEM image of CNTs from 1.0V electroplating and CVD at 800 °C.

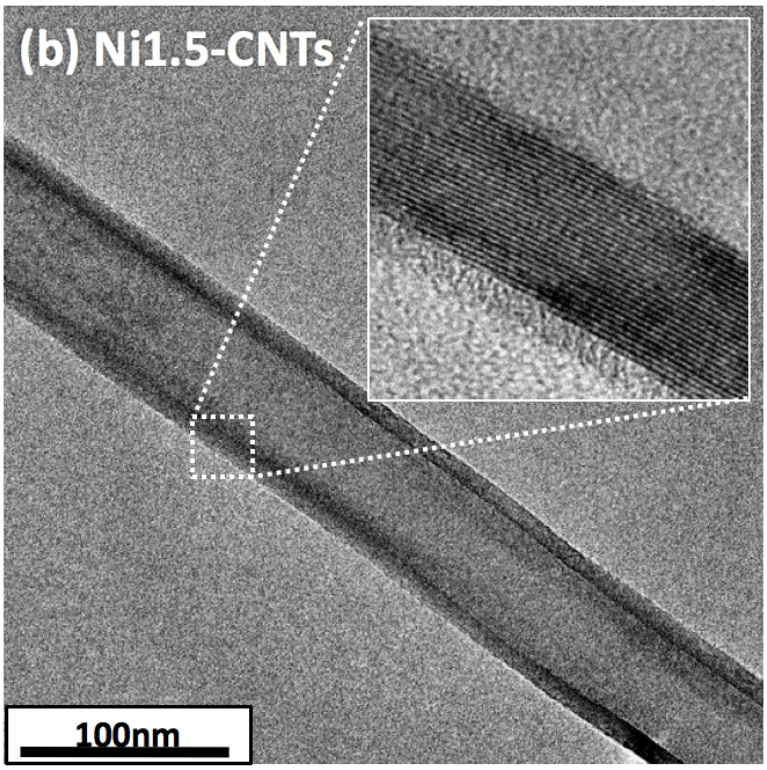

Figure 4.13 TEM image of CNTs from 1.5V electroplating and CVD at 800 °C.

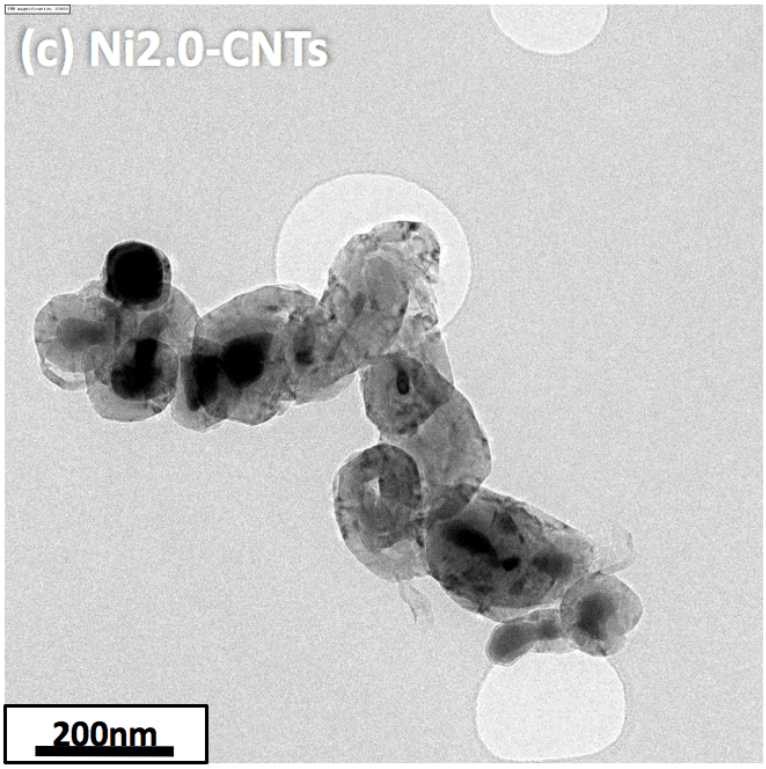

Figure 4.14 TEM image of CNTs from 2.0V electroplating and CVD at 800 °C.

Figure 4.12 – **Figure 4.14** show TEM images of Ni1.0-CNTs, Ni1.5- CNTs and Ni2.0-CNTs, respectively. The images taken at x50,000 magnification reveal the CNTs shape and graphitic wall arrangements. The images of Ni1.0-CNTs and Ni1.5-CNTs show that the CNTs had a tubular shape with diameters of approximately 45±7 nm and 60±5 nm, respectively. The darker contrast in TEM image of CNTs corresponds to the thickness of the wall. However, at high magnification up to x400,000, it was found that the wall layers were different. The inset in Figure 4.12 shows that the graphitic layers of Ni1.0-CNTs were at an angle to the tube axis wall (bamboo structure), while the inset in Figure 4.13 shows clearly that the graphitic layers of Ni1.5-CNTs were parallel to the tube axis. Furthermore, the structure of Ni2.0-CNTs was completely different from those of Ni1.0- CNTs and Ni1.5-CNTs. Ni2.0-CNTs were string bead [38] of nanoparticles with Ni catalyst inside and a wide distribution of tube diameters (Figure 4.14). These results imply that the small-sized Ni NPs with a narrow distribution is a key to uniform CNTs synthesis.

Although the TEM technique gives the advantage of high resolution with higher magnification examinations of CNTs internal structures but it was limited to a small area of CNTs. SEM, on the other hand, was appropriate for a large area observation and for external morphology. So both techniques, SEM and TEM, are complimentary for the CNTs characterization.

Figure 4.15 illustrates the structure models of CNTs growth from various electroplating voltages. The Figure 4.15(a) shows the stacking carbon layer of Ni1.0-CNTs condition, continuing growth up with stacking shape, so-called bamboo structure [37]. While the carbon growth in Figure 4.15(b) shows the carbon structure with continuous form the parallel walled carbon tube, so-called multiwall structure. In Figure 4.15(c), Ni2.0-CNTs condition, size of Ni NP was too big to form as carbon tube, as a result, the carbon layer formed around the Ni particle as string bead structure instead [38].

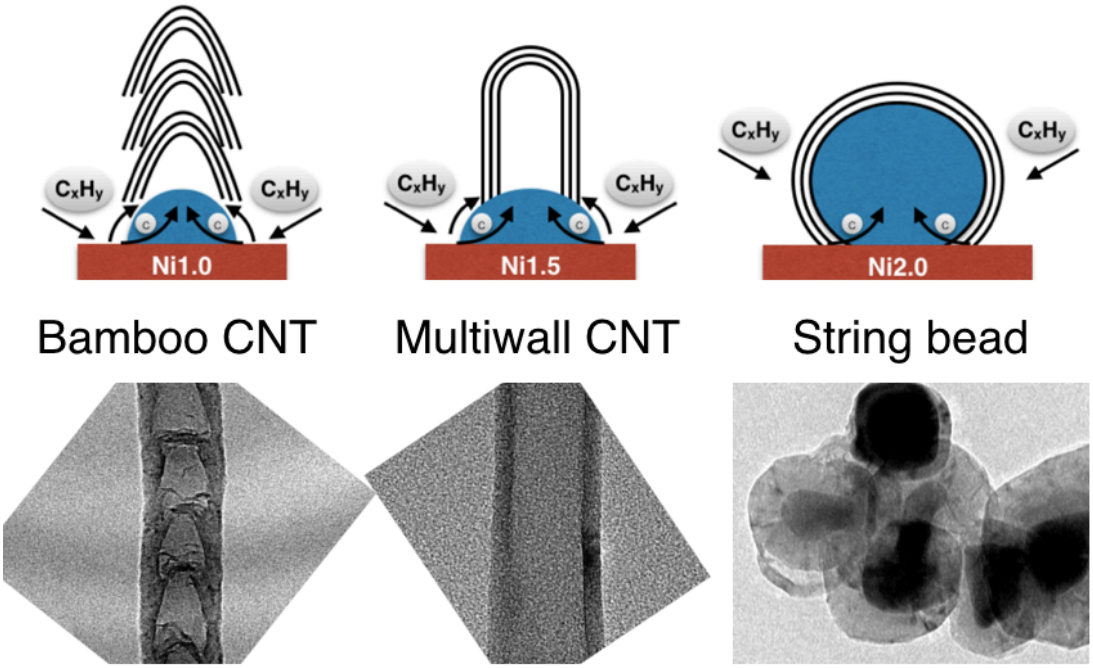

Figure 4.15 Model structures of carbon growth (a) Ni1.0-CNTs, (b) Ni1.5-CNTs and (c) Ni2.0-CNTs.

4.3.3 Raman spectroscopy investigation of carbon nanotube grown from different Ni electroplating voltages

Figure 4.16 shows Raman spectra of the synthesized CNTs. The light source was Ar ion laser with a wavelength of 532 nm (2.33 eV).

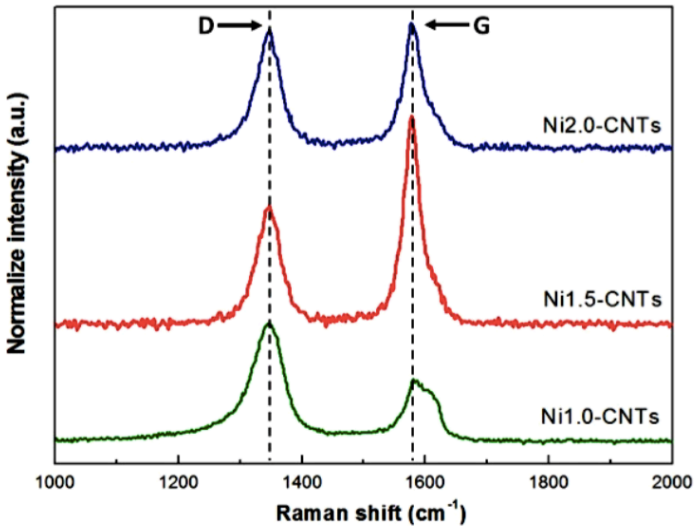

Figure 4.16 Typical Raman spectra of (a) Ni1.0-CNTs, (b) Ni1.5-CNTs and (c) Ni2.0-CNTs.

Generally, in carbon material characterization, Raman spectra are used to identify the existence of disordered carbon (*D*-band) and graphitic carbon (*G*-band). Two sharp peaks at Raman shift of approximately 1350 cm^{-1} (*D*-band) and 1590 cm^{-1} (*G*-band) were observed for all samples. The ratio of *G*-band and *D*- band (I_G/I_D) could be used to evaluate the crystallinity of the CNTs. A higher I_G/I_D ratio indicated a higher degree of structural ordering and purity of CNTs. In this study, it was found that the I_G/I_D of Ni1.0-CNTs, Ni1.5-CNTs and Ni2.0-CNTs were 0.53, 1.77 and 1.06, respectively. Ni1.5- CNTs show the highest I_G/I_D. These results corresponded well to the SEM and TEM results, demonstrating that Ni1.5-CNTs were relatively higher purity and/or had lower defects inside the parallel graphitic layers. Moreover, they also showed that the electroplating voltage directly affected the morphology of Ni NPs.

4.4 Electrochemical properties measurement

The electrochemical properties of the synthesized CNTs were investigated. The cyclic voltammetry (CV) of electrode was measured to obtain the CV curve for further specific capacitance calculation. The galvanostatic charge-discharge (CD) was measured the charge-discharge properties and the stability of the electrode. The electrochemical measurement was carried out using three-electrode system. The Ni1.5-CNTs was used as a working electrode, the Pt electrode was used as a counter electrode and the Ag/AgCl was used a reference electrode. Figure 4.17 shows a photograph of the Ni1.5-CNTs and the setup of the electrochemical test. Figure 4.18 shows cyclic voltammetry (CV) curves of the Ni1.5-CNTs in the potential range of -0.3 to 0.2 V at different scan rates.

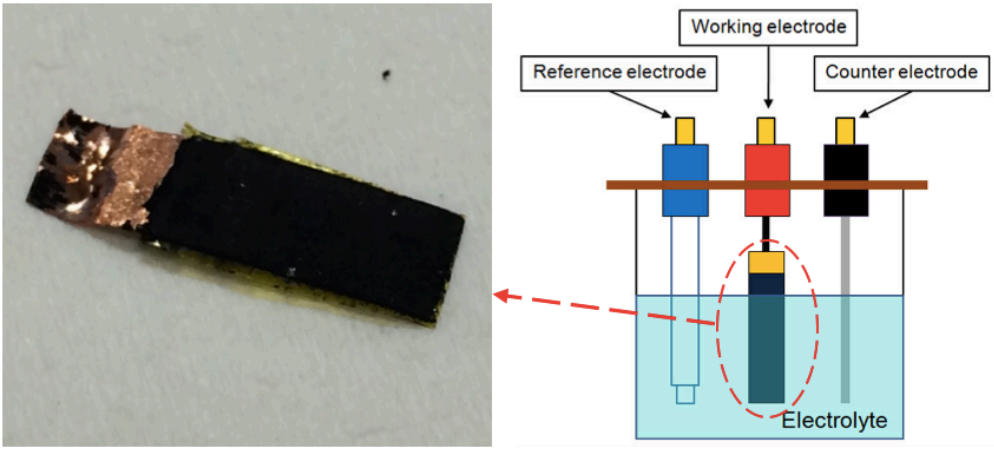

Figure 4.17 (a) Photograph of the Ni1.5-CNTs on Cu foil and schematic view of the setup of the electrochemical test.

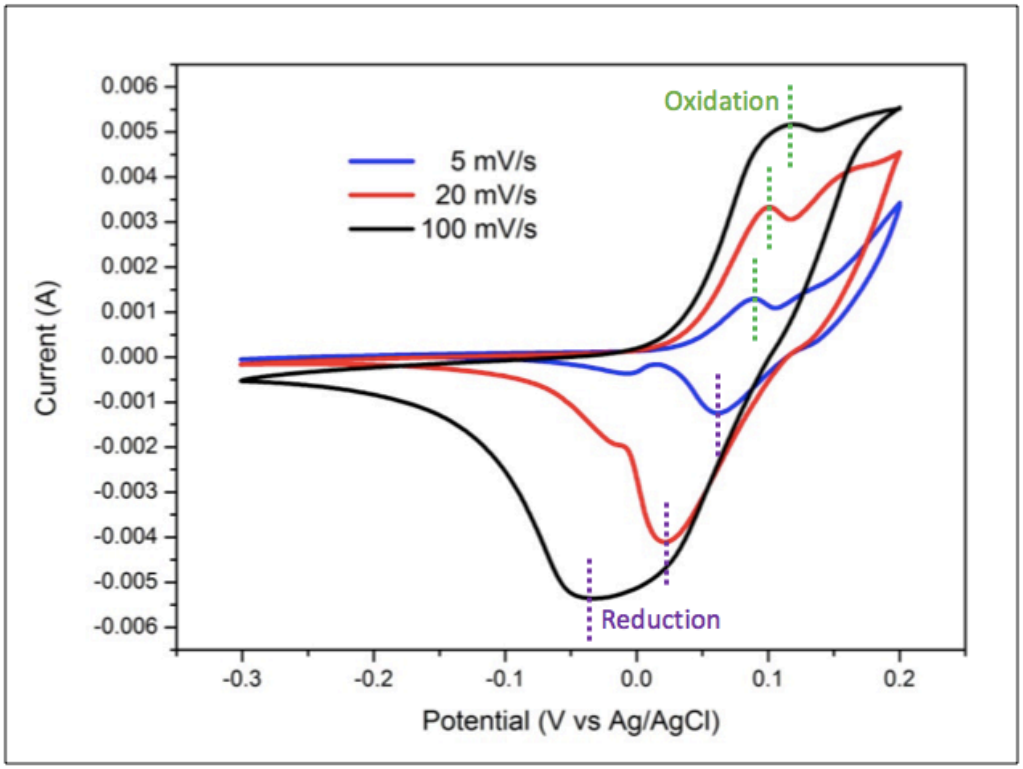

Figure 4.18 Cyclic voltammetry curves of Ni1.5-CNTs at different scan rates.

From the CV shown in Figure 4.18, instead of showing the expected rectangular shaped curve of ideal electric double-layer capacitor, all of CV curves showed a pair of redox current peaks with oxidation and reduction peaks (dot line in Figure 4.18),

indicating that faradic pseudocapacitance was the dominant electrochemical property. With increasing scan rate, the current increased and the gap between redox peaks widened while the shapes of the CV curves were retained, indicating reversibility of the redox reactions. This psesudocapacitive character might be caused by nickel oxide from CNTs synthesis [39]. Evidently, X-ray photoelectron spectroscopy spectrum of the Ni electroplated at 1.5V (Figure 4.4) shows a chemical shift of Ni 2p peaks with a composition of Ni metal, NiO and $Ni(OH)_2$. In addition, Ni NPs could also have been oxidized by residual oxygen inside the quartz tube during the CVD process. Besides Ni oxides, the effect of the CuO could not be discarded, even though the chemical shift of Cu could not be found in XPS results due to the technique limitation that sensitive only few nanometers in the depth direction. However, the potential window range in CV curve does not match for Cu-CuO redox reaction (E_0 = 34 V). Thus, under our measurement condition, the effect of Cu oxides could be neglected. However, the further experiment to prove the role of Cu oxides is required. Figure 4.19 shows galvanostatic charge-discharge curves of the Ni1.5-CNTs at current of 5 mA.

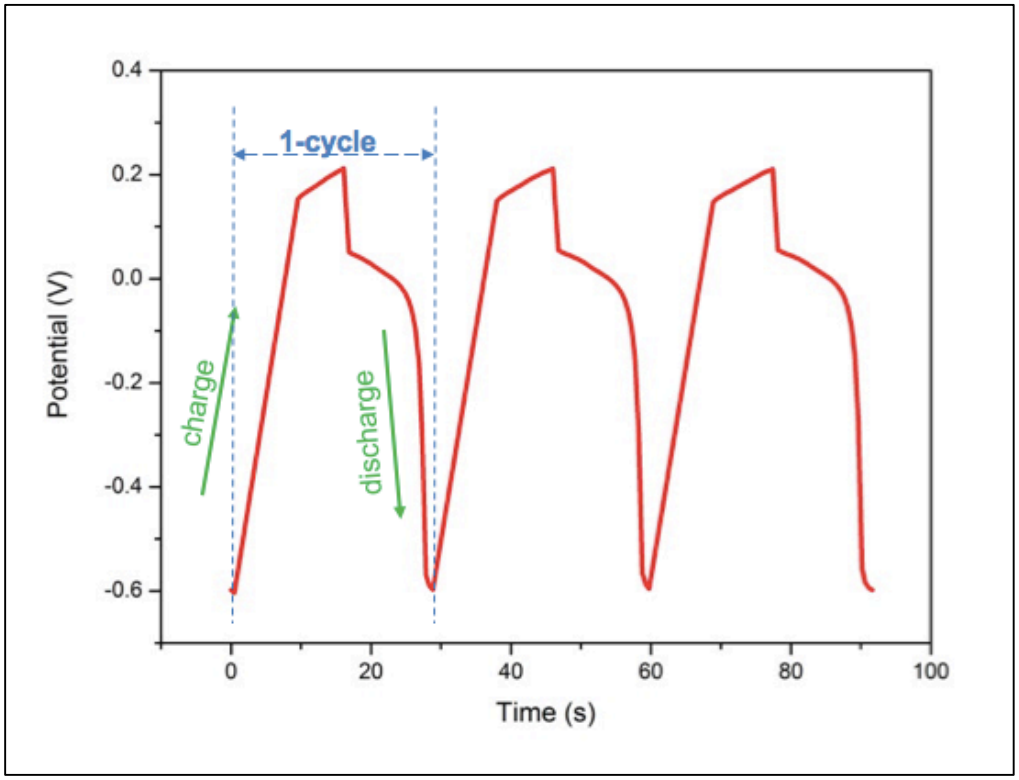

Figure 4.19 Galvanostatic charge-discharge (CD) curves of Ni1.5-CNTs at current of 5 mA.

The CD curves show the charge-discharge repeatability of the electrode. In contrast to the symmetrical triangular shape of a typical electric double-layer capacitor, the discharge curves showed nonlinearities. The discharge curves consist of the vertical line, the small curve and symmetric triangular line. The vertical line represents to the voltage drop from equivalent series resistance (ESR) in electrode. The small curve and the symmetric triangular line imply the combination of faradaic capacitive (small curve) and double-layer capacitive (triangular shape) in the active electrode material [40]. For the faradaic capacitive factor, charge transfer reaction gradually occurs. The slow discharge means the electrode discharge time increases, resulting in longer time in charge release usage. This discharge result also substantiates to the results from the CV curves. The specific capacitance calculated from the CV curve at a scan rate of 5 $mV \cdot s^{-1}$ was approximately 53 $F \cdot g^{-1}$. The energy density and power density of electrode were approximately 6.25 $Wh \cdot kg^{-1}$ and 0.49 $kW \cdot kg^{-1}$, respectively. Although, the result obtained showed a relatively small value compared to the other reports [41], the fabricated electrode also showed the potential use of supercapacitor.

All these preliminary results signified that facile growth of CNTs by Ni NPs catalyst, deposited using DC electroplating method, was fully achieved. The synthesized CNTs showed a real potential for supercapacitor electrode application. However, further work and optimization are still necessary.

CHAPTER 5
CONCLUSION

5.1 Summary conclusion

5.1.1 Novel CNTs synthesis that is simple and low-cost was proposed. This method uses controllable electroplated Ni NPs as catalyst and ethanol as carbon source for CVD process.

5.1.2 The electroplating voltage directly affects the size of Ni NPs, which, in turn, affecting the morphology and structure of the synthesized CNTs. By selecting the appropriate voltage, graphitic layers of CNTs are parallel to the tube axis with a narrow distribution of tube diameters at 60±5 nm.

5.1.3 The synthesized CNTs show a potential use as supercapacitor material with a specific capacitance of 53 $F \cdot g^{-1}$ at a scan rate of 5 $mV \cdot s^{-1}$. Further optimization of the amount ratio of oxidized Ni NPs and CNTs should improve the supercapacitor performance.

5.2 Suggestions and solutions

5.2.1 For more applicable use of the synthesized electrode, the electrode with larger dimension is required. The optimal parameter for large electroplating area such as plating voltage and size of electroplating equipment should be investigated.

5.2.2 For the CVD, the vacuum in rough to high regimes is recommended. The less contamination and controlled gas flow will provide high purification and uniform CNT.

REFERENCES

1) H.R. Kroto, J.R. Heath, S.C. O'Brien, R.F. Curl, and R.E. Smalley, **Nature** 318, 162 (1985).
2) S. Iijima, **Nature** 354, 56 (1991).
3) S. Iijima and T. Ichihashi, **Nature** 363, 603 (1993).
4) D.S. Bethune, C.H. Klang, M.S. de Vries, G. Gorman, R. Savoy, J. Vazquez, and R. Bayers, **Lett. to Nat**. 363, 605 (1993).
5) J. Prasek, J. Drbohlavova, J. Chomoucka, J. Hubalek, O. Jasek, V. Adam, and R. Kizek, **J. Mater. Chem.** 21, 15872 (2011).
6) V.N. Popov, **Mater. Sci. Eng.** 43, 61 (2004).
7) J.P. Gore and A. Sane, *Flame Synthesis of Carbon Nanotubes* (InTech, 2011).
8) T.W. Ebbesen and P.M. Ajayan, **Lett. to Nat.** 358, 220 (1992).
9) C. Journet, W.K. Maser, P. Bernier, A. Loiseau, M. Lamy de la Chapelle, S. Lafrant, P. Deniard, R. Lee, and J.E. Fischer, **Nature** 388, 756 (1997).
10) A. Thess, R. Lee, P. Nikolaev, H. Dai, P. Petit, J. Robert, C. Xu, Y.H. Lee, S.G. Kim, A.G. Rinzler, D.T. Colbert, G.E. Scuseria, D. Tomanek, J.E. Fischer, and R.E. Smalley, **Science** 273, 483 (1996).
11) Jose-Yacaman M., M. Miki-Yoshida, L. Rendon, and J.G. Santiesteban, **Appl. Phys. Lett.** 62, 657 (1993).
12) V. Ivanov, J.B. Nagy, P. Lambin, A. Lucas, X.B. Zhang, X.F. Zhang, D. Bernaerts, G. Van Tendeloo, S. Amelinckx, and J. Van Landuyt, **Chem. Phys. Lett.** 223, 329 (1994).
13) S. Amelinckx, X.B. Zhang, D. Bernaerts, X.F. Zhang, V. Ivanov, and J.B. Nagy, **Science** 265, 635 (1994).
14) W.Z. Li, S.S. Xie, L.X. Qian, B.H. Chang, B.S. Zou, W.Y. Zhou, R.A. Zhao, and G. Wang, **Science** 274, 1701 (1996).
15) S. Hofmann, G. Csanyi, A.C. Ferrari, M.C. Payne, and J. Robertson, **Phys. Rev. Lett.** 95, 36101 (2005).
16) R.S. Wagner and W.C. Ellis, **Appl. Phys. Lett.** 4, 89 (1964).
17) R.T.K. Baker, M.A. Barber, P.S. Harris, F.S. Feates, and R.J. Waite, **J. Catal.** 26, 51 (1972).
18) R.T.K. Baker and R.J. Waite, **J. Catal.** 37, 101 (1975).
19) M. Kumar, *Carbon Nanotube Synthesis and Growth Mechanism* (InTech, 2011).
20) S. Bhaviripudi, E. Mile, S.A. Steiner Iii, A.T. Zare, M.S. Dresselhaus, A.M. Belcher, and J. Kong, **J. Am. Chem. Soc.** 129, 1516 (2007).
21) Y. Takagi, D., Kobayashi, Y., Hlbirio, H., Suzuki, S., Homma, **Nano Lett.** 8, 832 (2008).

22) D. Yuan, L. Ding, H. Chu, Y. Feng, T.P. McNicholas, and J. Liu, **Nano Lett.** 8, 2576 (2008).

23) L. Ding, A. Tselev, J. Wang, D. Yuan, H. Chu, T.P. McNicholas, Y. Li, and J. Liu, **Nano Lett.** 9, 800 (2008).

24) L. Ding, D. Yuan, and J. Liu, J. **Am. Chem. Soc.** 130, 5428 (2008).

25) W. Zhou, Z. Han, J. Wang, Y. Zhang, Z. Jin, X. Sun, Y. Zhang, C. Yan, and Y. Li, **Nano Lett.** 6, 2987 (2006).

26) M. Ritschel, A. Leonhardt, D. Elefant, S. Oswald, and B. Bu, **J. Phys. Chem. C** 111, 8414 (2007).

27) Y. Li, W. Kim, Y. Zhang, M. Rolandi, D. Wang, and H. Dai, **J. Phys. Chem. B** 105, 11424 (2001).

28) H.C. Choi, W. Kim, D. Wang, and H. Dai, J. **Phys. Chem. B** 106, 12361 (2002).

29) G.-H. Jeong, A. Yamazaki, S. Suzuki, H. Yoshimura, Y. Kobayashi, and Y. Homma, J. **Am. Chem. Soc.** 127, 8238 (2005).

30) A. Javey and H. Dai, **J. Am. Chem. Soc.** 127, 11942 (2005).

31) L. An, J.M. Owens, L.E. McNeil, and J. Liu, **J. Am. Chem. Soc.** 124, 13688 (2002).

32) C. Lu and J. Liu, **J. Phys. Chem. B** 110, 20254 (2006).

33) *AJA* INTERNATIONAL, Inc. 2016. **Sputtering**. [online]. Available : http://www.ajaint.com/what-is-sputtering.html

34) Wikipedia. 2016. **Supercapacitors chart**. [online]. Available : https://commons.wikimedia.org/wiki/File:Supercapacitors_chart.svg

35) Wikipedia. 2016. **Capacitor**. [online]. Available : https://en.wikipedia.org/wiki/Capacitor

36) Princeton Applied Research. 2016. **A Review of Techniques for Electrochemical Analysis**. [online]. Available : http://www.ameteksi.com/-/media/ameteksi/download_links/documentations/library/princetonappliedresearch/application_note_e-4.pdf?la=en

37) X. Wang, W. Hu, Y. Liu, C. Long, Y. Xu, S. Zhou, D. Zhu, and L. Dai, **Carbon** 39, 1533 (2001).

38) S. Seraphin, S. Wang, D. Zhou, and J. Jiao, **Chem. Phys. Lett.** 228, 506 (1994).

39) H.B. Li, M.H. Yu, F.X. Wang, P. Liu, Y. Liang, J. Xiao, C.X. Wang, Y.X. Tong, and G.W. Yang, **Nat. Commun.** 4, 1894 (2013).

40) H.W. Wang, Z.A. Hu, Y.Q. Chang, Y.L. Chen, Z.Q. Lei, Z.Y. Zhang, and Y.Y. Yang, **Electrochim. Acta** 55, 8974 (2010).

41) P. Dulyaseree, V. Yordsri, and W. Wongwiriyapan, **Jpn. J. Appl. Phys**. 55, 02BD05 (2016).

AUTHOR BIOGRAPHY

Name-Surname Mr. Visittapong Yordsri

Date of Birth June 10, 1982

Present Address 123 Soi.113, Lardprow Rd., Klongjun, Bangkapi, Bangkok, Thailand 10240

Education

2001-2004 Bachelor of Engineering, Department of Materials, Faculty of Material Engineering, Kasetsart University, Thailand

Work Experience

2005-Present Senior Technician of Transmission Electron Microscope Laboratory, National Metal and Materials Technology Center

Recent/relevant publications:

(1) Worawut Muangrat, Visittapong Yordsri, Rungroj Maolanon, Sirapat Pratontep, Supanit Porntheeraphat, Winadda Wongwiriyapan
"Hybrid gas sensor based on platinum nanoparticles/poly(methyl methacrylate)-coated single-walled carbon nanotubes for dichloromethane detection with a high response magnitude"
Diamond & Related Materials 65 (2016), 183-190

(2) Phannee Saengkaew, Sakuntam Sanorpim, Manit Jitpukdee, Kulthawat Cheewajaroen, Chadet Yenchai, Decho Thong-aram, Visittapong Yordsri, Chanchana Thanachayanont, Noppadon Nuntawong
"Impact of precursor purity on optical properties and radiation detection of CsI:Tl scintillators"

Applied Physics A (2016), 122:729

(3) Paweena Dulyaseree, Visittapong Yordsri, Winadda Wongwiriyapan

"Effects of microwave and oxygen plasma treatments on capacitive characteristics of supercapacitor based on multiwalled carbon nanotubes"

Japanese Journal of Applied Physics, 55 (2016), 02BD05

(4) Pornsiri Wanarattikan, Sakuntam Sanorpim, Somyod Denchitcharoen, Visittapong Yordsri, Chanchana Thanachayanont, Kenjiro Uesugi, Shigeyuki Kuboya, Kentaro Onabe

"TEM Analysis of Planar Defects in InGaAsN and GaAs Grown on Ge (001) by MOVPE"

Key Engineering Materials, 675-676 (2016), 649-642

(5) Bralee Chayasombat, Visittapong Yordsri, Tetsuo Oikawa, Chanchana Thanachayanont

"Microstructural characterization of nickel hydroxide films deposited using an ammonia-induced method and subsequently calcined nickel oxide films"

Materials Science in Semiconductor Processing, 34 (2015), 224-229

(6) Phannee Saengkaew, Sakuntam Sanorpim, Visittapong Yordsri, Chanchana Thanachayanont, Kentaro Onabe

"Characterization of semi-polar GaN on GaAs substrates"

Journal of Crystal Growth, 411 (2015), 76-80

(7) Visittapong Yordsri, Winadda Wongwiriyapan, Chanchana Thanachayanont, **"Facile growth of carbon nanaotube electrode from electroplated Ni catalyst for supercapacitor"**
Advance Materials Letters, 6 (2015), 501-504

(8) Phannee Saengkaew, Sakuntam Sanorpim, Visittapong Yordsri, Chanchana Thanachayanont, Kentaro Onabe
"Characterization of semi-polar GaN on GaAs substrates"
Journal of Crystal Growth, 411 (2015), 76-80

(9) Chanchana Thanachayanont, Visittapong Yordsri, Suphakan Kijamnajsuk, Nawal Binhayeeniyi, Nantakan Muensit
"Microstructural investigation of sol–gel BZT powders"
Materials Letters, 82 (2012), 205-207

(10) Chanchana Thanachayanont, Visittapong Yordsri, Chris Boothroyd,
"Microstructural investigation and SnO nanodefects in spray-pyrolyzed SnO_2 thin films"
Materials Letters, 65 (2011), 2610-2613

Research Article Adv. Mater. Lett. 2015, **6**(6), 501-504 Advanced Materials *Letters*

www.amlett.com, www.vbripress.com/aml, DOI: 10.5185/amlett.2015.SMS6 Published online by the VBRI Press in 2015

Facile growth of carbon nanaotube electrode from electroplated Ni catalyst for supercapacitor

Visittapong Yordsri[1,2], Winadda Wongwiriyapan[1,3,4*], Chanchana Thanachayanont[2]

[1]*College of Nanotechnology, King Mongkut's Institute of Technology Ladkrabang, Chalongkrung Rd., Ladkrabang, Bangkok, Thailand*
[2]*National Metal and Materials Technology Center, 114 Thailand Science Park, Paholyothin Rd., Klong 1, Klong Luang, Pathumthani, Thailand*
[3]*Nanotec-KMITL Center of Excellence on Nanoelectronic Device, Chalongkrung Rd., Ladkrabang, Bangkok, Thailand*
[4]*Thailand Center of Excellence in Physics, CHE, Si Ayutthaya Rd., Bangkok, Thailand*

[*]Corresponding author. Tel: (+66) 23298000; E-mail: kwwinadd@kmitl.ac.th

Received: 15 October 2015, Revised: 20 March 2015 and Accepted: 22 March 2015

ABSTRACT

A facile growth of carbon nanotubes (CNTs) was facilitated by the use of direct-current plating technique for catalyst preparation. Ni nanoparticles (NPs) were deposited on Cu foil at different applied voltages of 1.0, 1.5 and 2.0 V. The Ni-deposited foil was subsequently used as catalyst for CNTs synthesis by chemical vapour deposition (CVD) method. CVD was carried out at 800 ºC using ethanol as carbon source. A voltage of 1.5 V was the optimum condition to deposit uniform Ni NPs that had a narrow size distribution of 55±3 nm, which in turn, yielded synthesized CNTs with a uniform diameter of approximately 60±5 nm with graphitic layers parallel to the CNTs axis. On the other hand, electroplated Ni at 1.0 V produced CNTs with graphitic layers at an angle to the CNTs axis, while electroplated Ni at 2.0 V produced curly CNTs with a wide distribution of diameters. These results show that Ni NPs size distribution could be controlled by electroplated voltage. Our observation was that Ni NPs with a narrow distribution of sizes and a uniform diameter is a key to uniform CNT synthesis. Furthermore, the synthesized CNTs electrode shows a faradic pseudo capacitance property, which can be attributed to the existence of oxidized Ni NPs. These results propose that the synthesized CNTs are promising materials for future super capacitor application. The optimization of ratio of Ni NPs and CNTs may improve the supercapacitors performance.

Keywords: Electroplating; carbon nanotube; chemical vapor deposition; pseudocapacitor.

Visittapong Yordsri is a technician of transmission electron microscope laboratory, National metal and materials technology center, Thailand. He is working on the nanocarbon characterization and the application of energy storage device as supercapacitor.

Introduction

Carbon nanotube (CNT) is one of the most promising materials in nanotechnology due to its large effective surface area and excellent mechanical and electrical properties. CNT shows a great potential for improving the performance of electronics devices, energy storage devices and sensors **[1-3]**. Important for large-scale applications, a simple synthesis method for mass production of CNT is required. Chemical vapor deposition (CVD) is one of the presently available methods for CNT synthesis. Metal catalyst is an essential ingredient in the CVD approach **[4, 5]**. As for catalyst film preparation, evaporation and sputtering techniques are normally utilized **[6-8]**, but these techniques are time-consuming and high cost. For practical application, facile catalyst preparation is absolutely required. Electroplating, a proposed technique for such preparation, is simple to set up, low cost, fast, can deposit to a selected area and does not need vacuum **[9-11]**. In this study, facile growth of CNTs was made possible by using direct-current (DC) electroplating for Ni nanoparticles (NPs) catalyst preparation; with the Ni-deposited catalyst, CNTs was synthesized by using CVD with ethanol as carbon source. The effects of DC-electroplating voltage on the morphology and structure of the CNTs were investigated. Furthermore, for demonstration of a potential application, supercapacitors based on the synthesized CNTs were fabricated and their electrochemical properties were determined.

Experimental

Materials

Cu foils 99.9% pure (0.05 mm × 4 mm × 20 mm) were used as a substrate for Ni NPs preparation (Nilaco Corporation, Japan). Ni ingot was applied as cathode and commercial Ni electroplating solution was used as electrolyte in the electroplating process. Prior to electroplating, Cu foils were cleaned in ethanol and acetone and then ultrasonically cleaned for 10 minutes in distilled water. For CNT synthesis, ethanol (99.9%, Labscan) was used as carbon source and Ar (99.995%) was used as carrier gas. H_2SO_4 (98%, Sigma Aldrich) was prepared in the concentration of 1 M for using as electrolyte in the measurements of electrochemical properties.

Ni catalyst preparation by electroplating

DC electroplating technique was used for Ni deposition on Cu foil. The Cu foil and the Ni ingot were connected as anode and cathode, respectively. Electroplating temperature, time and distance between electrodes were fixed at 45ºC, 5 min and 100 mm, respectively, while the applied voltages were varied from 1.0, 1.5 to 2.0V. The Ni catalyst-electroplated Cu foil was used for CNT synthesis by CVD.

CNT synthesis by chemical vapor deposition

The CNT synthesis procedure was as follows. A quartz tube reactor was filled with Ar gas at a flow rate of 500 sccm and the Ni catalyst-electroplated Cu foil was heated to 800ºC. Ethanol was vaporized and directed into the quartz tube by Ar bubbling for 20 min to grow the CNTs.

Characterization of Ni nanoparticles and CNTs

The morphology of the electroplated Ni was characterized by atomic force microscopy (AFM; SEIKO SPA400) with a monocrystal silicon tip (NT-MDT; HA_NC ETALON). The morphology, diameter and structure of the graphitic layer, and the crystallinity of the synthesized CNTs were characterized by field emission scanning electron microscopy (FESEM; Hitachi SU-8030), transmission electron microscopy (TEM; JEOL JEM-2010) and Raman spectroscopy (Thermal Scientific; DXR™ SmartRaman Spectroscopy), respectively.

Measurement of electrochemical properties

Electrochemical measurements were carried out in a three-electrode setup connected to an electrochemical workstation (Metrohm AUTOLAB PGSTAT 302). The CNT synthesized on Ni-electroplated Cu foil (an area of 4 mm × 10 mm) was used as working electrode. Pt and Ag/AgCl electrodes were used as counting and reference electrode, respectively. 1M H_2SO_4 aqueous solution was used as electrolyte. Electrochemical properties were characterized by cyclic voltammetry (CV) and galvanostatic charge/discharge (CD) technique. CV tests were done at the potential range of −0.3 to 0.2 V at a scan rate of 5, 20 and 100 mVs^{-1}. CD tests were performed at a current of 5 mA. The specific capacitance (C_{sp}, Fg^{-1}) was evaluated from CV curves according to the following equation;

$$C_{sp} = \frac{\int_{V_1}^{V_2} i(V)dV}{2(V_2 - V_1)mv} \quad (1)$$

where $\int_{V_1}^{V_2} i(V)dV$ is total voltammetric charge obtained by integration of positive and negative sweep in CV curve, V_2-V_1 is potential window width (V), m is a total mass of active materials (g), v is a scan rate (Vs^{-1}) **[12]**.

Results and discussion

Fig. 1(a-c) show the AFM images of the Ni NPs on Cu foils electroplated at the voltages of 1.0, 1.5 and 2.0 V, respectively. Ni NPs were formed at all of these electroplating voltages. At the applied voltage of 1.0 V, small and larger clusters of Ni NPS were formed; their average sizes were 44±7 nm and 120±14 nm, respectively. At the applied voltage of 1.5 V, Ni NPs with a narrow distribution of sizes were formed with an average size of 55±3 nm. When the applied voltage was increased to 2.0 V, the sizes of the formed Ni NPs increased to approximately 103±12 nm. Thus, the size of formed Ni NPs can be controlled by varying electroplating voltages.

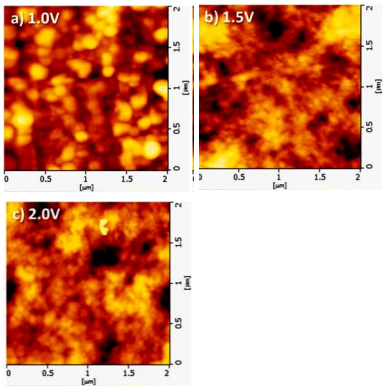

Fig. 1. AFM images of Ni NPs on Cu foils electroplated at the voltages of (a) 1.0 V, (b) 1.5 V and (c) 2.0 V.

Fig. 2(a-c) show SEM images of the CNTs synthesized by using Ni NPs catalysts that were deposited at electroplating voltages of 1.0, 1.5 and 2.0 V, respectively (hereafter referred to as Ni1.0-CNTs, Ni1.5-CNTs and Ni2.0-CNTs, respectively). After CVD, the surfaces of all Cu foils were visually observed to be wholly covered with black powder. All of the formed Ni NPs were able to act as catalyst producing tubular shaped CNTs, but the synthesized CNTs were different in their morphology and structure. The Ni1.0-CNTs were a tangled network while the Ni1.5-CNTs were straight with high aspect ratio and the Ni2.0-CNTs were curly and agglomerated.

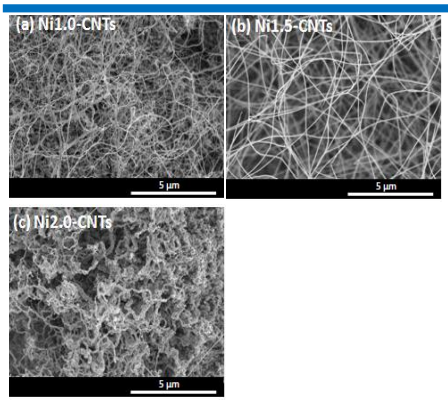

Fig. 2. SEM images of (a) Ni1.0-CNTs, (b) Ni1.5-CNTs and (c) Ni2.0-CNTs.

Fig. 3(a-c) shows TEM images of Ni1.0-CNTs, Ni1.5-CNTs and Ni2.0-CNTs, respectively. Insets are TEM images of graphitic layers of CNT walls at high magnification. Typical for TEM characterization, magnification in the range of x50000 to x400000 was used. Observed at low magnification, Ni1.0-CNTs and Ni1.5-CNTs were tubular in shape with diameters of approximately 45±7 nm and 60±5 nm, respectively. However, at high magnification, it was found that their graphitic layers were completely different. The inset in **Fig. 3(a)** shows that the graphitic layers of Ni1.0-CNTs were at an angle to the tube axis wall, while the inset in **Fig. 3b** shows clearly that the graphitic layers of Ni1.5-CNTs were parallel to the tube axis. Furthermore, the structure of Ni2.0-CNTs was completely different from those of Ni1.0-CNTs and Ni1.5-CNTs. Ni2.0-CNTs were largely curly with Ni catalyst inside and wide distribution of tube diameters (**Fig. 3(c)**).

Fig. 4 shows Raman spectra of the synthesized CNTs. The exciting light was Ar ion laser at the wavelength of 532 nm (2.33 eV). Generally, in carbon material characterization, Raman spectra can be used to identify the existence of disordered carbon (*D*-band) and graphitic carbon (*G*-band). Two sharp peaks at Raman shift of approximately 1350 cm^{-1} (*D*-band) and 1590 cm^{-1} (*G*-band) were observed for all samples. The ratio of *G*-band and *D*-band (I_G/I_D) can be used to evaluate the crystallinity of the CNTs. A higher I_G/I_D ratio indicates a higher degree of structural ordering and purity of CNTs **[13].** In this study, it was found that the I_G/I_D of Ni1.0-CNTs, Ni1.5-CNTs and Ni2.0-CNTs were 0.53, 1.77 and 1.06, respectively. Ni1.5-CNTs showed the highest I_G/I_D. These results corresponded well to the SEM and TEM results, demonstrating that Ni1.5-CNTs were relatively higher purity and/or had lower defects inside the parallel graphitic layers. Moreover, they also showed that the electroplating voltage directly affected the morphology of Ni NPs. Small-sized Ni NPs with narrow distribution is key to uniform CNT synthesis.

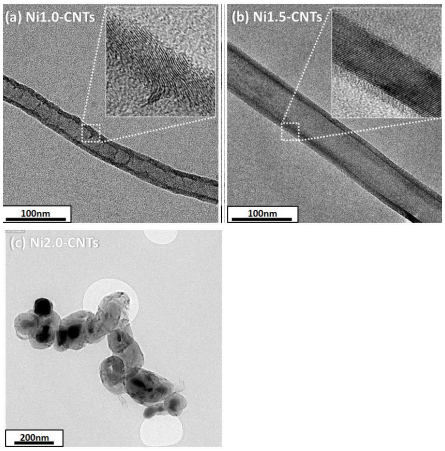

Fig. 3. TEM images (a) Ni1.0-CNTs, (b) Ni1.5-CNTs and (c) Ni2.0-CNTs. Insets are TEM images of graphitic layers of CNT walls at high magnification.

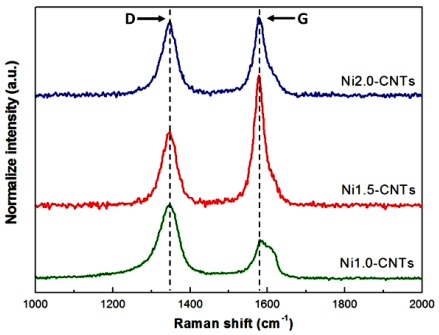

Fig. 4. Typical Raman spectra of (a) Ni1.0-CNTs, (b) Ni1.5-CNTs and (c) Ni2.0-CNTs.

To check their suitability for supercapacitor application, the electrochemical properties of Ni1.5-CNTs on Cu foil were determined. **Fig. 5(a)** shows cyclic voltammetry (CV) curves of Ni1.5-CNTs in the potential range of -0.3 to 0.2 V at different scan rates. Instead of showing the expected rectangular shaped curve of ideal electric double-layer capacitor, all of CV curves showed a pair of redox current peaks, indicating that faradic pseudocapacitance is the dominant electrochemical property. With increasing scan rate, the current increased and the gap between redox peaks widened while the shapes of the CV curves were retained, indicating reversibility of the redox reactions. This psesudocapacitive character might be caused by residual Ni NPs catalyst **[14]** from CNT synthesis. Evidently, X-ray photoelectron spectroscopy spectra showed a chemical shift of Ni 2p peaks, indicating that Ni_xO_y and $Ni(OH)_2$ were

formed after electroplating (data not shown). In addition, Ni NPs could also have been oxidized by residual oxygen inside the quartz tube during the CVD process. **Fig. 5(b)** shows a cycle of the galvanostatic charge-discharge curves at the current of 5 mA. In contrast to the symmetrical triangular shape of a typical electric double-layer capacitor, the discharge curves show nonlinearities, indicating an occurrence of faradaic reaction in the active electrode material and substantiating the results from the CV curves. The specific capacitance calculated from the CV curve at a scan rate of 5 mVs^{-1} was approximately 53 Fg^{-1}.

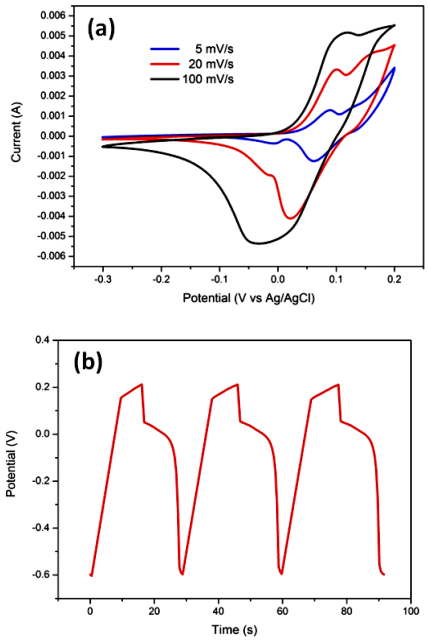

Fig. 5. (a) Cyclic voltammetry curves of Ni1.5-CNTs with different scan rate and (b) galvanostatic charge-discharge curves.

All of these preliminary results signified that facile growth of CNTs by Ni NPs catalyst, deposited using DC electroplating method was fully achieved. The synthesized CNTs showed a real potential for supercapacitor electrode application. However, further work and optimization are still necessary.

Conclusion

Novel CNTs synthesis method that is simple and low cost was proposed. This method uses controllable electroplated Ni NPs as catalyst and ethanol as carbon source for CVD process. The electroplating voltage directly affected the size of Ni NPs, which, in turn, affecting the morphology and structure of the synthesized CNTs. By selecting the appropriate voltage, graphitic layers of CNTs can be made parallel to the tube axis with a narrow distribution of tube diameters at 60±5 nm. The synthesized CNTs showed a real potential as supercapacitor with a specific capacitance of 53 Fg^{-1} at a scan rate of 5 mVs^{-1}. Further optimization of the amount ratio of oxidized Ni NPs and CNTs should improve the supercapacitor performance.

Acknowledgements

We acknowledge support from the Thailand Research Fund (DBG5580005) and from the National Nanotechnology Center (NANOTEC), NSTDA, Ministry of Science and Technology, Thailand, through its program of Center of Excellence Network and the Thailand Center of Excellence in Physics (ThEP).

Reference

1. Park, S.; Vosquerichian, M.; Bao, Z., *Nanoscale* **2013**, *5*. **DOI:** 10.1039/C3NR33560G
2. Karakaya, M.; Zhu, J.; Raghavendra, A.J.; Podila, R.; Parler Jr., S.G.; Kaplan, J.P.; Rao A.M.; *Appl. Phys. Lett.* **2014**, *105*, 263103. **DOI:** 10.1063/1.4905153
3. Esser, B.; Schnorr, J.M.; Swager, T.M.; *Angew. Chtm. Int. Ed.* **2012**, *51*, 5752. **DOI:** 10.1002/anie.201201042
4. Lee, C.J.; Park, J.; Yu, J.A., *Chem. Phys. Lett.* **2002**, *360*, 250. **DOI:** 10.1016/S0009-2614(02)00831-X
5. Muangrat, M.; Porntheeraphat, S.; Wongwiriyapan, W., *Engineering Journal* **2013**, *17*, 35. **DOI:** 10.4186/ej.2013.17.5
6. Zhang, R.Y.; Amlani, I.; Basker J.; Tresek, J. and Tsui, T.K, *Nano Lett.* **2003**, *3*, 731. **DOI:** 10.1021/nl034154z
7. Hata, K.; Futaba, D.N.; Mizuno, K.; Namai, T.; Yumura, M.; Iijima, S., *Science* **2004**, *306*, 1362. **DOI:** 10.1126/science.1104962
8. Teblum, E.; Noked, M.; Grinblat, J.; Kremen, A.; Muallem, M.; Fleger, Y.; Tischler, Y.R.; Aurbach, D.; Nessim, G.D.; *J. Phys. Chem. C* **2014**, *118*(33), 19345. **DOI:** 10.1021/jp5015719
9. Park, K.H.; Lee, S.; Koh, K.H., *Diamond & Related Materials* **2005**, *14*, 2094. **DOI:** 10.1016/j.diamond.2005.06.013
10. Singh, M.K.; Singh, P.P.; Titus, E.; Misra, D.S.; LeNormand, F., *Chem. Phys. Lett.* **2002**, *354*, 331. **DOI:** 10.1016/S0009-2614(02)00133-1
11. Sung, W.Y.; Kim, W.J.; Lee, H.Y.; Kim, Y.H.; *Vacuum* **2008**, *82*, 551. **DOI:** 10.1016/j.vacuum.2007.07.051
12. Chen, W.; Fan, Z.; Gu, L.; Bao, X.; Wang, C., *Chem. Commun.* **2010**, *46*, 3905. **DOI:** 10.1039/C000517G
13. Kataura, H.; Kumazawa, Y.; Maniwa, Y.; Umezu, I.; Suzuke, S.; Ohtsuka, Y.; Achiba, Y., *Synthetic Metals* **1999**, *103*, 2555. **DOI:** 10.1016/S0379-6779(98)00278-1
14. Li, H.B.; Yu, M.H.; Wang, F.X.; Liu, P.; Liang, Y.; Xiao, J.; Wang, C.X.; Tong, Y.X.; Yang, G.W., *Nature Communications* **2013**, *4*, 1. **DOI:** 10.1038/ncomms2932

THAI JOURNAL OF PHYSICS, SERIES 10, (2014)

Facile growth of carbon nanotube by electroplated Ni catalyst

Visittapong Yordsri[1],Winadda Wongwiriyapan[1-3]*, Wirat Jarernboon[1-3] and Chanchana Thanachayanont[4]

[1]*College of Nanotechnology, King Mongkut's Institute of Technology Ladkrabang,Chalongkrung Rd., Lardkrabang, Bangkok 10520, Thailand*

[2]*Nanotec-KMITL Center of Excellence on Nanoelectronic Device, Chalongkrung Rd., Ladkrabang, Bangkok, 10520 Thailand*

[3]*Thailand Center of Excellence in Physics, CHE, Si Ayutthaya Rd., Bangkok, 10400, Thailand*

[4]*National Metal and Materials Technology Center, 114 Thailand Science Park, Paholyothin Rd., Klong 1, Klong Luang, Pathumthani 12120, Thailand*

A facile growth of carbon nanotube (CNT) by electroplated Ni as catalyst was proposed. Ni catalyst layers were deposited on Cu sheet by direct-current electroplating technique. Electroplated voltages were varied at 1.0, 1.5 and 2.0 V. CNTs were synthesized on electroplated Ni by chemical vapor deposition (CVD) using ethanol as carbon source. Atomic force microscopy (AFM), scanning electron microscopy (SEM), transmission electron microscopy (TEM) and Raman spectroscopy were utilized for characterization of electroplated Ni catalyst and synthesized CNTs. Electroplated Ni at 1.0, 1.5, 2.0 V had particle sizes of 78, 75 and 113 nm, respectively. CNTs with a uniform diameter of approximately 54 nm with graphene layers being parallel to CNT axis, corresponding to multi-wall CNTs, were obtained by using electroplated Ni at 1.5 V. Electroplated Ni at 1.0 V produced CNTs with graphitic layers making an angle to CNT axis, while electroplated Ni at 2.0 V produced curly CNTs with a wide diameter distribution. These results show that electroplated voltage directly affects morphology and structure of Ni layers and Ni catalyst with a smaller size and uniform diameter is a key for uniform CNT synthesis

Keywords: Electroplating, Carbon nanotube, Chemical vapor deposition

1. INTRODUCTION

Carbon nanotube (CNT) is well-known as the promising materials in recent nanotechnology due to its great mechanical property, electrical property and the large effective surface area. These useful properties make CNT be suitable material for many applications such as electronics devices, energy storage devices and sensors [1,2]. Many researches study on techniques for CNT synthesis. Arc discharge and laser ablation [3,4] are generally used for CNT synthesis but these techniques are time-consuming process and high cost. Chemical vapor deposition (CVD) technique is one of the main methods for CNT synthesis with advantages of simple, low cost and no need vacuum in process. For CNT synthesis by CVD technique, metal catalyst is an essential ingredient for CNT nucleation growth [5,6]. Normally, evaporation and sputtering techniques are utilized for catalyst film preparation. However, these techniques are time-consuming process and high cost. Recently, high density of multiwalled CNTs was synthesized on Ni electroplated Cu substrates by microwave plasma CVD [7]. K. H Park *et al*. also proposed growth of carbon nanofiber films with electroplated Ni catalyst using methane (CH_4) as carbon source [8]. In this study, a facile growth of CNT was proposed by using direct-current (DC) electroplating for Ni film preparation and CNTs was synthesized by CVD using ethanol as carbon source. Effect of electroplated voltage on morphology and structure of CNTs was investigated. It was found that electroplated voltage directly affect yield, purity, diameter distribution and graphitic layer structure of CNTs.

*Corresponding author. *E-mail*: kwwinadd@kmitl.ac.th

2. EXPERIMENT

For the preparation of the Ni catalyst layers, direct-current electroplating technique was used. A commercial Ni electroplating bath for jewelry coating was used as electrolyte in an electroplating process. Ni ingot and Cu sheet (Nilaco Corporation, Japan) was connected to the cathode and the anode of the circuit, respectively. The applied voltages were varied at 1.0, 1.5 and 2.0 V. Distance between both electrodes, temperature and time were fixed at 10 cm, 45ºC and 5 min, respectively. Morphology and grain size of the deposited Ni catalysts on Cu sheets were characterized by atomic force microscopy (AFM; SEIKO SPA400) technique.

Next, Ni catalyst-electroplated Cu sheet was set into a quartz tube reactor for chemical vapor deposition (CVD) process. Firstly, the quartz tube was filled with Ar gas at a flow rate of 500 sccm for 30 min to eliminate oxygen and air. Next, Ni catalyst-electroplated Cu sheet was heated to 800ºC and ethanol (AR grade, Labscan) was vaporized and switched into the quartz tube by Ar bubbling at a flow rate of 300 sccm for 20 min for CNT growth. The synthesized CNTs were cooled down to room temperature under Ar ambient before taken out from the quartz tube. Morphology, diameter and structure of graphitic layer, and crystallinity of the synthesized CNTs were characterized by scanning electron microscopy (SEM; Hitachi S-3400N),

transmission electron microscopy (TEM; JEOL JEM-2010) and Raman spectroscopy (Thermal Scientific; DXR™ SmartRaman Spectrometer), respectively.

3. RESULTS AND DISCUSSIONS

Figs. 1(a)-1(c) show AFM images of the Ni catalyst layer on Cu sheets obtained from electroplated voltages of 1.0, 1.5 and 2.0 V, respectively. Ni nanoparticles were formed by all electroplated voltages. The average particle sizes formed at electroplated voltages of 1.0, 1.5 and 2.0 V were approximately 78±3 nm, 75±16 nm and 113±10 nm, respectively. Thus, under the controlled electroplating condition, Ni nanoparticles with controllable size for use as catalyst in CNT synthesis can be formed.

After CVD process, Cu sheet surface was wholly covered with a black powder by visual. The detailed morphology was observed by SEM. Figs. 2(a)-2(c) show SEM images of CNTs synthesized from electroplated voltages of 1.0, 1.5 and 2.0 V, respectively. Tubular structures were observed for all electroplated voltages but morphologies and structures were different. For electroplated voltages of 1.0 and 1.5 V, synthesized CNTs were straight with high aspect ratio while CNTs synthesized from electroplated voltage of 2.0 V were curly and agglomerated in cluster.

For TEM characterization, typically, magnification in a range of X20000 to X500000 was used for observation. The higher resolution in TEM images could precisely identify the graphitic layers of CNTs synthesized from different electroplated voltages. Figs. 3(a)-3(c) show TEM images of CNTs synthesized from electroplated voltages of 1.0, 1.5 and 2.0 V, respectively. Insets are TEM images of graphitic layer at high resolution. At electroplated voltages of 1.0 V and 1.5 V, the CNTs were in the same tubular shape with the diameter range of approximately 36 nm and 54 nm, respectively, at low resolution. However, at high resolution, it was found that their graphitic layers were completely different. Inset of Fig. 3(a) shows that graphitic layers of the CNTs were angle to the tube axis wall for electroplated voltage of 1.0 V, while inset of Fig. 3(b) shows clearly that graphitic layers of the CNTs were parallel to the tube axis. At electroplated voltage of 2.0 V, the structures of the synthesized resultants were completely different from those of 1.0 and 1.5 V. The resultants were largely curly with Ni catalyst inside with wide tube diameter distribution (Fig.3(c)).

Next, the synthesized CNTs were characterized by Raman spectroscopy. Generally, in carbon materials characterization, Raman spectra can identify the existence of graphitic carbon (*G*-band) and disordered carbon (*D*-band). Fig. 4 shows the Raman spectra of CNTs obtained from different electroplated voltages of (a) 1.0 V, (b) 1.5 V and (c) 2.0 V. The excited light was Ar ion laser with a wavelength of 532 nm (2.33 eV) Two sharp peaks at Raman shift of approximately 1350 cm^{-1} (*D*-band) and 1590 cm^{-1} (*G*-band) were observed from all samples. The ratio of *G*-band and D-band (I_G/I_D) can be used to evaluate the crystallinity of the CNTs. A higher I_G/I_D ratio indicates a higher degree of structural ordering and purity of the CNTs [9]. It was found that I_G/I_D of the CNTs obtained from the electroplated voltage of 1.0, 1.5 and 2.0V were 0.53, 1.77 and 1.06, respectively. The CNTs obtained from electroplated voltage of 1.5V had the highest I_G/I_D. These results correspond to the SEM and TEM results, showing that the CNTs obtained from electroplated voltage of 1.5 V were relatively higher purity and/or had lower defects

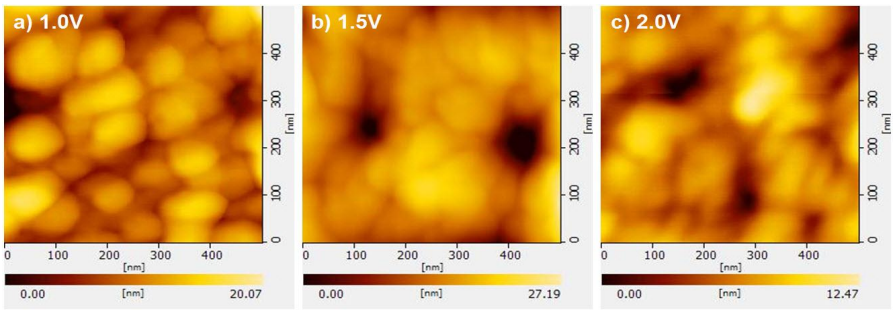

FIGURE 1. AFM images of Ni catalyst layer formed at electroplated voltages of (a) 1.0 V, (b) 1.5 V and (c) 2.0 V.

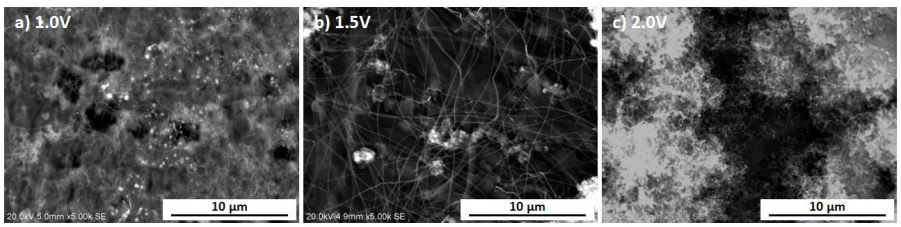

FIGURE 2. SEM images of CNTs obtained from different electroplated voltages of (a) 1.0 V, (b) 1.5 V and (c) 2.0 V.

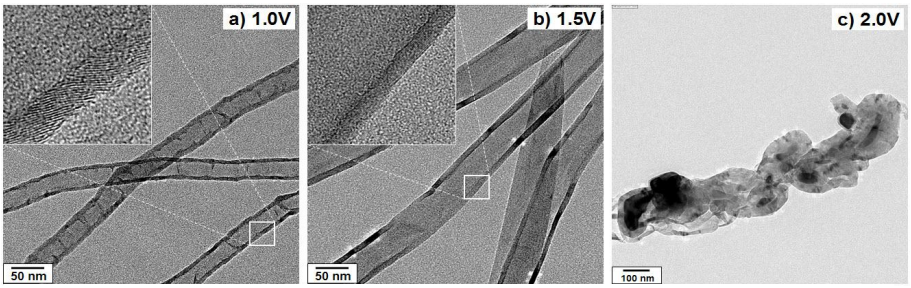

FIGURE 3. TEM micrographs with additional high resolution of CNTs obtained from different electroplated voltages of (a) 1.0 V, (b) 1.5 V and (c) 2.0 V.

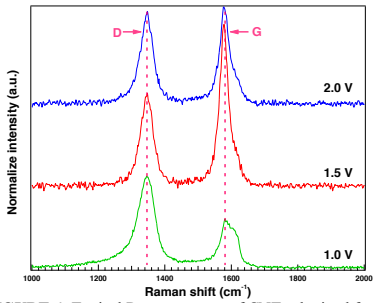

FIGURE 4. Typical Raman spectra of CNTs obtained from different electroplated voltages of (a) 1.0 V, (b) 1.5 V and (c) 2.0 V.

inside the parallel graphitic layers. These results show that electroplated voltage directly affects morphology and structure of Ni layers and Ni catalyst with a smaller size and uniform diameter is a key for uniform CNT synthesis

4. CONCLUSION

Novel synthesis of CNTs with simple and low cost method was proposed by the use of controllable electroplated Ni as catalyst and the use of ethanol as carbon source during CVD process. The electroplated voltages for Ni catalyst formation directly affect the morphology and structure of CNTs. The graphitic layers of CNTs can be selectively parallel or angle to the tube axis with a narrow tube diameter distribution of 54 nm. By the different CNTs structures obtained by controllable Ni catalyst, it could lead to further research with the mechanical property and electrical conductivity characterization in order to optimum suitable properties for devices and applications.

ACKNOWLEDGMENTS

This work is financially supported by the Thailand Research Fund (DBG5580005), the National Nanotechnology Center (NANOTEC), NSTDA, Ministry of Science and Technology, Thailand, through its program of Center of Excellence Network and the Thailand Center of Excellence in Physics (ThEP). We acknowledge facility support from National Metal and Materials Technology Center (MTEC).

1. Steve, P., Michael, V., Zhenan, Bao., A review of fabrication and applications of carbon nanotube film-based flexible electronics, Nanoscale, Issue 5. 2013
2. Yu, J., Hongyuan, C., Minghai, C., et al., Graphene-patched CNT/MnO2 nanocomposite papers for the electrode of high-performance flexible asymmetric supercapacitors, Applied Materials & Interfaces, Vol. 5, pp. 3408-3416. 2013
3. Ando, Y., Zhao, X., Hataura, H., et. al., Multiwalled carbon nanotubes prepared by hydrogen arc, Diamond and Related Materials, Vol. 9, pp. 847-851. 2000
4. Shiang-Kuo, C., Jeng-Rong, H., John, C., Fabrication of transparent double-walled carbon nanotubes flexible matrix touch panel by laser alation technique, Optics & Laser Technology, Vol. 43, pp. 1371-1376. 2011
5. Lee, C.J., Park, J., Yu, J.A., Catalyst effect on carbon nanotubes synthesized by thermal chemical vapor deposition, Chemical Physics Letters, vol. 360, pp. 250-255. 2002
6. Worawut, M., Supanit, P., Winadda, W., Effect of Metal Catalysts on Synthesis of Carbon Nanomaterials by Alcohol Catalytic Chemical Vapor Deposition, Engineering Journal, Vol. 17, Issue 5, pp. 35-39. 2013
7. Singh, M.K., Singh, P.P., Titus, E., et al., High density of multiwalled carbon nanotubes observed on nickel electroplated copper substrates by microwave plasma chemical vapor deposition, Chemical Physics Letters, Vol. 354, pp. 331-336. 2002
8. Kyung, H.P., Soonil, L., Ken, H.K., Growth and high current field emission of carbon nanofiber films with electroplated Ni catalyst, Diamond & Related Materials, Vol. 14, pp. 2094-2098. 2005
9. Kataura, H., Kumazawa, Y., Maniwa, Y., et al., Optical properties of single-wall carbon nanotubes, Synthetic Metals, Vol. 103, pp. 2555-2558. 1999

การสังเคราะห์ท่อนาโนคาร์บอนจากตัวเร่งปฏิกิริยาโลหะนิเกิลที่เตรียมด้วยวิธีการเคลือบด้วยไฟฟ้าและการใช้งานด้านตัวเก็บประจุยิ่งยวด

SYNTHESIS OF CARBON NANOTUBES BY ELECTROPLATED NICKEL CATALYST AND ITS SUPERCAPACITOR APPLICATION

วิศิษฏพงศ์ ยอดศรี
VISITTAPONG YORDSRI

วิทยานิพนธ์นี้เป็นส่วนหนึ่งของการศึกษาตามหลักสูตรปริญญาวิทยาศาสตรมหาบัณฑิต
สาขาวิชานาโนวิทยาและนาโนเทคโนโลยี
วิทยาลัยนาโนเทคโนโลยีพระจอมเกล้าลาดกระบัง
สถาบันเทคโนโลยีพระจอมเกล้าเจ้าคุณทหารลาดกระบัง
พ.ศ. 2559
KMITL-2016-NT-M-001-002

SYNTHESIS OF CARBON NANOTUBES BY ELECTROPLATED NICKEL CATALYST AND ITS SUPERCAPACITOR APPLICATION

VISITTAPONG YORDSRI

A THESIS SUBMITTED IN PARTIAL FULFILLMENT
OF THE REQUIREMENT FOR THE DEGREE OF
MASTER OF SCIENCE IN NANOSCIENCE AND NANOTECHNOLOGY
COLLEGE OF NANOTECHNOLOGY
KINGMONGKUT'S INSTITUTE OF TECHNOLOGY LADKRABANT
2016
KMITL-2016-NT-M-001-002

หัวข้อวิทยานิพนธ์	การสังเคราะห์ท่อนาโนคาร์บอนจากตัวเร่งปฏิกิริยาโลหะนิกเกิลที่เตรียม ด้วยวิธีการเคลือบด้วยไฟฟ้าและการใช้งานด้านตัวเก็บประจุยิ่งยวด
นักศึกษา	นายวิศิษฏพงศ์ ยอดศรี
รหัสประจำตัว	56607003
ปริญญา	วิทยาศาสตรมหาบัณฑิต
สาขาวิชา	นาโนวิทยาและนาโนเทคโนโลยี
พ.ศ.	2559
อาจารย์ที่ปรึกษาวิทยานิพนธ์	ผศ.ดร.วินัดดา วงศ์วิริยะพันธ์
อาจารย์ที่ปรึกษาวิทยานิพนธ์ร่วม	ดร.ชัญชณา ธนชยานนท์

บทคัดย่อ

การวิจัยนี้ได้ศึกษาการสังเคราะห์ท่อนาโนคาร์บอนอย่างง่ายบนแผ่นทองแดงด้วยเทคนิคการเคลือบผิวด้วยไอเคมีเพื่อนำไปประยุกต์ใช้งานด้านอุปกรณ์กักเก็บพลังงานโดยเป็นขั้วของตัวเก็บประจุยิ่งยวด ในกระบวนการเคลือบผิวด้วยไอเคมี โลหะคะตะลิสต์เป็นส่วนประกอบที่สำคัญสำหรับการสังเคราะห์ท่อนาโนคาร์บอน ในงานวิจัยนี้จึงเลือกใช้นิกเกิลเป็นคะตะลิสต์ อนุภาคนาโนของนิกเกิลถูกปลูกลงบนแผ่นทองแดง ด้วยวิธีการเคลือบผิวด้วยไฟฟ้ากระแสตรง เนื่องด้วยเป็นกระบวนการที่ง่าย ค่าใช้จ่ายน้อย ทำได้อย่างรวดเร็ว สามารถเลือกพื้นที่สำหรับการปลูกได้ และไม่ต้องใช้ระบบสุญญากาศ โดยในงานวิจัยได้ศึกษาผลของแรงดันไฟฟ้าต่อสัณฐานวิทยาของคะตะลิสต์ และโครงสร้างของท่อนาโนคาร์บอน ในขั้นตอนการปลูกคะตะลิสต์กำหนดให้แรงดันไฟฟ้าที่จ่ายในระบบการเคลือบผิวด้วยไฟฟ้ากระแสตรงมีค่า 1.0, 1.5 และ 2.0 โวลต์ โดยตัวแปรอื่นมีค่าคงที่ได้แก่ อุณหภูมิ 45 องศาเซลเซียส ระยะห่างระหว่างขั้ว 100 มิลลิเมตร และเวลาในการปลูก 5 นาที สำหรับกระบวนการสังเคราะห์ท่อนาโนคาร์บอนด้วยเทคนิคการเคลือบผิวด้วยไอเคมี สังเคราะห์ในเตาท่อที่อุณหภูมิ 800 องศาเซลเซียสเป็นเวลา 20 นาที และใช้เอทานอลเป็นแหล่งกำเนินคาร์บอน ทำการวิเคราะห์ลักษณะทางด้านสัณฐานวิทยาของอนุภาคนาโนนิกเกิลด้วยเทคนิคกล้องจุลทรรศน์แรงอะตอม ทำการวิเคราะห์ลักษณะทางด้านสัณฐานวิทยาและลักษณะโครงสร้างของชั้นกราไฟต์ของท่อนาโนคาร์บอนด้วยเทคนิคกล้องจุลทรรศน์อิเล็กตรอนแบบส่องกราด กล้องจุลทรรศน์อิเล็กตรอนแบบส่องผ่าน และรามานสเปกโทรสโกปี นอกจากนี้ท่อนาโนคาร์บอนที่สังเคราะห์ลงบนแผ่นทองแดงที่เคลือบด้วยอนุภาคนาโนนิกเกิล ถูกนำไปประยุกต์ใช้เป็นขั้วสำหรับตัวเก็บประจุยิ่งยวด โดยทำการทดสอบสมบัติทางไฟฟ้าเคมีด้วยเทคนิคไซคลิกโวลแทมเมทรีและกัลวานอสแตติกชาร์จดิสชาร์จ จากผลการวิจัย พบว่าเงื่อนไขแรงดันไฟฟ้า 1.5 โวลต์เป็นเงื่อนไขที่ดีที่สุด คือได้ขนาดอนุภาคนาโนนิกเกิลเฉลี่ยประมาณ 55$\pm$3 นาโนเมตร และได้ท่อนาโนคาร์บอนที่มีผนังท่อซึ่งเป็นชั้นของกราไฟต์ขนานกับแนวแกนยาวของท่อนาโนคาร์บอน ในขณะที่เงื่อนไขแรงดันไฟฟ้าที่ 1.0 โวลต์ เกิดท่อนาโนคาร์บอนที่มีผนังท่อทำมุมทแยงกับแนวแกนยาวของท่อนาโนคาร์บอน ส่วนในเงื่อนไขแรงดันไฟฟ้าที่ 2.0 โวลต์ สิ่งที่ได้คือท่อนาโนคาร์บอนที่เป็นเกลียวใหญ่และมีขนาดไม่คงที่ จากผลวิจัยดังกล่าวชี้ให้เห็นว่า เงื่อนไขแรงดันไฟฟ้าที่จ่ายในระบบการเคลือบผิวด้วยกระแสไฟฟ้ากระแสตรงมีผลโดยตรงกับขนาดและการกระจายตัวของขนาดของอนุภาคนาโนนิกเกิล โดยอนุภาคนาโนนิกเกิลที่มี

ขนาดเล็กและมีการกระจายตัวของขนาดที่แคบเป็นปัจจัยสำคัญสำหรับการสังเคราะห์ท่อนาโนคาร์บอนที่มีลักษณะคงที่ นอกจากนี้ จากการวิเคราะห์สมบัติทางไฟฟ้าเคมีพบว่า ขั้วท่อนาโนคาร์บอนที่สังเคราะห์ได้ มีสมบัติทางด้านการเก็บประจุด้วยค่าสัมประสิทธ์การเก็บประจุที่ 53 ฟารัดต่อกรัม จากผลการวิจัยเบื้องต้นนี้แสดงให้เห็นว่าสามารถสังเคราะห์ท่อนาโนคาร์บอนอย่างง่ายโดยใช้อนุภาคนาโนนิกเกิลที่เตรียมด้วยเทคนิคการเคลือบด้วยไฟฟ้ากระแสตรง และสามารถพัฒนาสมบัติทางไฟฟ้าเคมีของขั้วท่อนาโนคาร์บอนได้ด้วยการศึกษาเงื่อนไขโครงสร้างของอนุภาคนาโนนิกเกิลและท่อนาโนคาร์บอนที่เหมาะสมที่สุด

คำสำคัญ : การเคลือบด้วยไฟฟ้ากระแสตรง ท่อนาโนคาร์บอน การเคลือบผิวด้วยไอเคมี ซุปเปอร์คาปาซิเตอร์

Thesis Title	Synthesis of Carbon Nanotubes by Electroplated Metal Catalyst and its Supercapacitor Application
Student	Mr. Visittapong Yordsri
Student ID	56607003
Degree	Master of Science
Program	Nanoscience and Nanotechnology
Year	2016
Thesis advisor	Assit. Prof. Dr. Winadda Wongwiriyapan
Thesis Co-advisor	Dr. Chanchana Thanachayanont

ABSTRACT

This research studies facile synthesis of carbon nanotube (CNT) on copper sheets by chemical vapor deposition (CVD) and its energy storage application as an electrode in supercapacitor. In CVD process, metal catalyst is an essential ingredient in the synthesis of CNT. In this work, nickel (Ni) was chosen as a catalyst. Ni nanoparticles were deposited on the copper sheet by the direct current (DC) electroplating technique. The DC electroplating is simple to set up, low cost, fast, can deposit to a selected area and does not need vacuum system. The effects of DC-electroplating voltage on the morphology and structure of the CNTs was investigated. The applied voltage was varied from 1.0, 1.5 to 2.0 V, while the electroplating temperature, time and distance between electrodes were fixed at 45°C, 5 min and 100 mm, respectively. The CNTs synthesis by CVD was carried out in the tube furnace at 800 °C using ethanol as carbon source for 20 min. The morphology of the electroplated Ni was characterized by atomic force microscopy (AFM). The morphology, diameter and structure of the graphitic layer, and the crystallinity of the synthesized CNTs were characterized by field emission scanning electron microscopy (FESEM), transmission electron microscopy (TEM) and Raman spectroscopy, respectively. Furthermore, the CNTs synthesized on Ni-electroplated Cu sheet was used as a supercapacitor electrode. The electrochemical measurements were carried out in a three-electrode setup connected to an electrochemical work station. Electrochemical properties were characterized by cyclic voltammetry (CV) and galvanostatic charge/discharge (CD) technique. The results show that at the applied voltage of 1.5 V, Ni nanoparticles with a narrow distribution of sizes were formed with an average size of 55±3 nm, which in turn, yielded synthesized CNTs with a uniform diameter of approximately 60±5 nm with graphitic layers parallel to the CNTs axis. On the other hand, the electroplated Ni at 1.0 V produced CNTs with graphitic layers with an angle to the CNTs axis, while the

electroplated Ni at 2.0 V produced curly CNTs with a wide diameters distribution. These results show that the Ni nanoparticle size distribution could be controlled by electroplated voltage. Our observation was that the Ni nanoparticles with a narrow distribution of sizes and a uniform diameter was a key for uniform CNTs synthesis. The synthesized CNTs showed a specific capacitance of 53 $F.g^{-1}$. All these results signified that facile growth of CNTs by Ni NPs catalyst, deposited using DC electroplating method was fully achieved. Further optimization of structures of Ni catalyst and CNTs should improve the supercapacitor performance.

Keywords : Electroplating, Carbon nanotube**,** Chemical vapor deposition, Supercapacitor

ACKNOWLEDGEMENTS

First, I would like to express my deep and sincere gratitude to my advisor, Asst. Prof. Dr. Winadda Wongwiriyapan (College of Nanotechnology, King Mongkut's Institute of Technology Ladkrabang, KMITL) and co-advisor, Dr. Chanchana Thanachayanont (National Metal and Materials Technology Center, MTEC) for their encouragement, helpful suggestions, remarkable patience, and kind support.

I am deeply grateful to Asst. Prof. Dr. Benchapol Tunhoo, Asst. Prof. Dr. Apiluck Eiad-ua, Dr. Mayuree Phonyium (College of Nanotechnology, KMITL), Dr. Supanit Porntheeraphat (National Electronics and Computer Technology Center, NECTEC) and Prof. Dr. Supapan Seraphin (The University of Arizona) for their comments and suggestions on this dissertation.

Finally, I would like to thank all the colleagues and friends, especially those who are the members of Nanocarbon Materials Research Laboratory, College of Nanotechnology, KMITL for their supports and kindnesses.

Visittapong Yordsri

CONTENTS

CONTENTS (Cont.)

LIST OF FIGURES

Page

LIST OF FIGURES (Cont.)

Page

LIST OF TABLES

Page

CHAPTER 1
INTRODUCTION

1.1 Background and Problem

Carbon nanotube (CNTs) is one of the most promising materials in nanotechnology due to its great properties such as large effective surface area, excellent mechanical properties and electrical properties. In recent researches, CNTs show many great potentials for improving the performance of electronics devices, energy storage devices and sensors. For future application, the method of synthesis with a large-scale production and a simple synthesis method is very important. Chemical vapor deposition (CVD) is one of the presently available methods that matched for CNTs synthesis requirement. Metal catalyst is an essential ingredient for the CVD process. As for catalyst preparation, evaporation and sputtering techniques are normally utilized, but these techniques are time-consuming, high cost with vacuum system and limited in size. For practical application, the simple catalyst preparation is absolutely required. Electroplating, a proposed technique for such catalyst preparation, is simple to set up, low cost, fast and does not need vacuum.

In this study, facile growth of CNTs was made possible by using direct-current (DC) electroplating for Ni nanoparticles (NPs) catalyst preparation; with the Ni-deposited catalyst, CNTs was synthesized by using CVD with ethanol vapor as carbon source. The effects of DC-electroplating voltage on the morphology and structure of the CNTs were investigated. Furthermore, for demonstration of a potential application, supercapacitors based on the synthesized CNTs were fabricated and their electrochemical properties were determined.

1.2 Objectives of the study

1.2.1 To fabricate Ni nanoparticles by direct-current electroplating technique for CNTs synthesis.

1.2.2 To optimize the synthesis of CNTs by chemical vapor deposition technique using electroplated Ni nanoparticles as catalyst.

1.2.3 To demonstrate the potential application of the synthesized CNTs as supercapacitor.

1.3 Scope of the study

1.3.1 Deposition of Ni nanoparticles on the substrate by electroplating technique and characterization by atomic force microscopy and X-ray photoelectron spectroscopy.

1.3.2 Synthesis of CNTs by CVD and characterization by scanning electron microscopy, transmission electron microscopy and Raman spectroscopy.

1.3.3 Characterization the electrochemical properties of the synthesized CNTs (such as cyclic voltammetry and galvanostatic charge-discharge).

1.4 Expected Results

1.4.1 Deposition of the Ni nanoparticle on the substrate with a narrow size distribution by electroplating technique.

1.4.2 Growth of CNTs from the electroplated Ni nanoparticle with a uniform size and high quality.

1.4.3 Demonstration of the CNTs electrode as supercapacitor.

CHAPTER 2
THEORETICAL BACKGROUND

2.1 Carbon nanotube

Normally, the sp^2 hybridization of carbon is the basis for the well-known graphite structure. Besides this, carbon can form other structures, such as the closed cages with honeycomb carbon arrangement, C_{60}, which was discovered by H.R. Kroto *et al*. in 1985 [1]. From this, various structures of carbon cages were discovered. In 1991, Iijima first observed the tubular carbon structure as "a new type of finite carbon structure consisting of needle-like tubes" [2]. The observed carbon structure consists of few graphitic shells with the spacing between shell of 0.34 nm. Two years later (1993), Iijima and Ichihashi [3] and Bethune *et al*. [4] achieved the synthesis of single-wall carbon nanotube (SWNT).

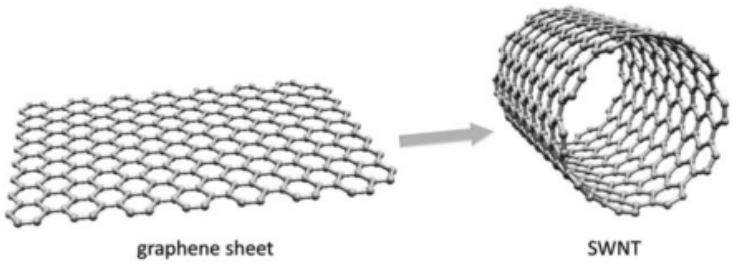

Figure 2.1 Wrapping of graphene sheet to form SWCNT [5].

Structurally, SWCNT can be compared to ''rolled up'' one- atom-thick sheets of graphite called graphene as shown in Figure 2.1. The way the graphene is wrapped along the honeycomb graphene structure is given by chiral vector *C* which is a result of a pair *(n,m)* of integers that corresponds to graphene vectors a_1 and a_2. The principle of SWNT construction from a graphene sheet along the chiral vector *C* is shown in Figure 2.2. There are two standard types of SWNT constructions from a single graphene sheet according to integers *(n,m)*. The *(n,0)* structure is called ''zigzag'' and the structure where *n=m (n,n)* is called ''armchair''. The third non-standard type of CNTs construction, which can be characterized by the equation where $n > m > 0$, is called ''chiral'' [5]. These different structures lead to the different properties of SWNT such as metallic or semiconducting [6].

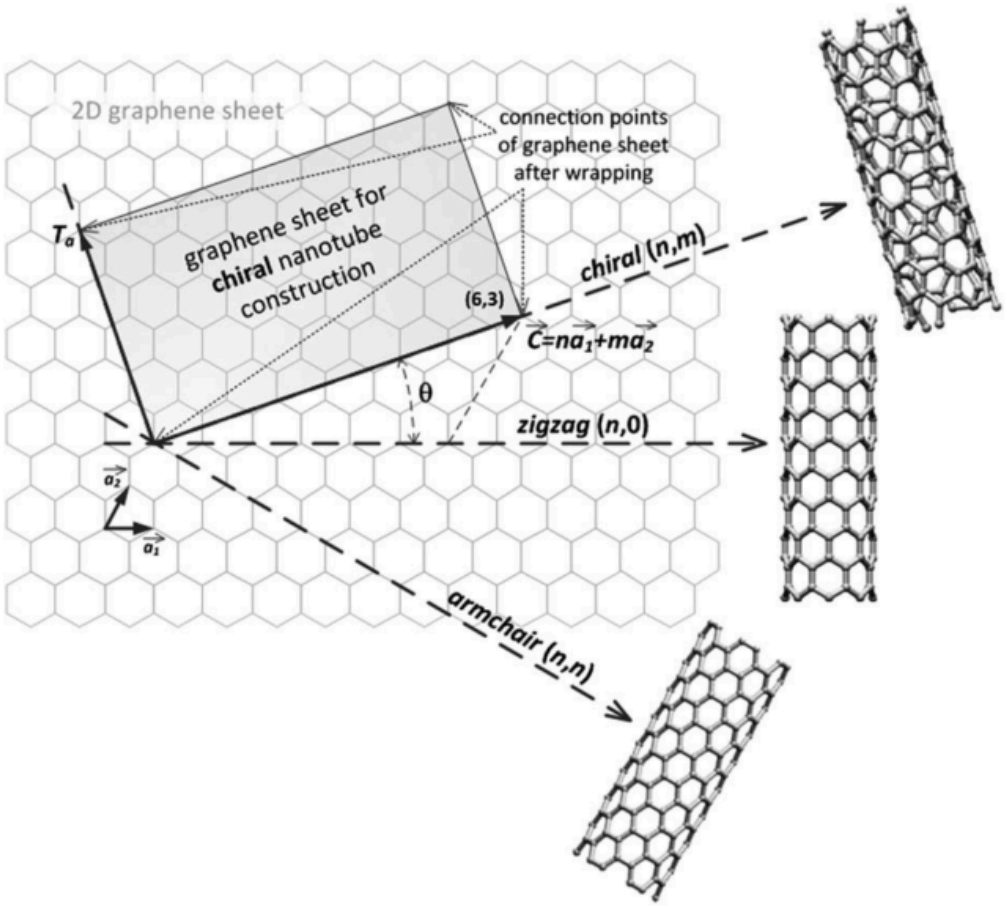

Figure 2.2 The principle of CNTs construction from graphene sheet along the chiral vector C [6].

CNTs can be either SWNT, the only one layer of graphene layer roll into tube structure, or multi-wall carbon nanotube (MWNT), the tubular that consists of many layers of graphene with the layer spacing of around 0.34 nm. For the MWNT, it can be few layers or more up to 100 layers.

CNTs have great properties with high surface area per unit weight, good mechanical properties (100 times stronger than steel, but 6 times lighter), high electrical conductivity, high thermal conductivity. Their unique properties are suitable for utilizing in composite materials for improvement of mechanical-properties and as additives to various structural materials. Some of the extraordinary properties of CNTs are shown in Table 2.1.

Table 2.1 The extra ordinary properties of CNTs.

	SWCNT	MWCNT
High surface area per unit weight	very broad scale from 50 - 1315 $m^2.g^{-1}$	10 - 500 $m^2.g^{-1}$
Good mechanical properties :		
Young's modulus	~ 1 TPa	~ 1.2 TPa
Tensile strength	~ 60 GPa (ropes)	~ 0.15 TPa
Thermal properties @ room temperature*	~ 1750-5800 $W.m^{-1}.K^{-1}$	> 3000 $W.m^{-1}.K^{-1}$
Electrical properties		
Typical resistivity	~ 10^{-4} ohm.cm	n/a
Typical current density	10^7-10^9 $A.cm^{-2}$	n/a
Electronic properties	• Metallic (bandgap=0 eV) if (n-m) is divisible by 3 • Semiconducting (bndgap=0.4-2 eV) if (n-m) is not divisible by 3	Non-semiconducting (bandgap ~0 eV)

2.2 Synthesis of carbon nanotube

Generally, MWNT and SWNT are normally produced by three main techniques, arc-discharge technique, laser-ablation technique and chemical vapor deposition (CVD).

2.2.1 Arc-discharge

Arc-discharge is a technique that normally used for synthesis of carbon fibers and fullerenes. However, Iijima used this technique to synthesize the MWNT in 1991 [2] and also SWCNTs [3] in 1993. For arc-discharge technique, a direct-current arc voltage is applied across two high-purity graphite electrodes as anode and cathode. The electrodes are vaporized by the direct-current through the separation of two graphite electrodes with around 1-2 mm in 400 mbar of helium atmosphere. The schematic experimental setup of arc-discharge is shown in

Figure **2.3**. From the process, if the anode and cathode are pure graphite, MWNTs are deposited on the cathode side. In the case of the graphite containing a metal catalyst (such as Fe, Co, Ni, Y or Mo), the SWNT can be produced either on anode or cathode side. The quality and quantity of CNTs such as lengths, diameters, purity are dependent on varied parameters and conditions such as inert gas pressure, gas type, current, system geometry, and metal concentration.

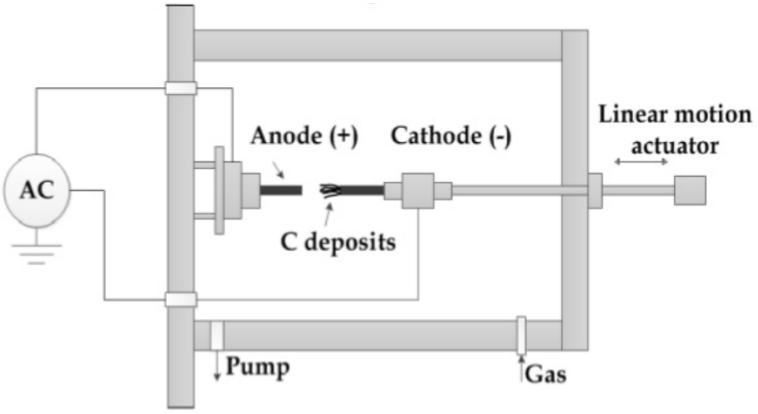

Figure 2.3 The schematic of arc-discharge technique [7].

Transmission electron microscopy (TEM) study of carbon nanotube morphology grown by arc-discharge revealed that there were many varieties in shape especially near the tube tips. Ebbesen and Ajayan [8] reported the large-scale synthesis of MWNTs by variant of standard arc-discharge technique. Two thin graphite rods were used and applied with direct-current potential of 18 V in helium atmosphere. With helium pressure at 500 Torr, the nanotubes give the maximum yield up to 75% relative to the starting graphitic material. The characterization by TEM revealed that the sample consisted of nanotubes with two or more carbon shells. The tube diameters are between 2 and 20 nm with length of several micrometers. The tube tips were capped with a combination of hexagons and pentagons.

In 1993, Iijima and Ichihashi [3] and Bethune *et al*. [4] almost simultaneously reported about arc-discharge and the SWNTs synthesis with catalyst-assisted process. Iijima used arc-discharge chamber filled with mixed gas of 10 Torr of methane and 40 Torr of argon. Two vertical thin electrodes were placed at the center of chamber. The lower electrode, cathode, had the thin layer of iron. The arc-discharge condition is running by a direct-current of 200 A at 20 V across both electrodes. The component of argon, iron and methane were the main critical parameters for SWNTs synthesis. The nanotubes obtained were curved and tangled into bundles with each tube having diameters of 1 nm and quite broad distribution from 0.7 to 1.65 nm. Bethune *et al*. reported the used of thin electrodes as anode with bored holes which were filled with mixture of pure powdered metals (Fe, Ni or Co) and graphite. The electrodes were vaporized in arc-discharge with a current of 95-105 A in 100-500 Torr of helium atmosphere. The TEM characterization showed that only cobalt metal catalyst can yield the nanotubes with single atomic layer walls with uniform diameter of 1.2 ± 0.1 nm.

Large scale synthesis of SWNTs by arc-discharge was reported by Journet *et al*. [9]. The two graphite electrodes were used with 600 mbar of helium atmosphere. The anode had a hole drilled at the end which was filled with a mixture of metallic catalyst (such as Ni-Co, Co-Y or Ni-Y) and graphite powder. The arc-discharge was processed by a current of 100 A and a constant voltage of 30 V. From scanning electron microscopy (SEM), the obtained product consists of a large amount (80%) of entangled carbon ropes. The high-resolution TEM images indicated that the ropes obtained had diameters from 5 to 20 nm and each rope consisted of bundle of tubes. Each tube diameters were around 1.4 with the separation of 1.7 nm. The spectra from X-ray diffraction (XRD) showed the period arrangement of tubes in the ropes. This pattern of XRD spectra of Journet et al. [9] is similar to the XRD data report from Thess *et al.* [10] (using laser-ablation technique) that obtained in 70-90% yield and tube diameter around 1.4 nm. The nanotubes also form into bundle of a few tens of nanotubes. Both reports lead to the nanotubes growth mechanism that does not depend on the method conditions. It depends much more on the kinetics of carbon condensation in a non-equilibrium situation. Furthermore, between the two methods, the arc-discharge technique is much cheaper than the laser-ablation technique.

2.2.2 Laser-ablation

Laser-ablation is a technique that the laser is focused on the graphite target under high temperature with argon atmosphere (around 500 Torr). The carbon that was vaporized by laser will be flowed with argon gas carrier to the outer heating zone and form CNTs at the collector (cooler zone behind heating zone), Figure 2.4. In case of SWNTs synthesis, the graphite target contained with metal particles is needed. The CNTs produced by laser-ablation technique are much more purified and have smaller size distribution than the previous technique, i.e. the arc-discharge technique.

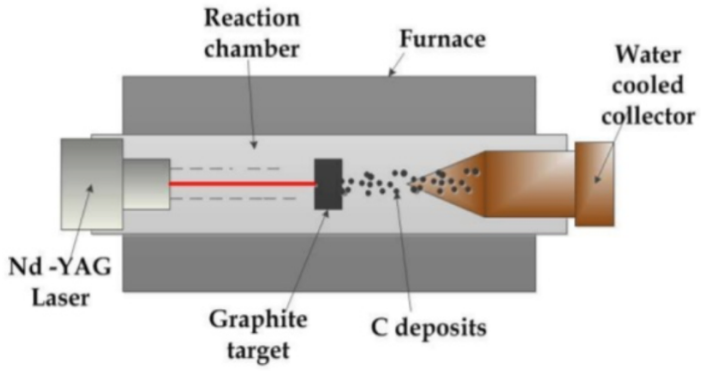

Figure 2.4 The schematic of Laser-ablation technique [7].

Smalley *et al.* (1996) reported the high yield (>70%) production of SWNTs using laser-ablation technique by vaporizing the graphite rods that contained small amounts of Ni and Co at 1200 °C [10]. By TEM and XRD characterization, the obtained SWNTs were uniform in diameters and formed as bundles with micrometer length. The bundles show the triangular lattice with a lattice constant, a = 1.7 nm (van der Waals bonding). The nanotubes represent as metallic structure with a main tube *(10,10)* structure. Therefore, both MWNTs and SWNTs can be obtained by this technique. The metal particles added in the graphite rod as catalysts were important factor for SWNTs forming.

2.2.3 Chemical vapor deposition

Chemical vapor deposition (CVD) is the technique that is widely used for CNTs synthesis, due to its advantage above the others that have less complicate setup, low cost due to do not need vacuum, variety of carbon source and can scale up for mass production.

For CVD process, catalyst is an essential parameter for CNTs growth. The substrates with catalyst deposited have been placed in the reactor that is heated up to 600 – 1000 °C and the hydrocarbon source is supplied to react in a reaction over surface of catalyst for 15-60 min. Then, CNTs grown on catalyst in reactor are collected after cooling the system to room temperature, Figure 2.5.

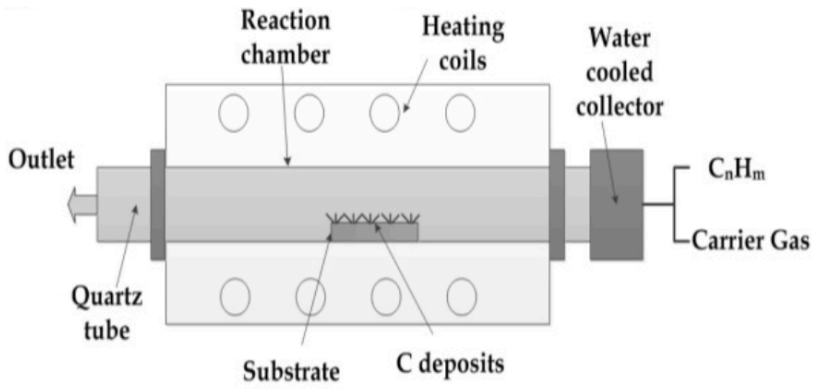

Figure 2.5 The schematic of chemical vapor deposition [7].

Carbon fibers and filaments have been produced by chemical vapor deposition, CVD, technique using the hydrocarbon source with catalyst added since 1960. Yacaman *et al*. (1993) [11] and Ivanov *et al* (1994) [12,13] were the first group that reported the growth of MWNTs by CVD technique. The CVD technique normally used with the catalyst-assisted for carbon nanotube forming and has been improved and optimized. Generally, ethylene or acetylene were used for the carbon source in a

tube reactor at temperature around 550 to 750 °C. The catalyst used for CNTs is metal. The best results obtained for catalyst chosen are Fe, Ni or Co nanoparticles. These are the same optimal catalysts with the previous arc-discharge and laser-ablation techniques, implying the common nanotube growth mechanism.

Li *et al*. [14] reported the large-scale synthesis of aligned CNTs by CVD technique. The mesoporous silica with iron nanoparticles catalyst was used as substrate. The carbon source was mixture of 9% acetylene in nitrogen gas that flown into the reactor with 110 cm^3/min flow rate. The carbon atoms from acetylene that decomposed at 700˚C were formed on the substrate as the carbon nanotube. SEM and the energy-dispersive X-ray spectroscopy (EDX) used for the obtained CNTs characterization. The SEM image showed that the nanotubes continuously grew from bottom to the top as thin film with length of around 50 to 100 mm. The nanotubes structure was multi-wall that had the diameters around 30 nm (40 shells) and formed arrays with each tube spacing of around 100 nm, equal to the spacing of pores on mesoporous silica substrate.

For the average yield of SWNTs, both arc-discharge and laser-ablation technique can be more than 70% yields. But the big disadvantage of these techniques are the carbon solid source temperature that needs to be high up to 3000 °C and the nanotubes structure that usually form in tangle. The tangled CNTs obtained is difficult in purification and the applications. In the other hand, CVD is the technique that the CNTs obtained can be controlled by the catalyst with additional low cost and high yield. Table 2.2 below shows the comparison of CVD with other synthesis techniques.

Table 2.2 Comparison of CVD with other popular CNTs synthesis techniques [6].

Parameter	Chemical vapor deposition	Arc discharge	Lase ablation
Process	Place substrate in oven, heat to high temperature, and slowly add a carbon source. A decomposed source frees up carbon atoms, which recombine in the form of CNTs	Connect two graphite rods to a power supply, place them a few millimeters apart. At 100 amps, carbon vaporizes and forms hot Plasma	Blast graphite with intense laser pulses; use laser pulses rather than electricity to generate carbon gas from which the CNTs form, try various conditions until hit on one that produces amounts of SWNTs
Condition	Low-pressure inert gas (argon)	Argon or nitrogen gas at 500 Torr	High temperatures within 500-1000 C at atmospheric pressure
Yield	High	Low	Low
Operating temperature	500-1200	~4000	Room temperature to 1000
Product	SWCNT : long tubes with diameter ranging from 0.6 to 4 nm. MWCNT : long tubes with diameter ranging from 10 to 240 nm.	SWCNT : short tubes with diameter of 0.6-1.4 nm. MWCNT : short tube with inner diameter of 1-3 nm and outer diameter of approximately 10 nm.	SWCNT : long bundles of tubes (5-20 um), with individual diameter from 1 to 2 nm. MWCNT : not vary much interest in this technique, as it is too expensive, but MWNT synthesis is possible.
Carbon source	Fossil-based hydrocarbon and botanical hydrocarbon	Pure graphite	Graphite
Purity	Medium to high	Medium	Low
Cost	Low	High	High
Average	Easiest to scale up to industrial production, long length, simple process, SWNT diameter controllable, and quite pure	Can easily produce SWCNT, MWNTs. SWNTs have few structural defects, MWNTs without catalyst, not too expensive, open air synthesis possible	Good quality, higher yield, and narrower distribution of SWNT than arc-discharge

2.3 Carbon nanotube growth mechanisms

The growth mechanisms of CNTs are still being debated since their first explored. Many different models have been proposed [15]. No single growth mechanism has been finalized to explain the CNTs growth mechanism. The most widely accepted model utilizing traditional catalysts of transition metals such as Fe, Ni, Co, is the vapor-liquid-solid (VLS) mechanism [16].

For CNTs growth formation, there are two general cases: (i) tip-growth [17] and (ii) base-growth [18]. In tip-growth model, the interaction between catalyst and substrate is weak where the molten metal catalyst has an acute contact angle with the substrate (Figure 2.6(a)) [19]. The carbon atoms that have decomposed from a hydrocarbon source diffuse into the metal top surface whereas the nanotube precipitates out at the bottom of the catalyst, thus lifting the catalyst above the substrate. Growth ceases when the surface of the particle is covered with excess carbon. In the latter case, the diffusion is similar to the first case, however, due to the strong catalyst-substrate interaction, the catalyst remains on the substrate (Figure 2.6(b)) [19]. The nanotube crystallizes out first as a fullerene hemispherical dome and extending into a hollow carbon cylinder as carbon continues diffuses upward.

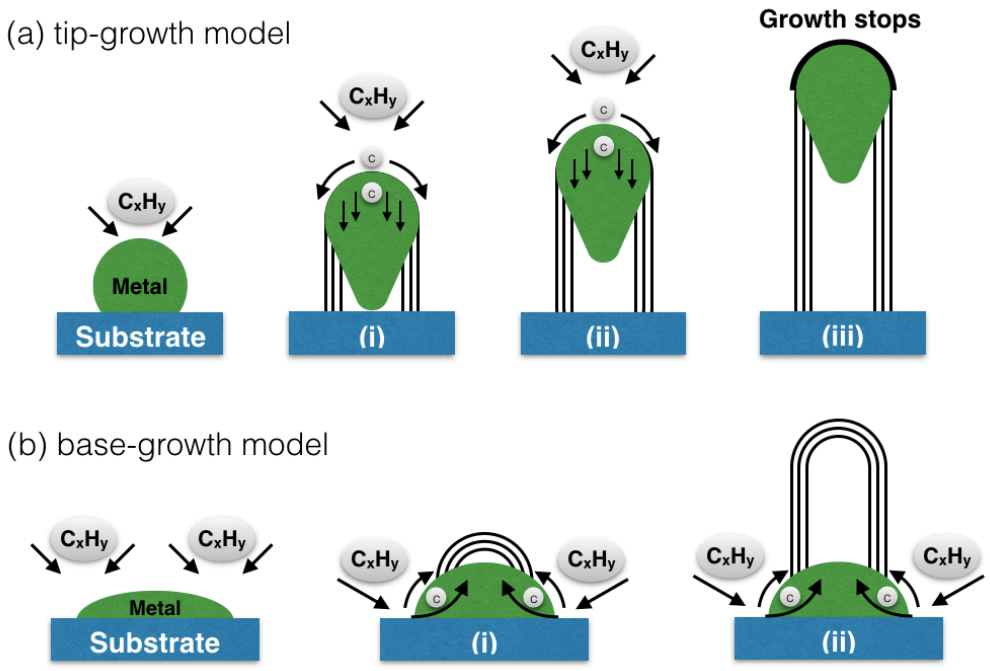

Figure 2.6 Widely-accepted growth mechanisms for CNTs: (a) tip-growth model, (b) base-growth model [19].

2.3.1 Types of catalysts

It is widely accepted that catalysts are essential ingredients for CNTs synthesis by CVD. The synthesis of both SWCNTs and MWNTs using transition metals such as Fe, Ni, Co, and Pd has become a routine process, which sometimes leads to a misconception that these metal catalysts are required for the formation of CNTs. During the past ten years, increasing attention has been made to search for new catalysts for nanotube growth. For instance, it has been shown that different metals such as Au, Ag, Cu, Pt, Rh, Mn, Mo, Sn, Mg, and Al can be used as catalysts [20–26].

2.3.2 Catalyst size

It is often assumed in the CNTs growth model by CVD process that one catalyst seed nucleates one nanotube; hence, the diameters of the nanotubes are determined by the sizes of the catalyst particles. It has been suggested that uniform nanotubes can be achieved if monodisperse catalyst nanoparticles are used. Although researchers have been able to produce a narrow diameter distribution of CNTs [27–31], it is often found that the majority of particles were not nucleating nanotubes. It has been proposed that under a given growth condition where carbon feeding and temperature are fixed, there is an optimal diameter of catalyst particles to nucleate CNTs [32]. According to this hypothesis, particles with a larger than optimal diameter are inactive due to “underfeeding” (Figure 2.7), whereas smaller particles are poisoned due to “overfeeding”. In “overfeeding” excessive carbon feeding creates a graphite shell which inhibits the CNTs nucleation. The “underfeeding” situation requires further investigation because the experimental study showed that large nanoparticles did not nucleate, even after prolonging growth time to allow the particles to collect more carbon.

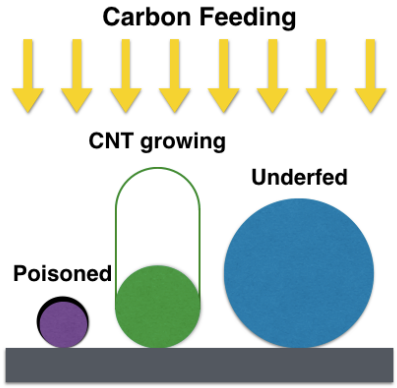

Figure 2.7 Schematic of overfeeding (poison) and underfeeding on various size particles.

Activation of nanoparticles is determined by their diameters under a given carbon feeding rate. Larger particles are underfed and not nucleating growth, while smaller particles are cutoff from carbon supplies by one or more layers of graphene sheet (the black layer in Figure 2.7). Only particles with a moderate and suitable size can nucleate growth.

2.4 Catalyst preparation

For the catalyst preparation, there are many methods such as evaporation, sputtering or chemical vapor deposition (CVD). Among of all, the CVD is the technique that has the advantage of easy setup, large area of substrate and low cost due to its common setup that do not need vacuum.

2.4.1 Evaporation

Thermal evaporation is one of the simplest of the physical vapor deposition (PVD) techniques. Basically, the material is heated in a vacuum chamber until its surface atoms have sufficient energy to leave the surface. At this point, they will traverse the vacuum chamber at thermal energy (less than 1 eV), and coat a substrate positioned above the evaporating material (average working distances are 200 mm to 1 meter). The pressure in the chamber must be below the point where the mean free path is longer than the distance between evaporation source and the substrate. The mean free path is the average distance an atom or molecule can travel in a vacuum chamber before it collides with another particle thereby disturbing its direction to some degree. This is typically 3.0×10^{-4} Torr or lower. The main reason to run at the high end of the pressure range is to allow an ion beam source to be employed simultaneously for film densification or other property modification.

2.4.2 Sputtering

Sputtering is a technique that is used to deposit thin film of material on the substrate. First, the gas plasma is created then accelerated the ions from plasma and bombarded onto the target materials. The target material is eroded by the arriving ions and is ejected in form of neutral particles (may be atoms, clusters of atoms or molecules). The ejected particles will move in a straight direction until they contact with something, other particles or some surface. If the substrate is placed in the path

of the ejected particles direction, it will be coated by the thin film of the target material.

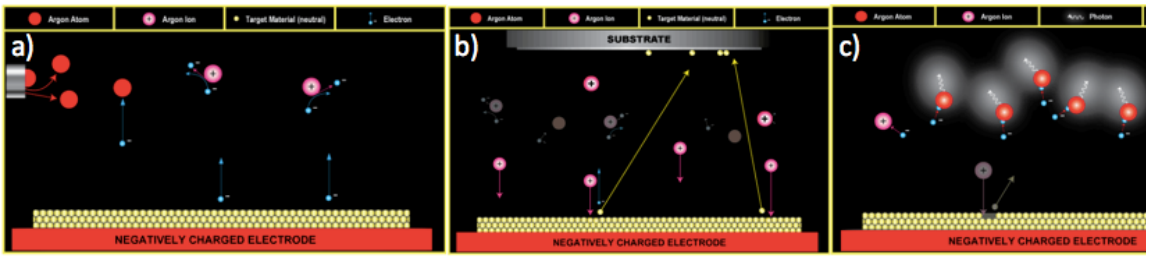

Figure 2.8 The schematic of sputtering process [33].

The sputtering process (Figure 2.8) can be explained as bellows;

a) The "free electrons" will immediately be accelerated away from the negatively charged electrode (cathode). These accelerated electrons will approach the outer shell electrons of neutral gas atoms in their path and, being of a like charge, will drive these electrons off the gas atoms. This leaves the gas atom electrically unbalanced since it will have more positively charged protons than negatively charged electrons (-) thus it is no longer a neutral gas atom but a positively charged "ion" (e.g. Ar^{+}).

b) At this point, the positively charged ions are accelerated into the negatively charged electrode (cathode) striking the surface and "blasting" loose electrode material and more free electrons by energy transfer. The additional free electrons feed the formation of ions and the continuation of the plasma. The blasted out materials move with straight direction than place onto the substrate upward as film coating.

c) All the while, free electrons find their way back into the outer electron shells of the ions thereby changing them back into neutral gas atoms. Due to the laws of conservation of energy, when these electrons return to a ground state, the resultant neutral gas atom gas gained energy and must release that same energy in the form of a photon. The release of these photons is the reason the plasma appears to be glowing.

2.4.3 Electroplating

Electroplating is the technique that passing an electric current through a solution called an electrolyte. The setup is done by immersing two electrodes into the electrolyte and connected both electrodes into circuit with power supply. The electrodes and electrolyte are carefully chosen of elements or compounds. While

current applied, the metal atoms will be generated from electrolyte as metal ion that will be deposited on the surface of one electrode. These called electroplating. All kinds of metals can be plating by this method such as gold, silver, tin, zinc and nickel. The electroplating technique is similar to the electrolysis (using electricity for splitting up the chemical solution), which is the reverse of the process.

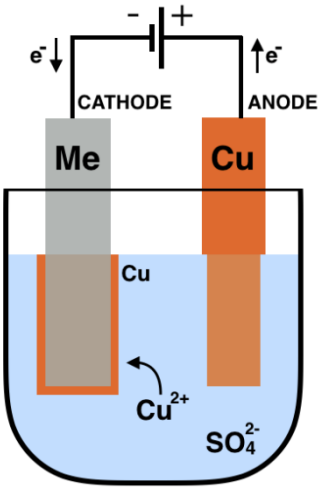

Figure 2.9 Electroplating of a metal (Me) with copper in a copper sulfate bath.

Figure 2.9 is the example process of electroplating, after voltage is applied, the copper anode is oxidized to Cu^{2+} by loss of two electrons. In the electrolyte solution, the Cu^{2+} and the anion SO_4^{2-} are from copper sulfate. At the cathode side, the Cu^{2+} is reduced to metallic copper by gaining two electrons from the current supplied that form the Cu plating on the cathode side. The plating technique is most common for a single metallic element.

2.5 Supercapacitor

Supercapacitor is an electrochemical capacitor that has very high capacitance compared with the conventional capacitor. They can store hundreds or thousands of times more charge then the conventional. However, the energy density of the supercapacitor is still lower in case of compared with batteries and fuel cells. From the Ragone plot in Figure 2.10, supercapacitor is between the conventional capacitor and batteries in term of energy density and power density but cannot give high power, while the conventional capacitors show high power but low energy density.

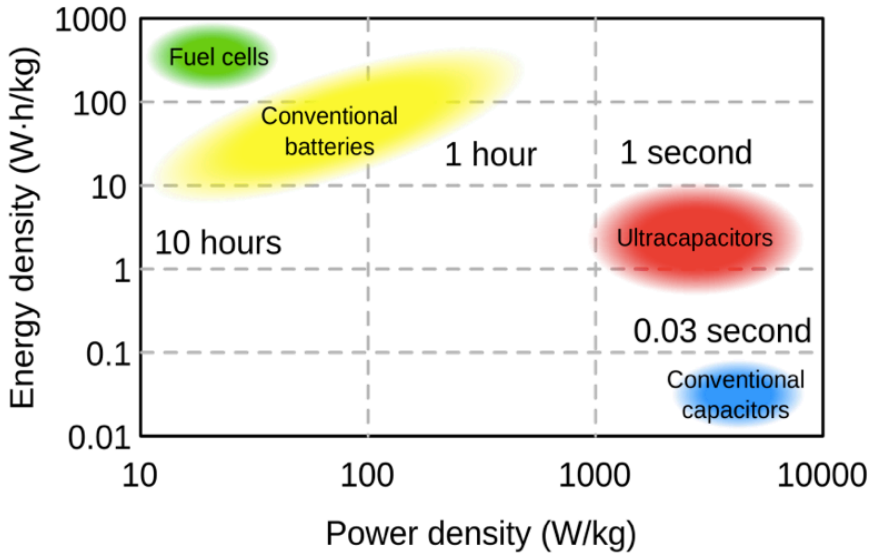

Figure 2.10 Ragone plot showing comparison for various energy storage devices [34].

In additional, from the charge-discharge process, the supercapacitor can be fully charged in seconds or minutes compared to the batteries that require to hours in charging. Supercapacitor also have longer life time (> 100,000 cycle) than batteries (around 3,000 cycle)

2.5.1 Conventional capacitor

Capacitor is an energy storage device, of which two passive metal plates are to store energy electrostatically in an electric field. The two plates with the same area of *A* and separated with dielectric thickness of *d*, were assembled as shown in Figure 2.11.

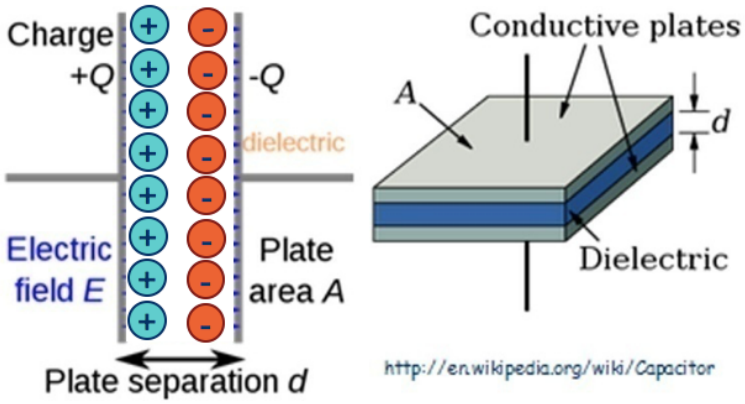

Figure 2.11 Schematic of capacitor with two parallel conductive plates [35].

Then, the capacitance *C* of the capacitor is defined as:

$$C = \frac{Q}{V} \tag{2.1}$$

where *Q* is the accumulated charge on each plate and *V* is the potential difference between the two plates. *C* is determined by the dimension of the capacitor and the property of dielectric between the plates, and can be calculated by:

$$C = \varepsilon_0 \varepsilon_r A/d \tag{2.2}$$

where ε_0 is the permittivity in vacuum and ε_r is the relative dielectric constant of the dielectric between the charged plates.

2.5.2 Supercapacitor

Generally, for the supercapacitor basic energy storage mechanism, it can be classified into two categories; (1) Electrical double layer capacitor (EDLC) and (2) Pseudocapacitor.

2.5.2.1 Electrochemical double layer capacitors (EDLC)

An electrochemical double layer capacitor (EDLC) stores its charge with electrostatic and consists of two layers of opposite charges that form at the interface of the electrode and electrolyte, separated by a distance at the atomic scale. For EDLC, the electrolyte can be either aqueous or non-aqueous liquid, or solid material as conducting polymer.

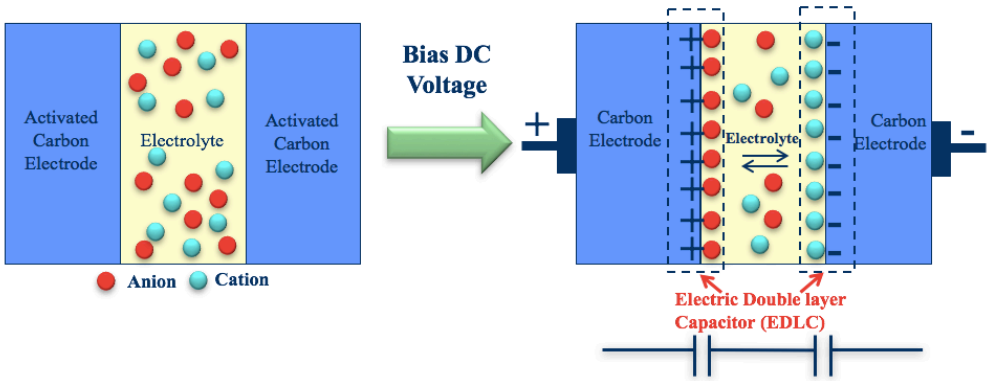

Figure 2.12 The schematic show the mechanism of electrochemical double layer capacitors (EDLC).

Figure 2.12 shows the schematic view of EDLC while charging by applying voltage. The process details are as follows;

- Before charging, in electrolyte, positive and negative ions are uniformly dispersed and there is no electric field at the electrode surface
- When a voltage is applied, the ions are attracted to the electrode with the opposite charge
- Energy is stored as a charge separation in double layers formed at the interface between the surface of electrode material and the electrolyte

2.5.2.2 Pseudocapacitor

Pseudocapacitor is a part of electrochemical capacitor, usually used together with the EDLC to form the supercapacitor. In pseudocapacitor, electrical energy stores by electron charge transfer between the electrode and electrolyte by reduction-oxidation reaction (redox reaction). A pseudocapacitor has chemical reaction that make electrical charge store faradaically at the electrode while in case of EDLC, the electrical charge is stored electrostatically with no interaction between electrode and ions. Electrochemical pseudocapacitors generally use metal oxide or conductive polymer electrodes with high amount of electrochemical pseudocapacitance.

EDLCs and pseudocapacitors also have different advantages, the EDLSs have higher power output but pseudocapacitors are greater in term of energy density. The comparison between both types shows in Table 2.3. In term of the lifetime usage, the EDLCs have much longer than the pseudocapacitors due to the materials limitation.

Table 2.3 The comparison of EDLCs and psudocapacitors [36].

Types	Mechanisms	Materials	Merits	Demerits
EDLCs	Charge separation at the electrode-electrolyte interface	Carbon materials	High power density, and good cycling behaviors	Low energy density, and low working voltage
Pseudo-capacitors	Reversible surface Faradic redox reactions	Transition metal oxides, conducting polymers	High capacitance and energy density	Poor cycling behavior, and low working voltage

2.5.3 Electrochemical measurement

Electrochemical is the study of the chemical response of a system to an electrical stimulation. This studies the loss of electrons (oxidation) or gain of electrons (reduction) occured during the electrical stimulation. These reduction and oxidation reactions are commonly known as redox reactions [36].

In electrochemical experiment, many parameters can be measured such as potential (*E*), current (*i*), charge (*Q*) and time (*t*), where as

- Potential (*E*) is the amount of electrical force of energy in a system. As the potential increases, more force is available to make a reaction happen. The base unit for potential is the volt (V).
- Current (*i*) is the magnitude of the electron flow in a system. Its base unit is amperes (A), but most electrochemical experiments measure currents on the microampere (10^{-6} A) or nanoampere (10^{-9} A) scale. Cathodic *i* is due to a reduction. Anodic *i* is due to an oxidation.
- Charge (*Q*) is a measure of the number of electrons used per equivalent. Its base unit is the coulomb (C). The charge can be directly measured or calculated by multiplying current and time.

In electrochemical techniques, there are three electrodes, the working electrode, the reference electrode and the counter electrode. The three electrodes are connected to a potentiostat instrument which controls the potential of the working electrode and measures the result current.

2.5.3.1 Cyclic voltammetry

Cyclic voltammetry (CV), is one of the commonly used electrochemical measurement techniques with the advantage of ability to characterize an electrochemical system. In CV measurement, the potentiostat applies a potential to the working electrode with specific scan rate then reverses the scan, returning to the initial potential (see triangular wave from in Figure 2.13).

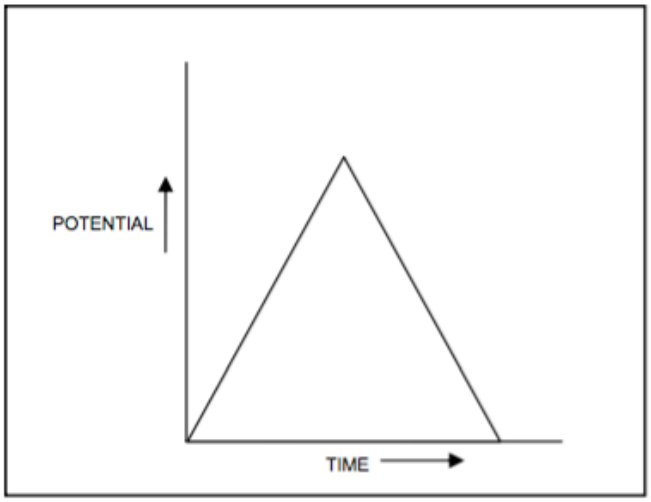

Figure 2.13 Typical excitation waveform for cyclic voltammetry.

During the potential sweep, the potentiostat measures the current result obtained from each applied potential. These values are collected then plot into CV graph of the current versus applied potential. The example of CV graph plot is shown in Figure 2.14.

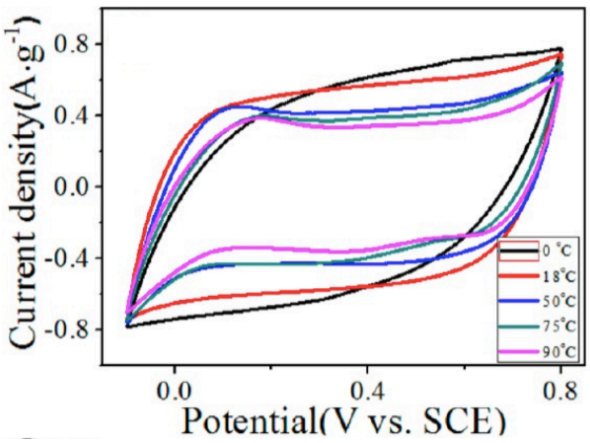

Figure 2.14 The example of cyclic voltammetry graph plot [37].

For the specific capacitance (C_s), can be calculated from the CV curve that obtained from the electrochemical measurement with equation 2.3

$$C_s = \frac{\int_{V_1}^{V_2} i(V)dV}{2(V_2 - V_1)mv} \quad (2.3)$$

where C_s is the specific capacitance ($F \cdot g^{-1}$), m is the mass of the electrode (g), v is the scan rate of CV curves ($V \cdot s^{-1}$), and $(V_2 - V_1)$ represents the potential window (V).

The energy density (E) and power density (P) of the assembled supercapacitor also can be calculated from CV curves by equation 2.4 and equation 2.5

$$E = \frac{1}{2} C V^2 \quad (2.4)$$

$$P = \frac{E}{t} \quad (2.5)$$

where C is the specific capacitance ($F \cdot g^{-1}$), V is the potential drop (V), and t is the discharge time.

2.5.3.2 Galvanostatic charge-discharge

Galvanostatic charge-discharge (CD), is the standard technique used to test the performance and cycle-life of EDLCs and batteries. A loop of charging and discharging is called as one cycle. Charge and discharge are conducted with constant current until reach the set voltage. The loop is repeated in cycle times to observe repeatable and the cycle-life time before performance is drop. The example of CD curve is shown in Figure 2.15.

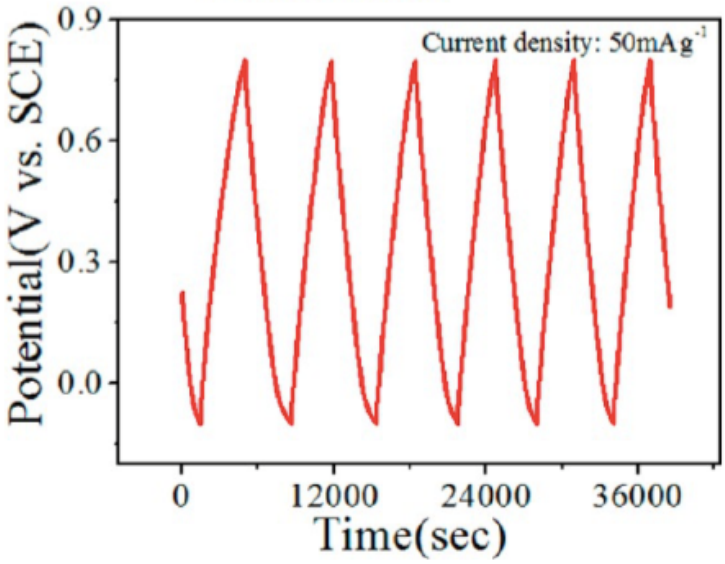

Figure 2.15 The example of galvanostatic charge-discharge curve [37].

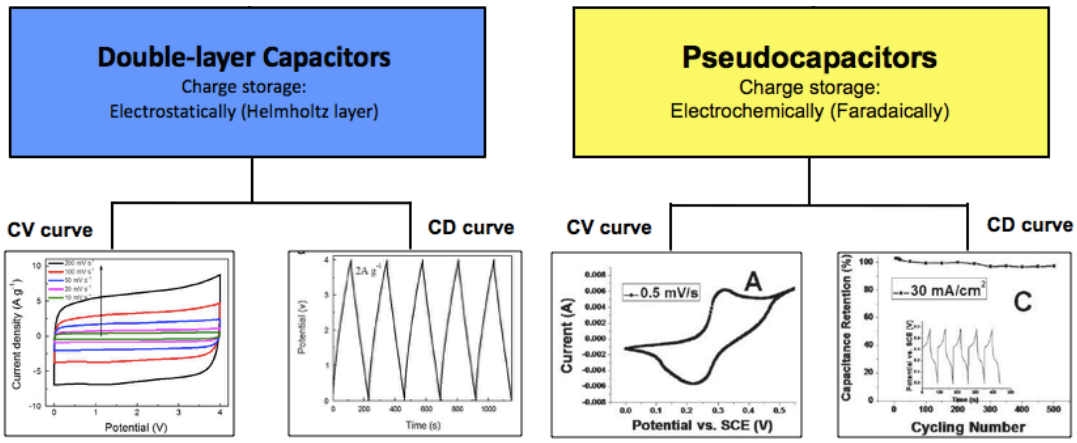

Figure 2.16 Example CV and CD curves from EDLC and pseudocapacitors.

The plot results of electrochemical measurement such as CV curve and CD curve from EDLC and pseudocapacitors are showed in Figure 2.16. The CV curve from EDLC is generally ploted as the rectangular shape while the pseudocapacitor usually generates with the additional redox reaction as oxidation and reduction peaks. In the case of CD curve, the EDLC shows with triangular repeatable charge-discharge curve but the pseudocapacitor shows with quasi-triangular representing the additional discharge time from redox reaction.

CHAPTER 3
RESEARCH METHODOLOGY

This research has focused on facile fabrication of CNTs electrode which is composed of two steps. The first step was to deposit Ni nanoparticles that acted as a catalyst on a copper (Cu) substrate by direct-current (DC) electroplating technique. The second step was to grow the CNTs on the Ni-electroplated Cu substrate by using chemical vapor deposition (CVD) technique. Several characterization techniques were utilized to investigate the optimum conditions for the fabrication of CNTs electrode. Finally, the optimized CNTs electrode was used to demonstrate its potential application as supercapacitor. Figure 3.1 shows a flow chart of the experimental procedure. The following section describes each step in detail.

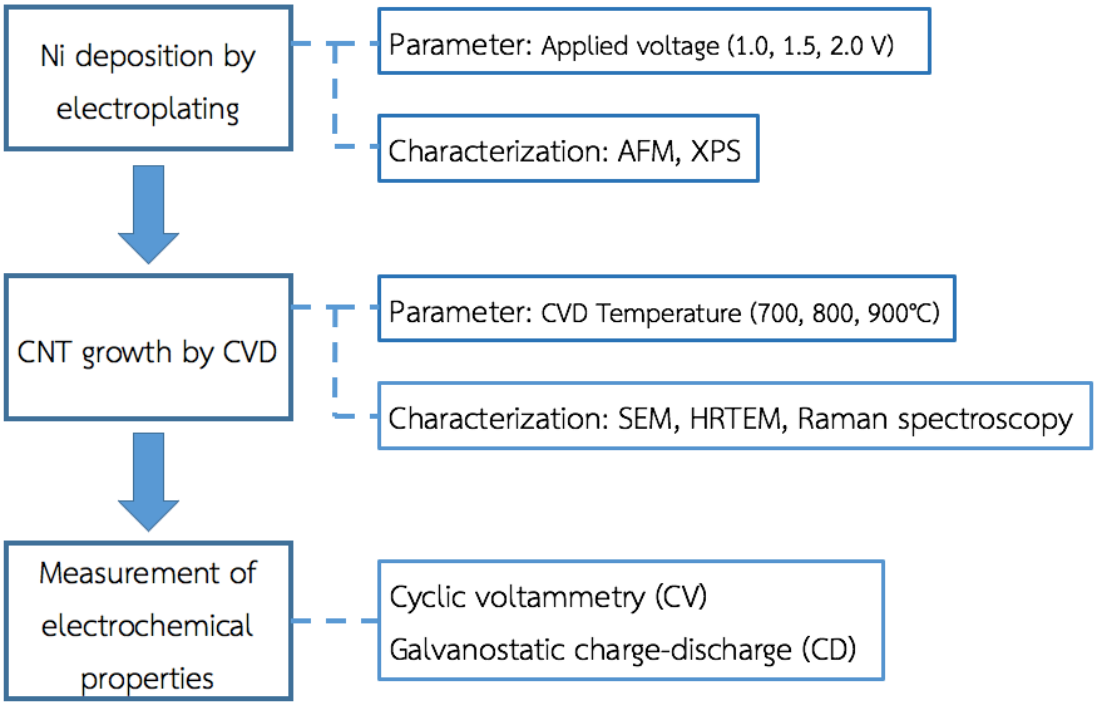

Figure 3.1 A flow of research procedure.

3.1 Deposition of Ni nanoparticles by direct-current electroplating

3.1.1 Materials and equipment

Materials and equipment used in this research for deposition of Ni catalyst are as follows:

(1) Cu sheet (99.9% purity, Nilaco Corporation, Japan)
(2) Ni Ingot (commercial grade)
(3) Ni solution electrolyte (commercial grade)
(4) Ethanol (AR grade, Labscan)
(5) Acetone (AR grade, Labscan)
(6) DC-Power supply
(7) Hot plate

3.1.2 Method of deposition of Ni nanoparticles by direct-current electroplating

99.9% pure Cu sheet (Nilaco Corporation, Japan) was cut to a size of 10 mm x 10 mm and was used as a substrate for Ni nanoparticle preparation by a direct-current (DC) electroplating technique. Prior to electroplating, Cu sheet was ultrasonically cleaned in ethanol, acetone and distilled water for 10 minutes, respectively. In electroplating process, the prepared Cu substrate was placed as an anode and Ni ingot was set to be a cathode with a 100 mm gap distance. Commercial Ni electroplating solution was used as electrolyte. The electrolyte temperature was fixed at 45^{o}C. Electroplating parameter studied in this research was the applied voltage. The applied voltages were varied at 1.0, 1.5 and 2.0 V. A schematic view of the setup and a photo of the setup are shown in Figure 3.2 (a) and (b), respectively.

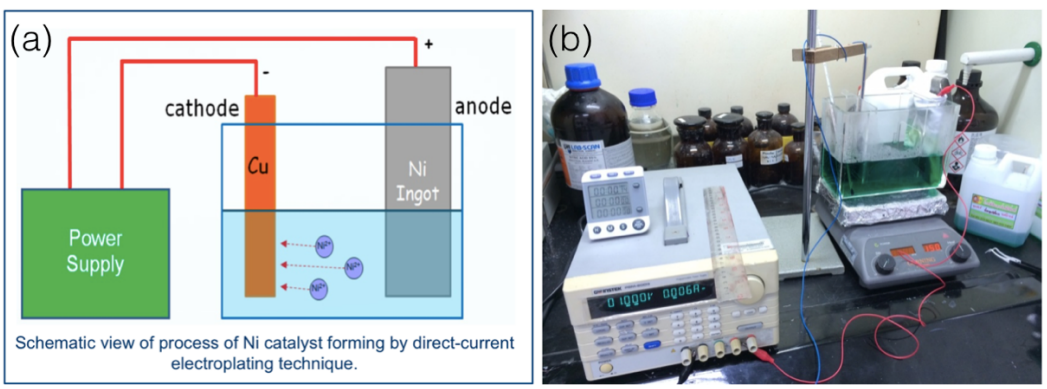

Figure 3.2 (a) Schematic view and (b) photograph of direct-current electroplating.

3.2 Growth of carbon nanotube on Ni-electroplated Cu by chemical vapor deposition

3.2.1 Materials and equipment for growth of carbon nanotube

Materials and equipment used in this research for growth of CNTs are as follows:

(1) Ethanol (AR grade, Labscan)

(2) Argon gas (99.95% purity)

(3) Tube furnace (Maximum temperature 1200 °C)

(4) Quartz tube (Diameter inside 21 mm, Length 120 cm)

(5) Quartz boat

(6) Mantle

(7) Gas control unit

3.2.2 Method of growth of carbon nanotube on Ni-electroplated Cu by chemical vapor deposition

Chemical vapor deposition (CVD) was used to synthesize CNTs on the Ni nanoparticle-electroplated Cu substrate prepared from the previous step (Section 3.1). For the CVD setup, a 120-cm long quartz tube was used as a reactor. The Ni nanoparticle-electroplated Cu substrates were set in the middle of the heating zone of the quartz tube as shown in Figure 3.3. Argon gas was purged in the quartz tube for 30 min at a flow rate of 0.6 LPM to replace oxygen and other gas contents in the reactor. Then, the reactor was heated up to setting temperature (varied with 700, 800 and 900°C) for 1 hr. Ethanol was vaporized and directly carried into the quartz tube by argon bubbling for 20 min to grow the CNTs. After CNTs growth, the reactor was cooled down to room temperature under atmosphere of argon gas flow. The profile of temperature and gas flow is shown in Figure 3.4.

For the CNTs growth by CVD, two parameters were studied (the CVD temperature and the electroplating voltage). First, to optimize CVD temperature, the electroplating voltage was fixed at 1.5 V and CVD temperatures were varied at 700, 800 and 900 °C. The CVD condition is shown in Table 3.1. Second, the CVD temperature was fixed at the optimum temperature and the electroplating voltages were varied at 1.0, 1.5 and 2.0 V.

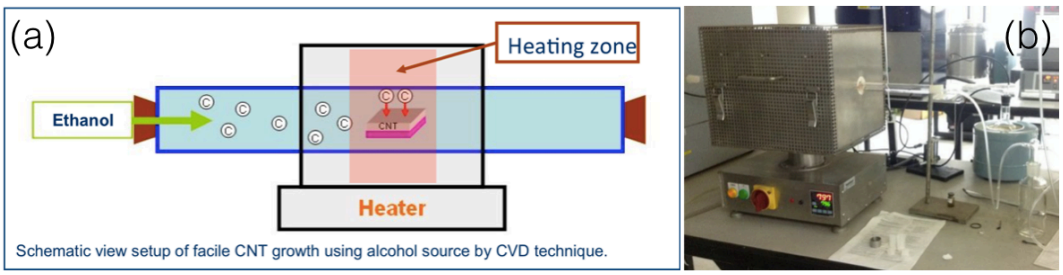

Figure 3.3 (a) Schematic view and (b) photograph of CVD setup.

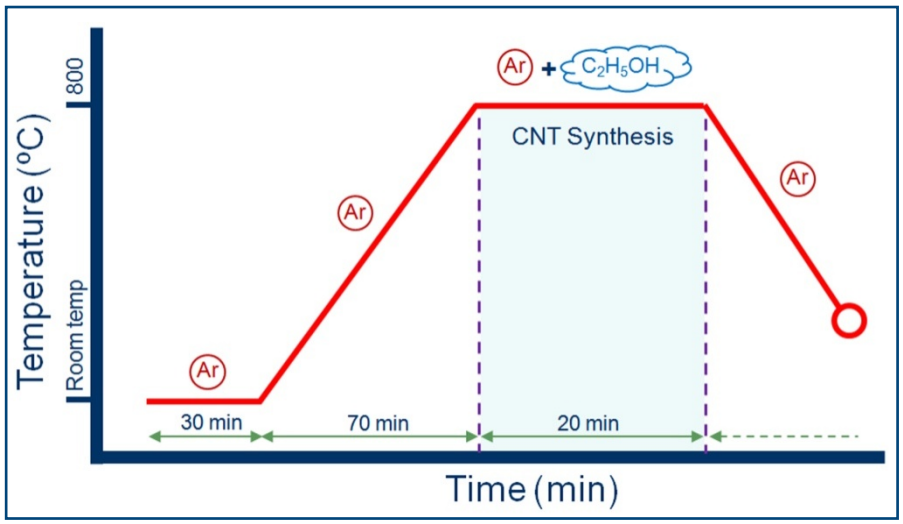

Figure 3.4 Temperature and gas profile for CVD process.

Table 3.1 Chemical vapor deposition conditions.

CVD condition	
Carbon source:	Ethanol (AR grade)
AR flow rate:	0.4 LPM
Ethanol flow rate	0.3 LPM
Pressure:	Atmospheric pressure
Temperature (varied):	700, 800, 900 °C
Time:	20 min

3.3 Characterization of Ni nanoparticles and CNTs

The morphology of the electroplated Ni was characterized by atomic force microscopy (AFM; SEIKO SPA400) with dynamic force mode (DFM) and a polysilicon

tip (NT-MDT; HA_NC ETALON) was used with resonance frequency = 235 kHz. The scan area was 2x2 μm^2. The chemical state of Ni was characterized by X-ray photoelectron spectroscopy (XPS; Kratos Analytical, AXIS Ultra DLD).

The morphology, diameter and structure of the graphitic layer, and the crystallinity of the synthesized CNTs were characterized by field emission scanning electron microscopy (FESEM; Hitachi, SU-8030) with an accelerated voltage at 1kV and a working distance of 10cm, transmission electron microscopy (TEM; JEOL, JEM-2010) using an accelerated voltage at 200 kV with LaB_6 filament and Raman spectroscopy (Thermal Scientific, DXR™ SmartRaman Spectrometer) with a laser wavelength of 532 nm, respectively. Table 3.2 shows a summary of analysis techniques and information that can be obtained from each technique.

Table 3.2 Characterization techniques and their corresponding information.

Techniques	Information
Atomic force microscopy (SEIKO, SPA400)	Ni catalyst size
X-ray photoelectron spectroscopy (Kratos Analytical, AXIS Ultra DLD)	Ni chemical state
Scanning electron microscopy (HITACHI, SU-8030)	CNTs morphology
High resolution transmission electron microscopy (JEOL, JEM-2010)	CNTs diameter and graphitic layer structure
Raman spectroscopy (Thermal Scientific, DXR™ SmartRaman Spectromete)	CNTs crystallinity

3.4 Measurement of electrochemical properties

3.4.1 Materials and equipment for measurement of electrochemical properties

Materials and equipment used in this research for measurement of electrochemical properties are as follows:

(1) 1M Sulfuric acid electrolyte
(2) Pt counter electrode
(3) Ag/AgCl reference electrode
(4) Faraday cage (to block electric field)
(5) Electrochemical instruments (Metrohm, Autolab PGSTAT302)

3.4.2 Method of measurement of electrochemical properties

Electrochemical properties were measured in a three-electrode setup as shown in Figure 3.5. It was connected to an electrochemical workstation (Metrohm, AUTOLAB PGSTAT 302). The CNTs synthesized on Ni-electroplated Cu sheet (an area of 10 mm x 10 mm) was used as a working electrode. Pt and Ag/AgCl electrodes were used as counter and reference electrode, respectively. 1M H_2SO_4 aqueous solution was used as electrolyte. Electrochemical properties were characterized by cyclic voltammetry (CV) and galvanostatic charge/discharge (CD) technique. CV tests were done at a potential range of -0.3 to 0.2 V at a scan rate of 5, 20 and 100 $mV{\cdot}s^{-1}$. CD tests were performed at a current of 5 mA. The specific capacitance (C_s, $F{\cdot}g^{-1}$) was evaluated from CV curves according to the following equation (2.3);

$$C_s = \frac{\int_{V_1}^{V_2} i(V)dV}{2(V_2 - V_1)mv} \tag{2.3}$$

Where $\int_{V_1}^{V_2} i(V)dV$ is a total voltammetric charge obtained by integration of positive and negative sweep in CV curve, V_2 - V_1 is a potential window width (V), m is a total mass of active materials (g) and v is a scan rate ($V{\cdot}s^{-1}$).

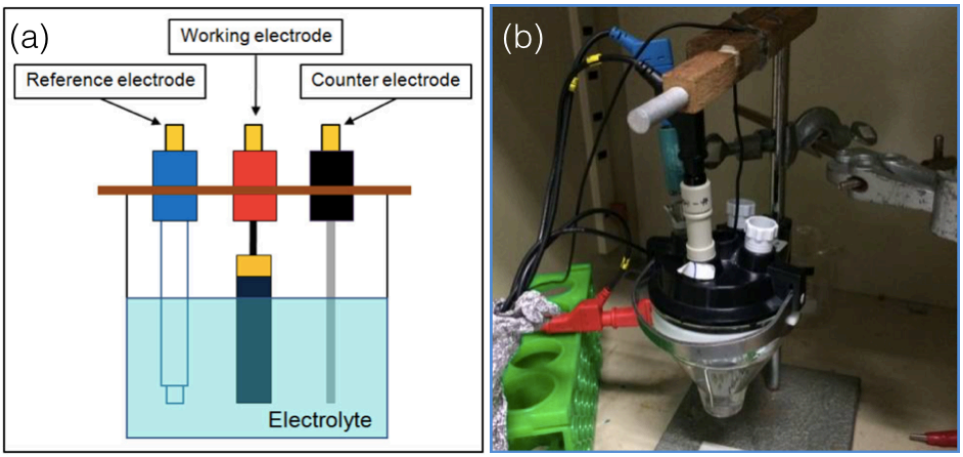

Figure 3.5 (a) Schematic diagram and (b) photograph of three electrode setup for electrochemical analysis.

CHAPTER 4
RESULTS AND DISCUSSIONS

This chapter explains the results of formation of Ni nanoparticles by DC-electroplating method and the synthesis of CNTs from the electroplated Ni by chemical vapor deposition. The effect of electroplated voltage on morphology and chemical states of the electroplated Ni and the quality of the synthesized CNTs were investigated. The DC electroplated Ni nanoparticles (NPs) were characterized the average size and the chemical states by atomic force microscope (AFM) and X-ray photoelectron spectroscopy (XPS) techniques, respectively. The synthesized CNTs by chemical vapor deposition (CVD) were characterized the morphology, internal structure and crystallinity by scanning electron microscopy (SEM), transmission electron microscopy (TEM) and Raman spectroscopy techniques, respectively. Figure 4.1 (a)-(c) shows photographs of Cu sheet before and after DC-electroplating, and after CVD process, respectively. The color of Cu sheet changed to silver color with Ni coating after DC-electroplating. After CVD process for CNTs growth, the obtained sample was obviously changed to black color wholly covered with black powder.

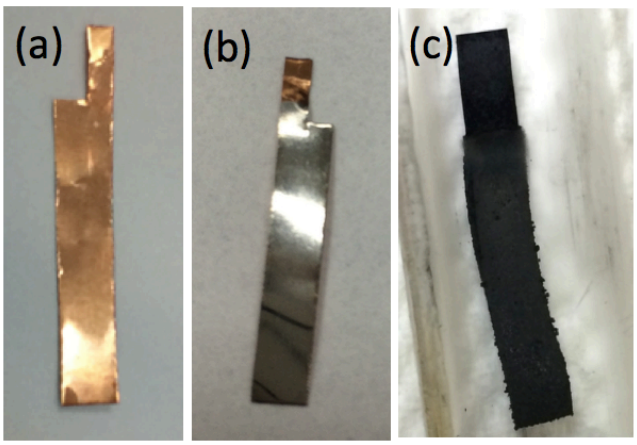

Figure 4.1 (a) Cu substrate, (b) Ni nanoparticles on Cu substrate by DC-electrplating and (c) CNTs synthesis by CVD.

4.1 Formation of Ni nanoparticles by direct-current electroplating

4.1.1 Atomic force microscopy investigation of Ni nanoparticles

After the DC-electroplating process on the Cu foils, the average sizes of the Ni nanoparticles formed by different electroplating voltages (1.0, 1.5 and 2.0 V) were measured by AFM.

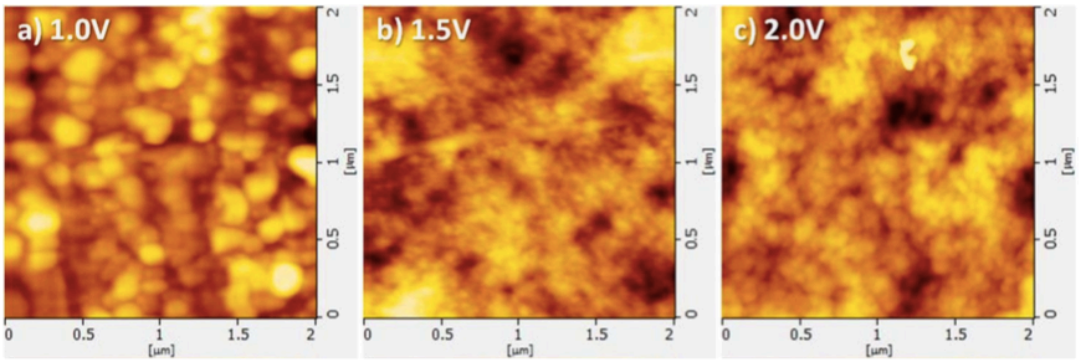

Figure 4.2 AFM images of Ni NPs on Cu foils electroplated at the voltages of (a) 1.0 V, (b) 1.5 V and (c) 2.0 V.

Figure 4.2 (a-c) shows the AFM images of the Ni NPs on Cu foils electroplated at the voltages of 1.0, 1.5 and 2.0 V, respectively. Ni NPs were formed at all of these electroplating voltages. At the applied voltage of 1.0 V, Ni NPs varied in small and larger clusters were formed; their average sizes were 44±7 nm and 120±14 nm, respectively. At the applied voltage of 1.5 V, Ni NPs with a narrow distribution of sizes were formed with an average size of 55±3 nm. When the applied voltage was increased to 2.0 V, the sizes of the formed Ni NPs increased to approximately 103±12 nm. Thus, the size of formed Ni NPs could be controlled by varying electroplating voltages.

The different size of NPs with increasing electroplating voltage can be explained by Faraday's Laws of electrolysis and Ohm's law as follows. Theoretically, Faraday's laws of electrolysis state that the amount of a material deposited on an electrode is proportional to the amount of electricity used. According to Ohm's law, the amount of current flow is proportional to the voltage. The higher the applied voltage, the higher amount and the higher energy of the positively charged Ni ions at the anode to migrate to the cathode, and reduce with the electrons to form Ni metal. The higher amount and the higher energy of the positively charged Ni ions will cause the high growth rate and large aggregation of the Ni metal.

4.1.2 X-ray photoelectron spectroscopy investigation of Ni nanoparticles

Figures 4.3-4.5 show XPS spectra of Ni NPs on Cu foils electroplated at the voltages of 1.0, 1.5 and 2.0 V, respectively.

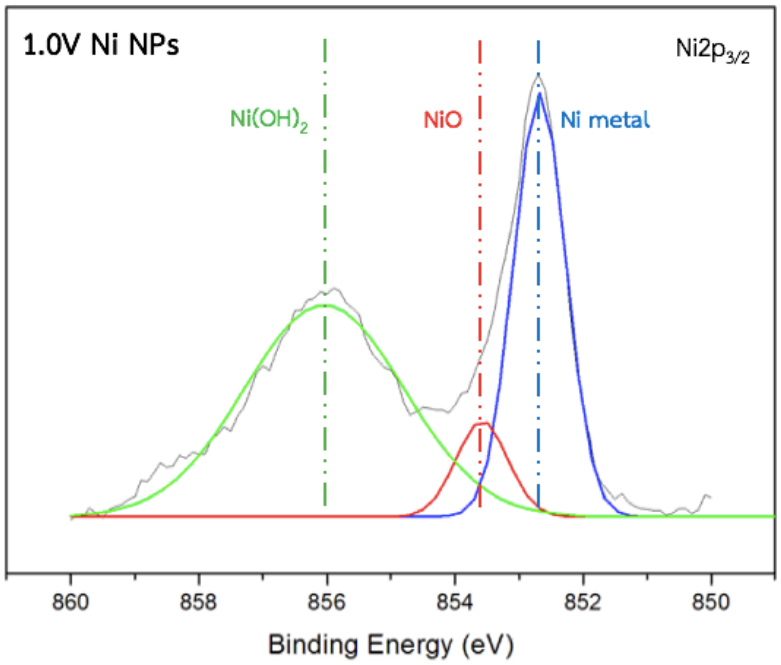

Figure 4.3 XPS spectra of Ni NPs on Cu foils electroplated at the voltages of 1.0 V.

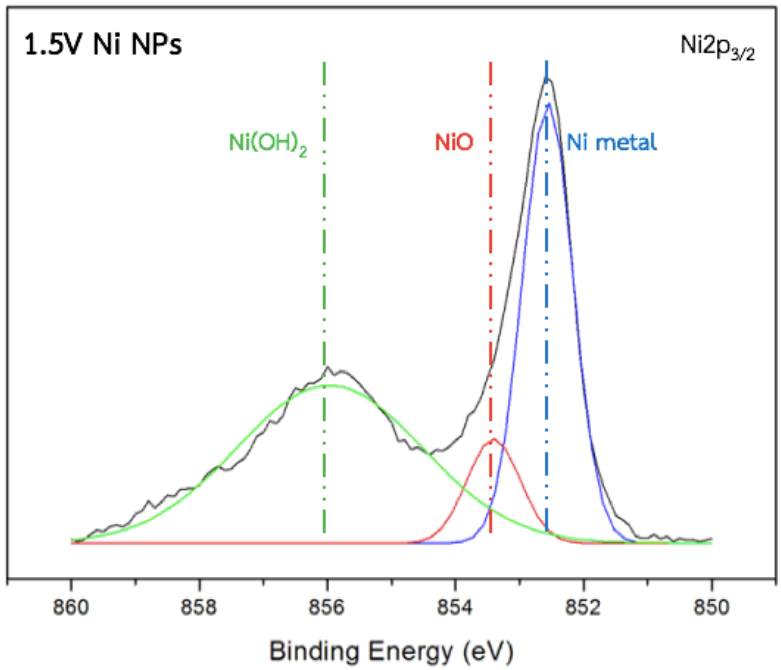

Figure 4.4 XPS spectra of Ni NPs on Cu foils electroplated at the voltages of 1.5 V.

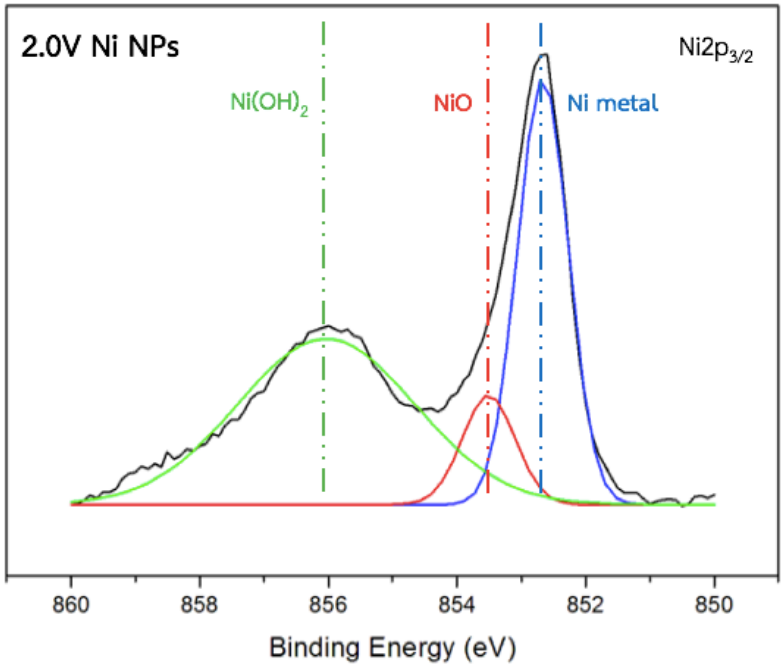

Figure 4.5 XPS spectra of Ni NPs on Cu foils electroplated at the voltages of 2.0 V.

From the XPS characterization of Ni $2p_{3/2}$, two main peaks were found at 852.8 and 856.0 eV. From peak deconvolution, the separated peaks were illustrated and match with binding energy at 852 eV, 853 eV and 856 eV that indicated to the Ni metal, NiO and $Ni(OH)_2$ formation, respectively. The atomic percentage of each oxidation states of Ni was showed in Table 4.1.

Table 4.1 The atomic percentage of each oxidation states of Ni from the electroplating voltages of 1.0, 1.5 and 2.0 V.

	Atomic % of Ni formation		
	Ni metal	NiO	$Ni(OH)_2$
1.0 V NPs	36.26	8.16	55.58
1.5 V NPs	39.13	9.69	51.18
2.0 V NPs	38.18	10.22	51.60

From XPS measurement results, the atomic percentage of each Ni oxidation states from the different electroplating voltages was similar value. The relatively same composition of Ni was formed although use the different electroplating voltages.

4.2 Effect of growth temperature on growth of carbon nanotube

In CNTs synthesis by CVD, temperature is the most important parameter that could affect to the quality of CNTs. In this experimental, the CVD temperatures were varied with 700, 800 and 900°C. The electroplating voltage for Ni NP formation was fixed at 1.5 V. SEM technique was used for characterization of the synthesized CNTs morphology

4.2.1 Scanning electron microscopy investigation of carbon nanotube grown from different growth temperatures

Figures 4.6-4.8 show SEM images of the synthesized CNTs at different temperatures recorded at the magnification of x5,000.

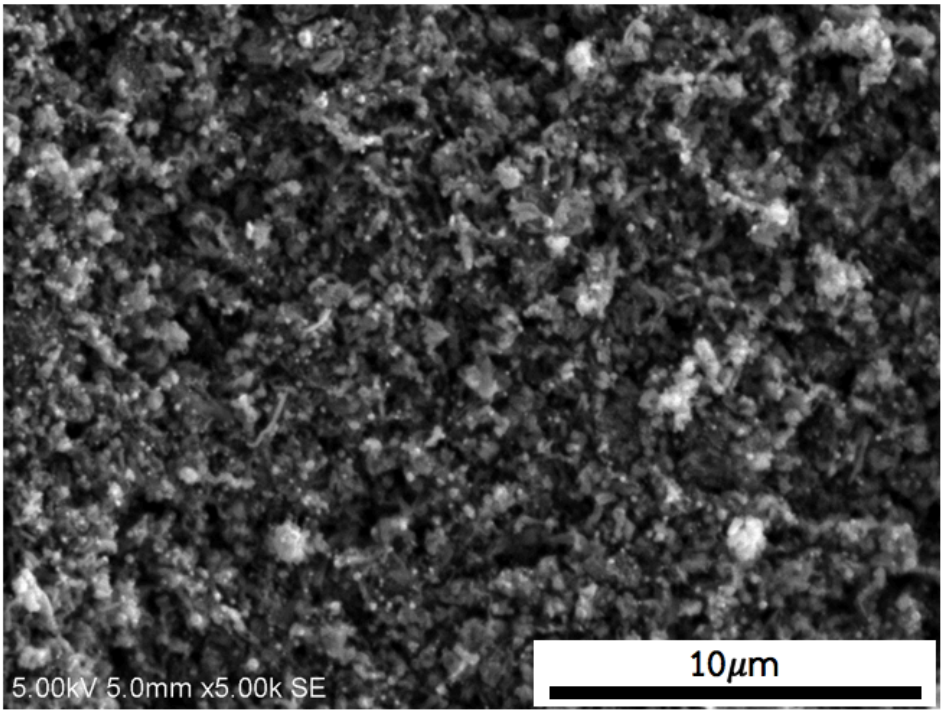

Figure 4.6 SEM image of CNTs from 1.5 V electroplating and CVD at 700°C.

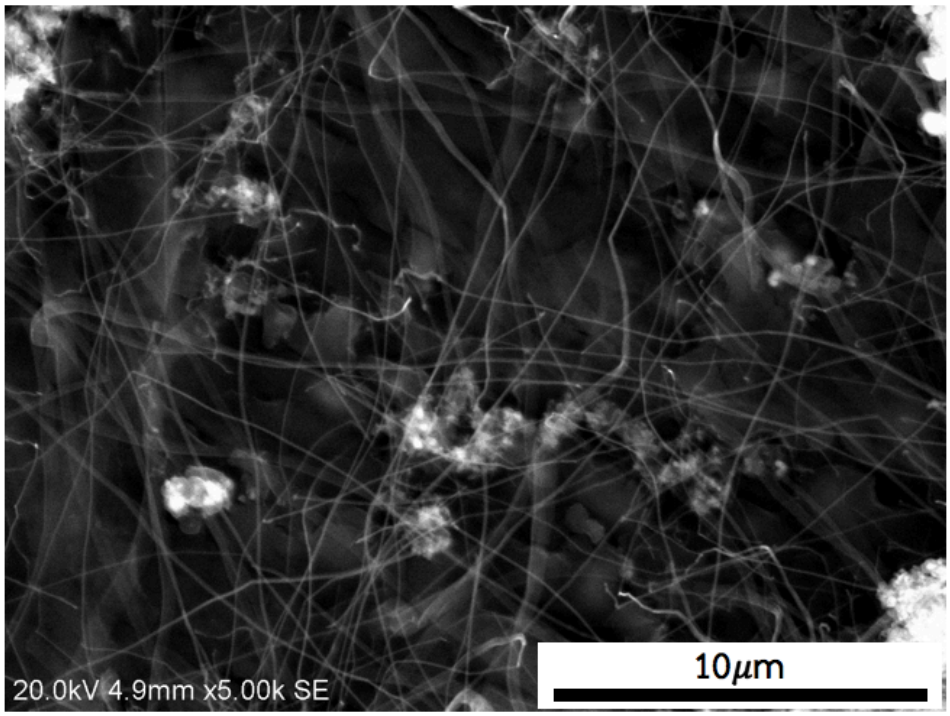

Figure 4.7 SEM image of CNTs from 1.5V electroplating and CVD at 800°C.

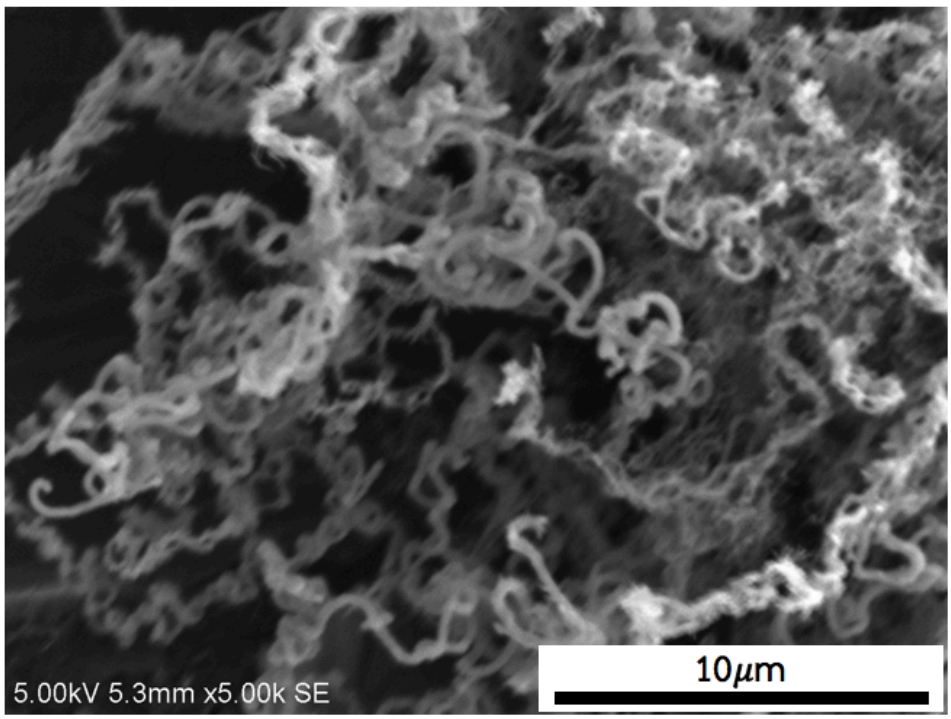

Figure 4.8 SEM image of CNTs from 1.5V electroplating and CVD at 900°C.

From the SEM results (Figure 4.6 – Figure 4.8), the morphology of CNTs grown at different growth temperature were totally different. At growth temperature of 700°C, a very short and curly CNTs were formed. The bright spots, corresponding to metal

NPs were clearly seen on the surface. At growth temperature of 800°C, the CNTs morphology was totally different from that of 700°C. The synthesized CNTs were relatively straight line with a relatively small diameter. At growth temperature of 900°C, the CNTs became curl shape and their diameter were larger compared to that of 800°C. From these results, the growth temperature of 800°C is the optimal condition to obtain the relative straight and small CNT. At low temperature (700°C), the temperature may be not sufficient for carbon diffusion on Ni NPs and saturation to form CNT, thus the nanotube structure cannot be formed. On the other hand, higher temperature (900°C), the diffusion rate of carbon is high and the Ni NPs possibly agglomerated in to a large size, resulting in the non-uniform CNT.

4.3 Effect of Ni electroplating voltage on growth of carbon nanotube

From experiment in section 4.2, it was found that the growth temperature of 800°C was the most appropriate condition for CNTs growth. Next, the effect of electroplating voltages, 1.0, 1.5 and 2.0 V, for Ni nanoparticle formation on CNTs morphology was investigated (hereinafter referred to as Ni1.0-CNTs, Ni1.5-CNTs and Ni2.0-CNTs, respectively). The CNTs growth temperature was fixed at 800°C. The synthesized CNTs were characterized by scanning electron microscopy (SEM), transmission electron microscopy (TEM) and Raman spectroscopy.

4.3.1 Scanning electron microscopy investigation of carbon nanotube grown from different Ni electroplating voltages

Figure 4.9 -Figure **4.11** show SEM images of CNTs synthesized from different Ni electroplating voltages at growth temperature of 800 °C.

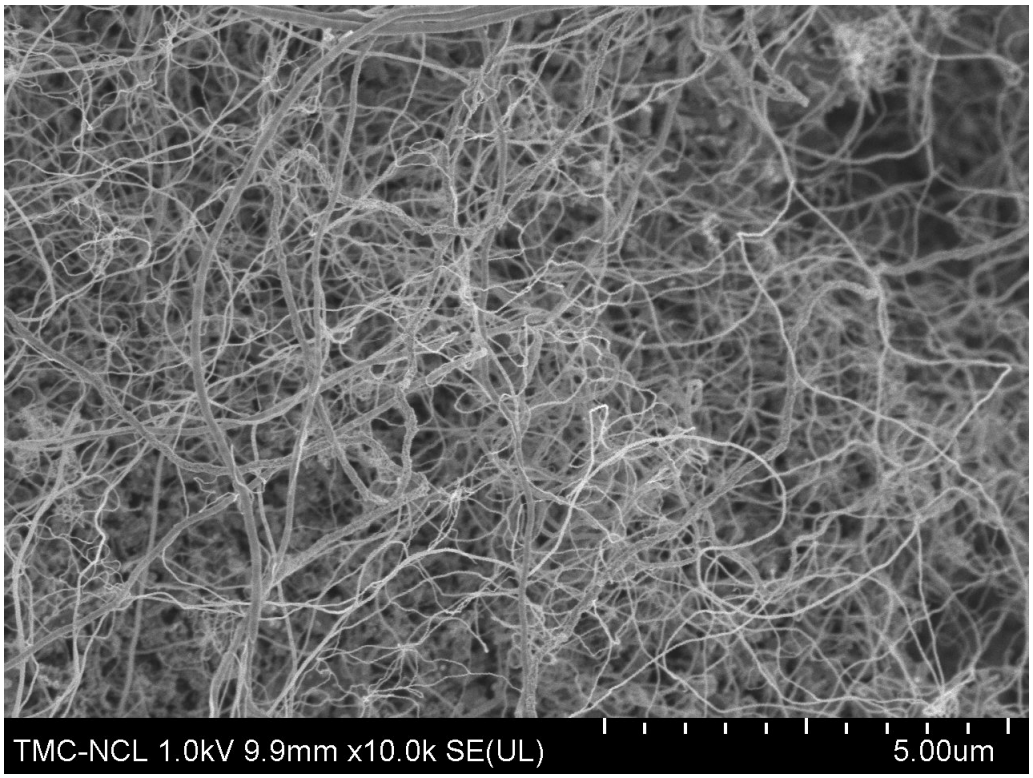

Figure 4.9 SEM image of CNTs from 1.0 V electroplating and CVD at 800 °C.

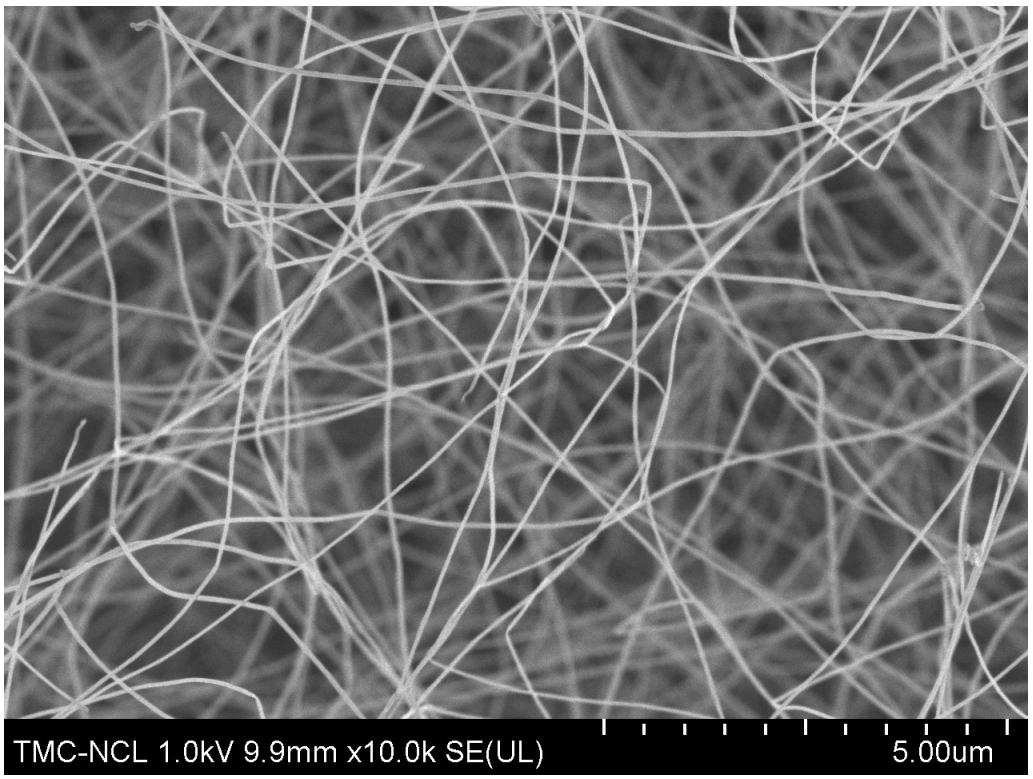

Figure 4.10 SEM image of CNTs from 1.5 V electroplating and CVD at 800 °C.

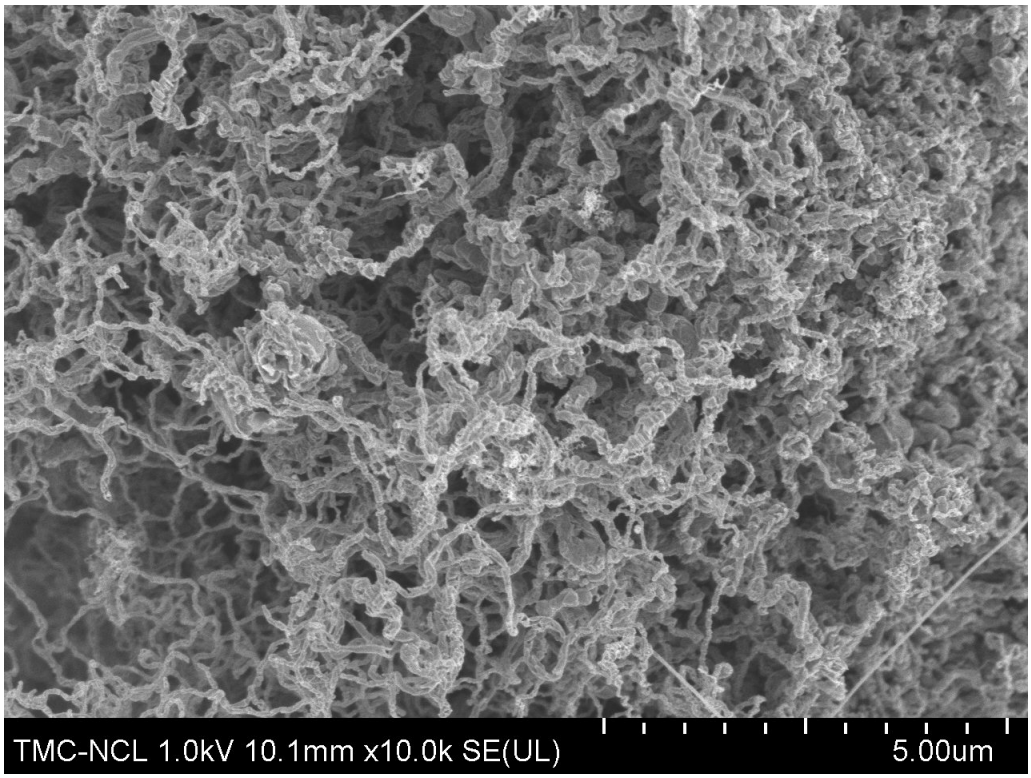

Figure 4.11 SEM image of CNTs from 2.0 V electroplating and CVD at 800 °C.

The overall morphology of the sample surfaces was examined by SEM technique. The SEM analysis was carried out with magnification at x10,000 that could reveal the CNTs in a wide area to confirm the uniformity of the synthesized CNTs. From the SEM images, it was obviously seen in Figure 4.11 that the Ni2.0-CNTs had the agglomerated clusters of curly-shape CNTs. While as seen in Figure 4.9 and Figure 4.10, Ni1.0-CNTs and Ni1.5-CNTs had a similar feature showing the high aspect ratio CNTs and non-agglomerated clusters. CNTs in Figure 4.10 were straighter and appear larger in diameters than those in Figure 4.9. For more details of the CNTs having diameters in a nanometer scale (less than 100 nanometers), TEM technique was a suitable technique that can provide sufficient resolution and internal structures of the CNTs.

4.3.2 Transmission electron microscopy investigation of carbon nanotube grown from different Ni electroplating voltages

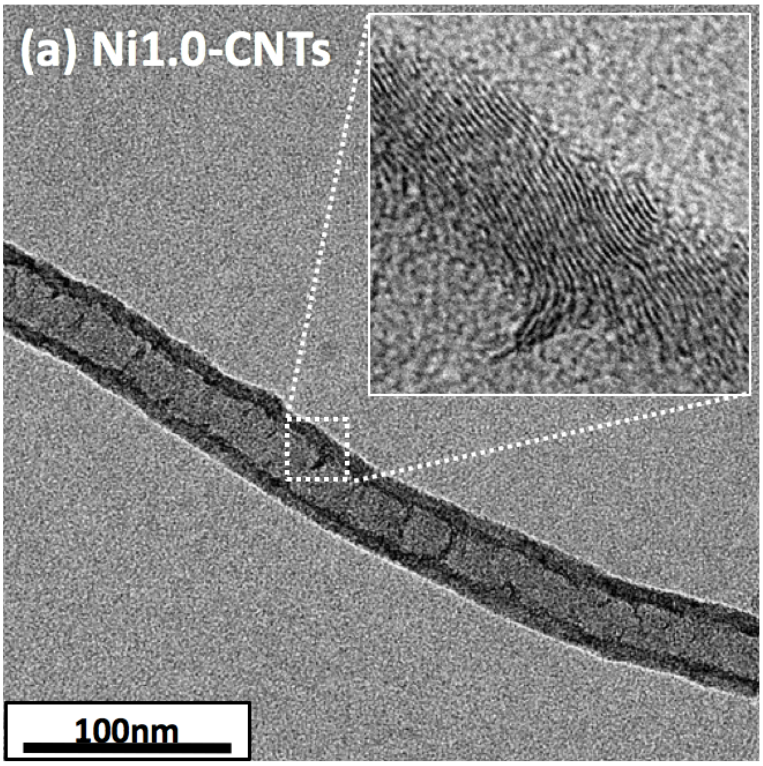

Figure 4.12 TEM image of CNTs from 1.0V electroplating and CVD at 800 °C.

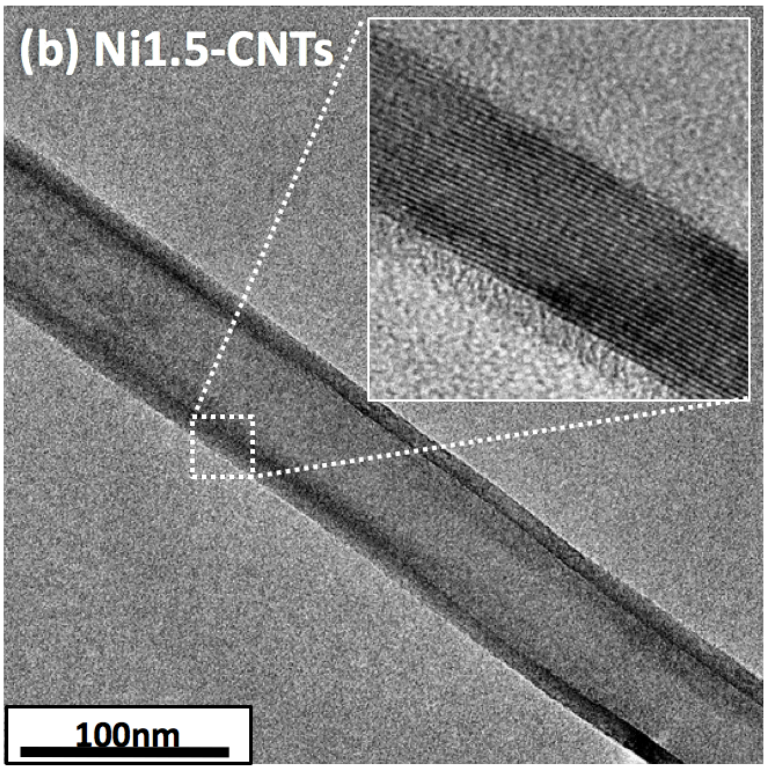

Figure 4.13 TEM image of CNTs from 1.5V electroplating and CVD at 800 °C.

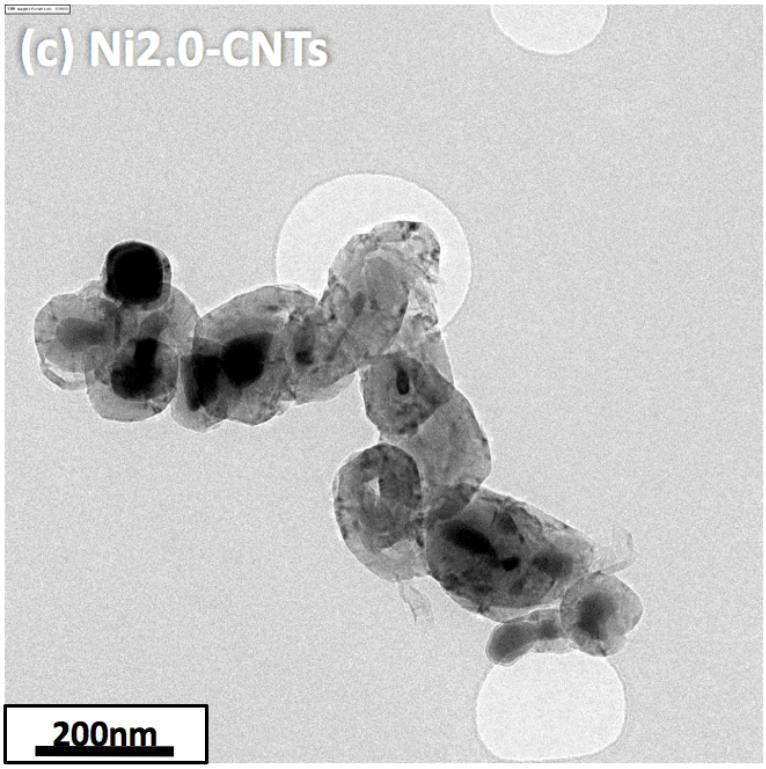

Figure 4.14 TEM image of CNTs from 2.0V electroplating and CVD at 800 °C.

Figure 4.12 – **Figure 4.14** show TEM images of Ni1.0-CNTs, Ni1.5- CNTs and Ni2.0-CNTs, respectively. The images taken at x50,000 magnification reveal the CNTs shape and graphitic wall arrangements. The images of Ni1.0-CNTs and Ni1.5-CNTs show that the CNTs had a tubular shape with diameters of approximately 45±7 nm and 60±5 nm, respectively. The darker contrast in TEM image of CNTs corresponds to the thickness of the wall. However, at high magnification up to x400,000, it was found that the wall layers were different. The inset in Figure 4.12 shows that the graphitic layers of Ni1.0-CNTs were at an angle to the tube axis wall (bamboo structure), while the inset in Figure 4.13 shows clearly that the graphitic layers of Ni1.5-CNTs were parallel to the tube axis. Furthermore, the structure of Ni2.0-CNTs was completely different from those of Ni1.0- CNTs and Ni1.5-CNTs. Ni2.0-CNTs were string bead [38] of nanoparticles with Ni catalyst inside and a wide distribution of tube diameters (Figure 4.14). These results imply that the small-sized Ni NPs with a narrow distribution is a key to uniform CNTs synthesis.

Although the TEM technique gives the advantage of high resolution with higher magnification examinations of CNTs internal structures but it was limited to a small area of CNTs. SEM, on the other hand, was appropriate for a large area observation and for external morphology. So both techniques, SEM and TEM, are complimentary for the CNTs characterization.

Figure 4.15 illustrates the structure models of CNTs growth from various electroplating voltages. The Figure 4.15(a) shows the stacking carbon layer of Ni1.0-CNTs condition, continuing growth up with stacking shape, so-called bamboo structure [37]. While the carbon growth in Figure 4.15(b) shows the carbon structure with continuous form the parallel walled carbon tube, so-called multiwall structure. In Figure 4.15(c), Ni2.0-CNTs condition, size of Ni NP was too big to form as carbon tube, as a result, the carbon layer formed around the Ni particle as string bead structure instead [38].

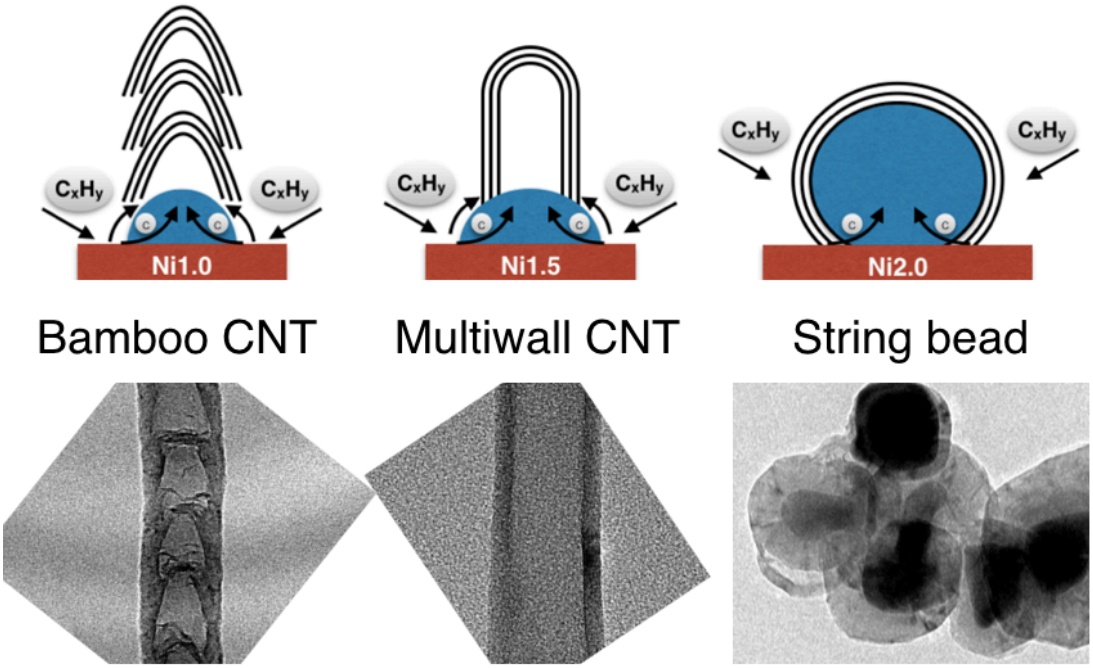

Figure 4.15 Model structures of carbon growth (a) Ni1.0-CNTs, (b) Ni1.5-CNTs and (c) Ni2.0-CNTs.

4.3.3 Raman spectroscopy investigation of carbon nanotube grown from different Ni electroplating voltages

Figure 4.16 shows Raman spectra of the synthesized CNTs. The light source was Ar ion laser with a wavelength of 532 nm (2.33 eV).

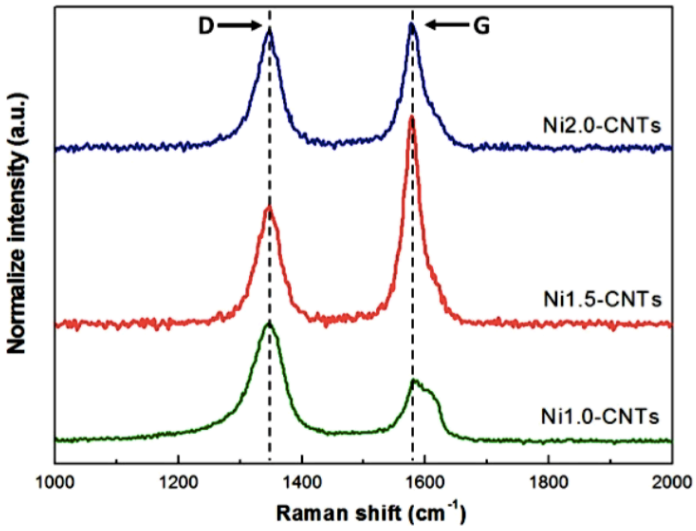

Figure 4.16 Typical Raman spectra of (a) Ni1.0-CNTs, (b) Ni1.5-CNTs and (c) Ni2.0-CNTs.

Generally, in carbon material characterization, Raman spectra are used to identify the existence of disordered carbon (*D*-band) and graphitic carbon (*G*-band). Two sharp peaks at Raman shift of approximately 1350 cm^{-1} (*D*-band) and 1590 cm^{-1} (*G*-band) were observed for all samples. The ratio of *G*-band and *D*- band (I_G/I_D) could be used to evaluate the crystallinity of the CNTs. A higher I_G/I_D ratio indicated a higher degree of structural ordering and purity of CNTs. In this study, it was found that the I_G/I_D of Ni1.0-CNTs, Ni1.5-CNTs and Ni2.0-CNTs were 0.53, 1.77 and 1.06, respectively. Ni1.5- CNTs show the highest I_G/I_D. These results corresponded well to the SEM and TEM results, demonstrating that Ni1.5-CNTs were relatively higher purity and/or had lower defects inside the parallel graphitic layers. Moreover, they also showed that the electroplating voltage directly affected the morphology of Ni NPs.

4.4 Electrochemical properties measurement

The electrochemical properties of the synthesized CNTs were investigated. The cyclic voltammetry (CV) of electrode was measured to obtain the CV curve for further specific capacitance calculation. The galvanostatic charge-discharge (CD) was measured the charge-discharge properties and the stability of the electrode. The electrochemical measurement was carried out using three-electrode system. The Ni1.5-CNTs was used as a working electrode, the Pt electrode was used as a counter electrode and the Ag/AgCl was used a reference electrode. Figure 4.17 shows a photograph of the Ni1.5-CNTs and the setup of the electrochemical test. Figure 4.18 shows cyclic voltammetry (CV) curves of the Ni1.5-CNTs in the potential range of -0.3 to 0.2 V at different scan rates.

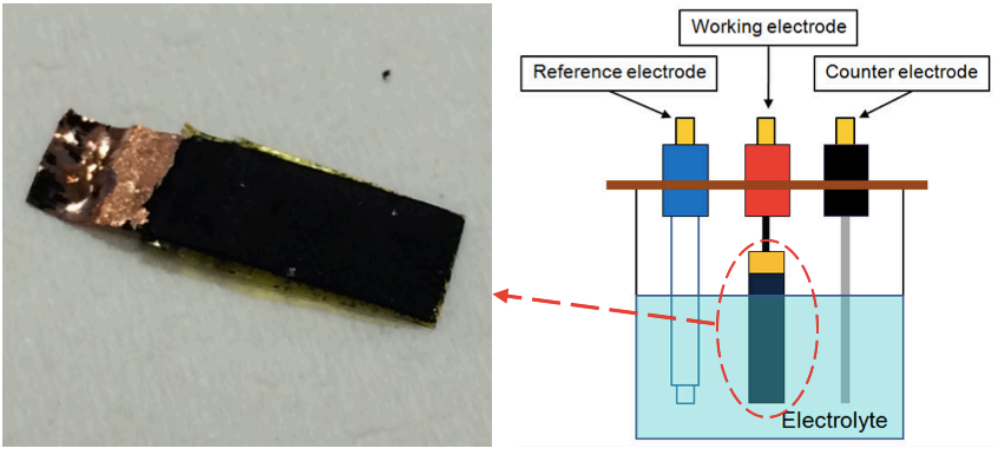

Figure 4.17 (a) Photograph of the Ni1.5-CNTs on Cu foil and schematic view of the setup of the electrochemical test.

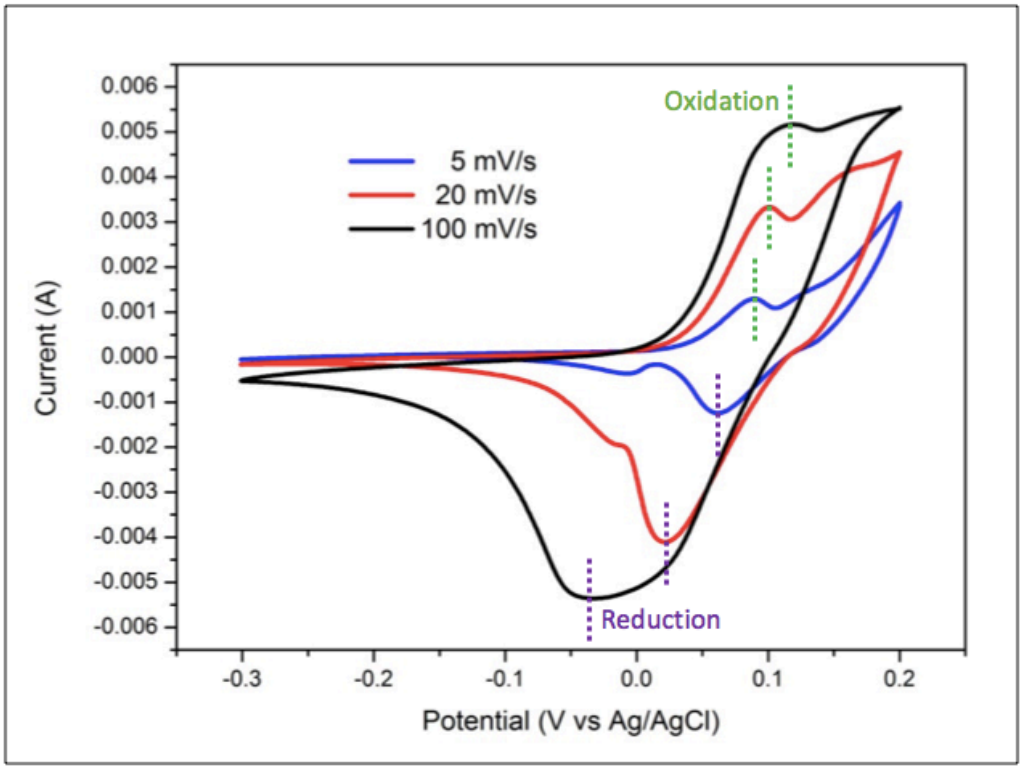

Figure 4.18 Cyclic voltammetry curves of Ni1.5-CNTs at different scan rates.

From the CV shown in Figure 4.18, instead of showing the expected rectangular shaped curve of ideal electric double-layer capacitor, all of CV curves showed a pair of redox current peaks with oxidation and reduction peaks (dot line in Figure 4.18),

indicating that faradic pseudocapacitance was the dominant electrochemical property. With increasing scan rate, the current increased and the gap between redox peaks widened while the shapes of the CV curves were retained, indicating reversibility of the redox reactions. This psesudocapacitive character might be caused by nickel oxide from CNTs synthesis [39]. Evidently, X-ray photoelectron spectroscopy spectrum of the Ni electroplated at 1.5V (Figure 4.4) shows a chemical shift of Ni 2p peaks with a composition of Ni metal, NiO and $Ni(OH)_2$. In addition, Ni NPs could also have been oxidized by residual oxygen inside the quartz tube during the CVD process. Besides Ni oxides, the effect of the CuO could not be discarded, even though the chemical shift of Cu could not be found in XPS results due to the technique limitation that sensitive only few nanometers in the depth direction. However, the potential window range in CV curve does not match for Cu-CuO redox reaction (E_0 = 34 V). Thus, under our measurement condition, the effect of Cu oxides could be neglected. However, the further experiment to prove the role of Cu oxides is required. Figure 4.19 shows galvanostatic charge-discharge curves of the Ni1.5-CNTs at current of 5 mA.

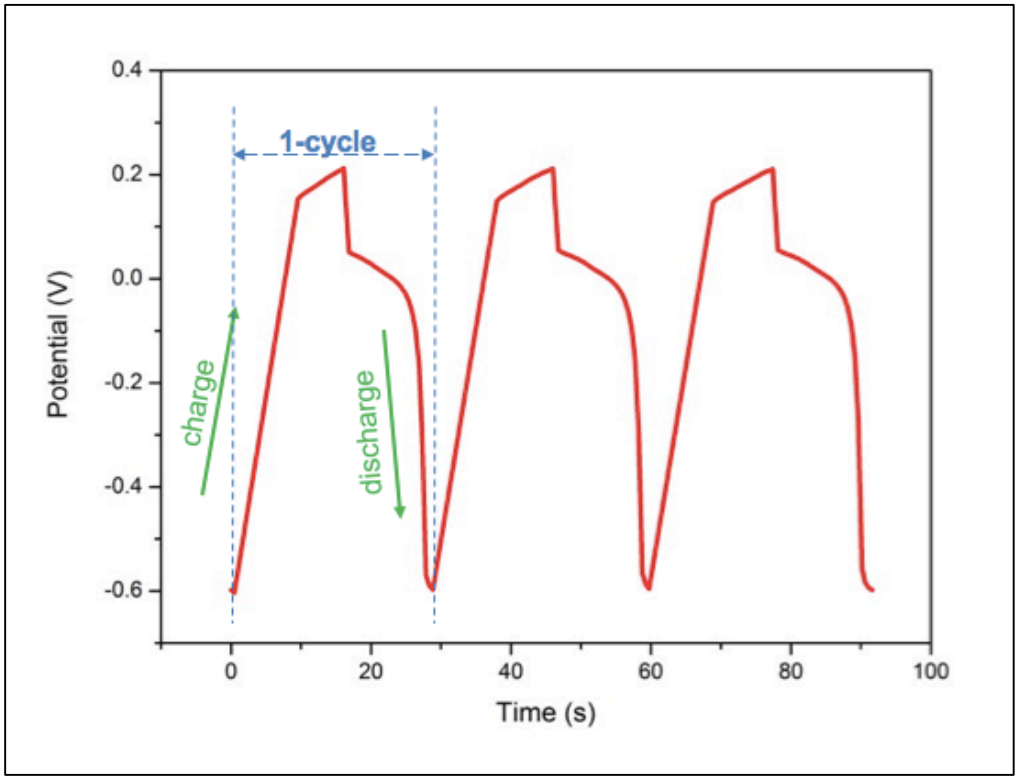

Figure 4.19 Galvanostatic charge-discharge (CD) curves of Ni1.5-CNTs at current of 5 mA.

The CD curves show the charge-discharge repeatability of the electrode. In contrast to the symmetrical triangular shape of a typical electric double-layer capacitor, the discharge curves showed nonlinearities. The discharge curves consist of the vertical line, the small curve and symmetric triangular line. The vertical line represents to the voltage drop from equivalent series resistance (ESR) in electrode. The small curve and the symmetric triangular line imply the combination of faradaic capacitive (small curve) and double-layer capacitive (triangular shape) in the active electrode material [40]. For the faradaic capacitive factor, charge transfer reaction gradually occurs. The slow discharge means the electrode discharge time increases, resulting in longer time in charge release usage. This discharge result also substantiates to the results from the CV curves. The specific capacitance calculated from the CV curve at a scan rate of 5 $mV \cdot s^{-1}$ was approximately 53 $F \cdot g^{-1}$. The energy density and power density of electrode were approximately 6.25 $Wh \cdot kg^{-1}$ and 0.49 $kW \cdot kg^{-1}$, respectively. Although, the result obtained showed a relatively small value compared to the other reports [41], the fabricated electrode also showed the potential use of supercapacitor.

All these preliminary results signified that facile growth of CNTs by Ni NPs catalyst, deposited using DC electroplating method, was fully achieved. The synthesized CNTs showed a real potential for supercapacitor electrode application. However, further work and optimization are still necessary.

CHAPTER 5
CONCLUSION

5.1 Summary conclusion

5.1.1 Novel CNTs synthesis that is simple and low-cost was proposed. This method uses controllable electroplated Ni NPs as catalyst and ethanol as carbon source for CVD process.

5.1.2 The electroplating voltage directly affects the size of Ni NPs, which, in turn, affecting the morphology and structure of the synthesized CNTs. By selecting the appropriate voltage, graphitic layers of CNTs are parallel to the tube axis with a narrow distribution of tube diameters at 60±5 nm.

5.1.3 The synthesized CNTs show a potential use as supercapacitor material with a specific capacitance of 53 $F \cdot g^{-1}$ at a scan rate of 5 $mV \cdot s^{-1}$. Further optimization of the amount ratio of oxidized Ni NPs and CNTs should improve the supercapacitor performance.

5.2 Suggestions and solutions

5.2.1 For more applicable use of the synthesized electrode, the electrode with larger dimension is required. The optimal parameter for large electroplating area such as plating voltage and size of electroplating equipment should be investigated.

5.2.2 For the CVD, the vacuum in rough to high regimes is recommended. The less contamination and controlled gas flow will provide high purification and uniform CNT.

REFERENCES

1) H.R. Kroto, J.R. Heath, S.C. O'Brien, R.F. Curl, and R.E. Smalley, **Nature** 318, 162 (1985).
2) S. Iijima, **Nature** 354, 56 (1991).
3) S. Iijima and T. Ichihashi, **Nature** 363, 603 (1993).
4) D.S. Bethune, C.H. Klang, M.S. de Vries, G. Gorman, R. Savoy, J. Vazquez, and R. Bayers, **Lett. to Nat**. 363, 605 (1993).
5) J. Prasek, J. Drbohlavova, J. Chomoucka, J. Hubalek, O. Jasek, V. Adam, and R. Kizek, **J. Mater. Chem.** 21, 15872 (2011).
6) V.N. Popov, **Mater. Sci. Eng.** 43, 61 (2004).
7) J.P. Gore and A. Sane, *Flame Synthesis of Carbon Nanotubes* (InTech, 2011).
8) T.W. Ebbesen and P.M. Ajayan, **Lett. to Nat.** 358, 220 (1992).
9) C. Journet, W.K. Maser, P. Bernier, A. Loiseau, M. Lamy de la Chapelle, S. Lafrant, P. Deniard, R. Lee, and J.E. Fischer, **Nature** 388, 756 (1997).
10) A. Thess, R. Lee, P. Nikolaev, H. Dai, P. Petit, J. Robert, C. Xu, Y.H. Lee, S.G. Kim, A.G. Rinzler, D.T. Colbert, G.E. Scuseria, D. Tomanek, J.E. Fischer, and R.E. Smalley, **Science** 273, 483 (1996).
11) Jose-Yacaman M., M. Miki-Yoshida, L. Rendon, and J.G. Santiesteban, **Appl. Phys. Lett.** 62, 657 (1993).
12) V. Ivanov, J.B. Nagy, P. Lambin, A. Lucas, X.B. Zhang, X.F. Zhang, D. Bernaerts, G. Van Tendeloo, S. Amelinckx, and J. Van Landuyt, **Chem. Phys. Lett.** 223, 329 (1994).
13) S. Amelinckx, X.B. Zhang, D. Bernaerts, X.F. Zhang, V. Ivanov, and J.B. Nagy, **Science** 265, 635 (1994).
14) W.Z. Li, S.S. Xie, L.X. Qian, B.H. Chang, B.S. Zou, W.Y. Zhou, R.A. Zhao, and G. Wang, **Science** 274, 1701 (1996).
15) S. Hofmann, G. Csanyi, A.C. Ferrari, M.C. Payne, and J. Robertson, **Phys. Rev. Lett.** 95, 36101 (2005).
16) R.S. Wagner and W.C. Ellis, **Appl. Phys. Lett.** 4, 89 (1964).
17) R.T.K. Baker, M.A. Barber, P.S. Harris, F.S. Feates, and R.J. Waite, **J. Catal.** 26, 51 (1972).
18) R.T.K. Baker and R.J. Waite, **J. Catal.** 37, 101 (1975).
19) M. Kumar, *Carbon Nanotube Synthesis and Growth Mechanism* (InTech, 2011).
20) S. Bhaviripudi, E. Mile, S.A. Steiner Iii, A.T. Zare, M.S. Dresselhaus, A.M. Belcher, and J. Kong, **J. Am. Chem. Soc.** 129, 1516 (2007).
21) Y. Takagi, D., Kobayashi, Y., Hlbirio, H., Suzuki, S., Homma, **Nano Lett.** 8, 832 (2008).

22) D. Yuan, L. Ding, H. Chu, Y. Feng, T.P. McNicholas, and J. Liu, **Nano Lett.** 8, 2576 (2008).

23) L. Ding, A. Tselev, J. Wang, D. Yuan, H. Chu, T.P. McNicholas, Y. Li, and J. Liu, **Nano Lett.** 9, 800 (2008).

24) L. Ding, D. Yuan, and J. Liu, J. **Am. Chem. Soc.** 130, 5428 (2008).

25) W. Zhou, Z. Han, J. Wang, Y. Zhang, Z. Jin, X. Sun, Y. Zhang, C. Yan, and Y. Li, **Nano Lett.** 6, 2987 (2006).

26) M. Ritschel, A. Leonhardt, D. Elefant, S. Oswald, and B. Bu, **J. Phys. Chem. C** 111, 8414 (2007).

27) Y. Li, W. Kim, Y. Zhang, M. Rolandi, D. Wang, and H. Dai, **J. Phys. Chem. B** 105, 11424 (2001).

28) H.C. Choi, W. Kim, D. Wang, and H. Dai, J. **Phys. Chem. B** 106, 12361 (2002).

29) G.-H. Jeong, A. Yamazaki, S. Suzuki, H. Yoshimura, Y. Kobayashi, and Y. Homma, J. **Am. Chem. Soc.** 127, 8238 (2005).

30) A. Javey and H. Dai, **J. Am. Chem. Soc.** 127, 11942 (2005).

31) L. An, J.M. Owens, L.E. McNeil, and J. Liu, **J. Am. Chem. Soc.** 124, 13688 (2002).

32) C. Lu and J. Liu, **J. Phys. Chem. B** 110, 20254 (2006).

33) *AJA* INTERNATIONAL, Inc. 2016. **Sputtering**. [online]. Available : http://www.ajaint.com/what-is-sputtering.html

34) Wikipedia. 2016. **Supercapacitors chart**. [online]. Available : https://commons.wikimedia.org/wiki/File:Supercapacitors_chart.svg

35) Wikipedia. 2016. **Capacitor**. [online]. Available : https://en.wikipedia.org/wiki/Capacitor

36) Princeton Applied Research. 2016. **A Review of Techniques for Electrochemical Analysis**. [online]. Available : http://www.ameteksi.com/-/media/ameteksi/download_links/documentations/library/princetonappliedresearch/application_note_e-4.pdf?la=en

37) X. Wang, W. Hu, Y. Liu, C. Long, Y. Xu, S. Zhou, D. Zhu, and L. Dai, **Carbon** 39, 1533 (2001).

38) S. Seraphin, S. Wang, D. Zhou, and J. Jiao, **Chem. Phys. Lett.** 228, 506 (1994).

39) H.B. Li, M.H. Yu, F.X. Wang, P. Liu, Y. Liang, J. Xiao, C.X. Wang, Y.X. Tong, and G.W. Yang, **Nat. Commun.** 4, 1894 (2013).

40) H.W. Wang, Z.A. Hu, Y.Q. Chang, Y.L. Chen, Z.Q. Lei, Z.Y. Zhang, and Y.Y. Yang, **Electrochim. Acta** 55, 8974 (2010).

41) P. Dulyaseree, V. Yordsri, and W. Wongwiriyapan, **Jpn. J. Appl. Phys**. 55, 02BD05 (2016).

AUTHOR BIOGRAPHY

Name-Surname Mr. Visittapong Yordsri

Date of Birth June 10, 1982

Present Address 123 Soi.113, Lardprow Rd., Klongjun, Bangkapi, Bangkok, Thailand 10240

Education

2001-2004 Bachelor of Engineering, Department of Materials, Faculty of Material Engineering, Kasetsart University, Thailand

Work Experience

2005-Present Senior Technician of Transmission Electron Microscope Laboratory, National Metal and Materials Technology Center

Recent/relevant publications:

(1) Worawut Muangrat, Visittapong Yordsri, Rungroj Maolanon, Sirapat Pratontep, Supanit Porntheeraphat, Winadda Wongwiriyapan
"Hybrid gas sensor based on platinum nanoparticles/poly(methyl methacrylate)-coated single-walled carbon nanotubes for dichloromethane detection with a high response magnitude"
Diamond & Related Materials 65 (2016), 183-190

(2) Phannee Saengkaew, Sakuntam Sanorpim, Manit Jitpukdee, Kulthawat Cheewajaroen, Chadet Yenchai, Decho Thong-aram, Visittapong Yordsri, Chanchana Thanachayanont, Noppadon Nuntawong
"Impact of precursor purity on optical properties and radiation detection of CsI:Tl scintillators"

Applied Physics A (2016), 122:729

(3) Paweena Dulyaseree, Visittapong Yordsri, Winadda Wongwiriyapan

"Effects of microwave and oxygen plasma treatments on capacitive characteristics of supercapacitor based on multiwalled carbon nanotubes"

Japanese Journal of Applied Physics, 55 (2016), 02BD05

(4) Pornsiri Wanarattikan, Sakuntam Sanorpim, Somyod Denchitcharoen, Visittapong Yordsri, Chanchana Thanachayanont, Kenjiro Uesugi, Shigeyuki Kuboya, Kentaro Onabe

"TEM Analysis of Planar Defects in InGaAsN and GaAs Grown on Ge (001) by MOVPE"

Key Engineering Materials, 675-676 (2016), 649-642

(5) Bralee Chayasombat, Visittapong Yordsri, Tetsuo Oikawa, Chanchana Thanachayanont

"Microstructural characterization of nickel hydroxide films deposited using an ammonia-induced method and subsequently calcined nickel oxide films"

Materials Science in Semiconductor Processing, 34 (2015), 224-229

(6) Phannee Saengkaew, Sakuntam Sanorpim, Visittapong Yordsri, Chanchana Thanachayanont, Kentaro Onabe

"Characterization of semi-polar GaN on GaAs substrates"

Journal of Crystal Growth, 411 (2015), 76-80

(7) Visittapong Yordsri, Winadda Wongwiriyapan, Chanchana Thanachayanont, **"Facile growth of carbon nanaotube electrode from electroplated Ni catalyst for supercapacitor"**
Advance Materials Letters, 6 (2015), 501-504

(8) Phannee Saengkaew, Sakuntam Sanorpim, Visittapong Yordsri, Chanchana Thanachayanont, Kentaro Onabe
"Characterization of semi-polar GaN on GaAs substrates"
Journal of Crystal Growth, 411 (2015), 76-80

(9) Chanchana Thanachayanont, Visittapong Yordsri, Suphakan Kijamnajsuk, Nawal Binhayeeniyi, Nantakan Muensit
"Microstructural investigation of sol–gel BZT powders"
Materials Letters, 82 (2012), 205-207

(10) Chanchana Thanachayanont, Visittapong Yordsri, Chris Boothroyd,
"Microstructural investigation and SnO nanodefects in spray-pyrolyzed SnO_2 thin films"
Materials Letters, 65 (2011), 2610-2613

Research Article Adv. Mater. Lett. 2015, **6**(6), 501-504 Advanced Materials *Letters*

www.amlett.com, www.vbripress.com/aml, DOI: 10.5185/amlett.2015.SMS6 Published online by the VBRI Press in 2015

Facile growth of carbon nanaotube electrode from electroplated Ni catalyst for supercapacitor

Visittapong Yordsri[1,2], Winadda Wongwiriyapan[1,3,4*], Chanchana Thanachayanont[2]

[1]*College of Nanotechnology, King Mongkut's Institute of Technology Ladkrabang, Chalongkrung Rd., Ladkrabang, Bangkok, Thailand*
[2]*National Metal and Materials Technology Center, 114 Thailand Science Park, Paholyothin Rd., Klong 1, Klong Luang, Pathumthani, Thailand*
[3]*Nanotec-KMITL Center of Excellence on Nanoelectronic Device, Chalongkrung Rd., Ladkrabang, Bangkok, Thailand*
[4]*Thailand Center of Excellence in Physics, CHE, Si Ayutthaya Rd., Bangkok, Thailand*

[*]Corresponding author. Tel: (+66) 23298000; E-mail: kwwinadd@kmitl.ac.th

Received: 15 October 2015, Revised: 20 March 2015 and Accepted: 22 March 2015

ABSTRACT

A facile growth of carbon nanotubes (CNTs) was facilitated by the use of direct-current plating technique for catalyst preparation. Ni nanoparticles (NPs) were deposited on Cu foil at different applied voltages of 1.0, 1.5 and 2.0 V. The Ni-deposited foil was subsequently used as catalyst for CNTs synthesis by chemical vapour deposition (CVD) method. CVD was carried out at 800 ºC using ethanol as carbon source. A voltage of 1.5 V was the optimum condition to deposit uniform Ni NPs that had a narrow size distribution of 55±3 nm, which in turn, yielded synthesized CNTs with a uniform diameter of approximately 60±5 nm with graphitic layers parallel to the CNTs axis. On the other hand, electroplated Ni at 1.0 V produced CNTs with graphitic layers at an angle to the CNTs axis, while electroplated Ni at 2.0 V produced curly CNTs with a wide distribution of diameters. These results show that Ni NPs size distribution could be controlled by electroplated voltage. Our observation was that Ni NPs with a narrow distribution of sizes and a uniform diameter is a key to uniform CNT synthesis. Furthermore, the synthesized CNTs electrode shows a faradic pseudo capacitance property, which can be attributed to the existence of oxidized Ni NPs. These results propose that the synthesized CNTs are promising materials for future super capacitor application. The optimization of ratio of Ni NPs and CNTs may improve the supercapacitors performance.

Keywords: Electroplating; carbon nanotube; chemical vapor deposition; pseudocapacitor.

Visittapong Yordsri is a technician of transmission electron microscope laboratory, National metal and materials technology center, Thailand. He is working on the nanocarbon characterization and the application of energy storage device as supercapacitor.

Introduction

Carbon nanotube (CNT) is one of the most promising materials in nanotechnology due to its large effective surface area and excellent mechanical and electrical properties. CNT shows a great potential for improving the performance of electronics devices, energy storage devices and sensors **[1-3]**. Important for large-scale applications, a simple synthesis method for mass production of CNT is required. Chemical vapor deposition (CVD) is one of the presently available methods for CNT synthesis. Metal catalyst is an essential ingredient in the CVD approach **[4, 5]**. As for catalyst film preparation, evaporation and sputtering techniques are normally utilized **[6-8]**, but these techniques are time-consuming and high cost. For practical application, facile catalyst preparation is absolutely required. Electroplating, a proposed technique for such preparation, is simple to set up, low cost, fast, can deposit to a selected area and does not need vacuum **[9-11]**. In this study, facile growth of CNTs was made possible by using direct-current (DC) electroplating for Ni nanoparticles (NPs) catalyst preparation; with the Ni-deposited catalyst, CNTs was synthesized by using CVD with ethanol as carbon source. The effects of DC-electroplating voltage on the morphology and structure of the CNTs were investigated. Furthermore, for demonstration of a potential application, supercapacitors based on the synthesized CNTs were fabricated and their electrochemical properties were determined.

Experimental

Materials

Cu foils 99.9% pure (0.05 mm × 4 mm × 20 mm) were used as a substrate for Ni NPs preparation (Nilaco Corporation, Japan). Ni ingot was applied as cathode and commercial Ni electroplating solution was used as electrolyte in the electroplating process. Prior to electroplating, Cu foils were cleaned in ethanol and acetone and then ultrasonically cleaned for 10 minutes in distilled water. For CNT synthesis, ethanol (99.9%, Labscan) was used as carbon source and Ar (99.995%) was used as carrier gas. H_2SO_4 (98%, Sigma Aldrich) was prepared in the concentration of 1 M for using as electrolyte in the measurements of electrochemical properties.

Ni catalyst preparation by electroplating

DC electroplating technique was used for Ni deposition on Cu foil. The Cu foil and the Ni ingot were connected as anode and cathode, respectively. Electroplating temperature, time and distance between electrodes were fixed at 45ºC, 5 min and 100 mm, respectively, while the applied voltages were varied from 1.0, 1.5 to 2.0V. The Ni catalyst-electroplated Cu foil was used for CNT synthesis by CVD.

CNT synthesis by chemical vapor deposition

The CNT synthesis procedure was as follows. A quartz tube reactor was filled with Ar gas at a flow rate of 500 sccm and the Ni catalyst-electroplated Cu foil was heated to 800ºC. Ethanol was vaporized and directed into the quartz tube by Ar bubbling for 20 min to grow the CNTs.

Characterization of Ni nanoparticles and CNTs

The morphology of the electroplated Ni was characterized by atomic force microscopy (AFM; SEIKO SPA400) with a monocrystal silicon tip (NT-MDT; HA_NC ETALON). The morphology, diameter and structure of the graphitic layer, and the crystallinity of the synthesized CNTs were characterized by field emission scanning electron microscopy (FESEM; Hitachi SU-8030), transmission electron microscopy (TEM; JEOL JEM-2010) and Raman spectroscopy (Thermal Scientific; DXR™ SmartRaman Spectroscopy), respectively.

Measurement of electrochemical properties

Electrochemical measurements were carried out in a three-electrode setup connected to an electrochemical workstation (Metrohm AUTOLAB PGSTAT 302). The CNT synthesized on Ni-electroplated Cu foil (an area of 4 mm × 10 mm) was used as working electrode. Pt and Ag/AgCl electrodes were used as counting and reference electrode, respectively. 1M H_2SO_4 aqueous solution was used as electrolyte. Electrochemical properties were characterized by cyclic voltammetry (CV) and galvanostatic charge/discharge (CD) technique. CV tests were done at the potential range of −0.3 to 0.2 V at a scan rate of 5, 20 and 100 mVs^{-1}. CD tests were performed at a current of 5 mA. The specific capacitance (C_{sp}, Fg^{-1}) was evaluated from CV curves according to the following equation;

$$C_{sp} = \frac{\int_{V_1}^{V_2} i(V)dV}{2(V_2 - V_1)mv} \quad (1)$$

where $\int_{V_1}^{V_2} i(V)dV$ is total voltammetric charge obtained by integration of positive and negative sweep in CV curve, V_2-V_1 is potential window width (V), m is a total mass of active materials (g), v is a scan rate (Vs^{-1}) **[12]**.

Results and discussion

Fig. 1(a-c) show the AFM images of the Ni NPs on Cu foils electroplated at the voltages of 1.0, 1.5 and 2.0 V, respectively. Ni NPs were formed at all of these electroplating voltages. At the applied voltage of 1.0 V, small and larger clusters of Ni NPS were formed; their average sizes were 44±7 nm and 120±14 nm, respectively. At the applied voltage of 1.5 V, Ni NPs with a narrow distribution of sizes were formed with an average size of 55±3 nm. When the applied voltage was increased to 2.0 V, the sizes of the formed Ni NPs increased to approximately 103±12 nm. Thus, the size of formed Ni NPs can be controlled by varying electroplating voltages.

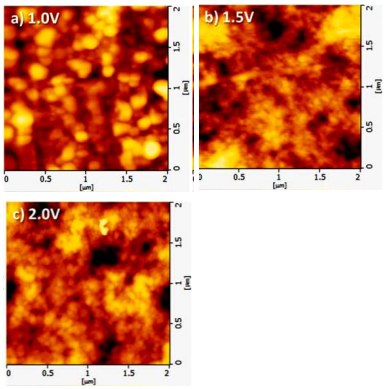

Fig. 1. AFM images of Ni NPs on Cu foils electroplated at the voltages of (a) 1.0 V, (b) 1.5 V and (c) 2.0 V.

Fig. 2(a-c) show SEM images of the CNTs synthesized by using Ni NPs catalysts that were deposited at electroplating voltages of 1.0, 1.5 and 2.0 V, respectively (hereafter referred to as Ni1.0-CNTs, Ni1.5-CNTs and Ni2.0-CNTs, respectively). After CVD, the surfaces of all Cu foils were visually observed to be wholly covered with black powder. All of the formed Ni NPs were able to act as catalyst producing tubular shaped CNTs, but the synthesized CNTs were different in their morphology and structure. The Ni1.0-CNTs were a tangled network while the Ni1.5-CNTs were straight with high aspect ratio and the Ni2.0-CNTs were curly and agglomerated.

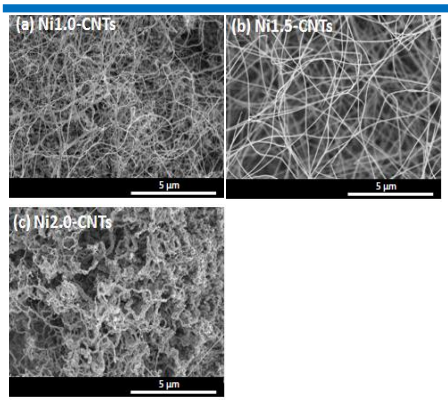

Fig. 2. SEM images of (a) Ni1.0-CNTs, (b) Ni1.5-CNTs and (c) Ni2.0-CNTs.

Fig. 3(a-c) shows TEM images of Ni1.0-CNTs, Ni1.5-CNTs and Ni2.0-CNTs, respectively. Insets are TEM images of graphitic layers of CNT walls at high magnification. Typical for TEM characterization, magnification in the range of x50000 to x400000 was used. Observed at low magnification, Ni1.0-CNTs and Ni1.5-CNTs were tubular in shape with diameters of approximately 45±7 nm and 60±5 nm, respectively. However, at high magnification, it was found that their graphitic layers were completely different. The inset in **Fig. 3(a)** shows that the graphitic layers of Ni1.0-CNTs were at an angle to the tube axis wall, while the inset in **Fig. 3b** shows clearly that the graphitic layers of Ni1.5-CNTs were parallel to the tube axis. Furthermore, the structure of Ni2.0-CNTs was completely different from those of Ni1.0-CNTs and Ni1.5-CNTs. Ni2.0-CNTs were largely curly with Ni catalyst inside and wide distribution of tube diameters (**Fig. 3(c)**).

Fig. 4 shows Raman spectra of the synthesized CNTs. The exciting light was Ar ion laser at the wavelength of 532 nm (2.33 eV). Generally, in carbon material characterization, Raman spectra can be used to identify the existence of disordered carbon (*D*-band) and graphitic carbon (*G*-band). Two sharp peaks at Raman shift of approximately 1350 cm^{-1} (*D*-band) and 1590 cm^{-1} (*G*-band) were observed for all samples. The ratio of *G*-band and *D*-band (I_G/I_D) can be used to evaluate the crystallinity of the CNTs. A higher I_G/I_D ratio indicates a higher degree of structural ordering and purity of CNTs **[13].** In this study, it was found that the I_G/I_D of Ni1.0-CNTs, Ni1.5-CNTs and Ni2.0-CNTs were 0.53, 1.77 and 1.06, respectively. Ni1.5-CNTs showed the highest I_G/I_D. These results corresponded well to the SEM and TEM results, demonstrating that Ni1.5-CNTs were relatively higher purity and/or had lower defects inside the parallel graphitic layers. Moreover, they also showed that the electroplating voltage directly affected the morphology of Ni NPs. Small-sized Ni NPs with narrow distribution is key to uniform CNT synthesis.

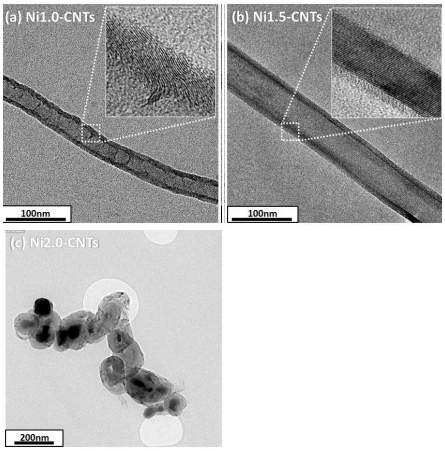

Fig. 3. TEM images (a) Ni1.0-CNTs, (b) Ni1.5-CNTs and (c) Ni2.0-CNTs. Insets are TEM images of graphitic layers of CNT walls at high magnification.

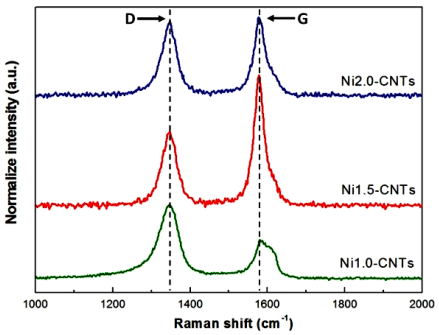

Fig. 4. Typical Raman spectra of (a) Ni1.0-CNTs, (b) Ni1.5-CNTs and (c) Ni2.0-CNTs.

To check their suitability for supercapacitor application, the electrochemical properties of Ni1.5-CNTs on Cu foil were determined. **Fig. 5(a)** shows cyclic voltammetry (CV) curves of Ni1.5-CNTs in the potential range of -0.3 to 0.2 V at different scan rates. Instead of showing the expected rectangular shaped curve of ideal electric double-layer capacitor, all of CV curves showed a pair of redox current peaks, indicating that faradic pseudocapacitance is the dominant electrochemical property. With increasing scan rate, the current increased and the gap between redox peaks widened while the shapes of the CV curves were retained, indicating reversibility of the redox reactions. This psesudocapacitive character might be caused by residual Ni NPs catalyst **[14]** from CNT synthesis. Evidently, X-ray photoelectron spectroscopy spectra showed a chemical shift of Ni 2p peaks, indicating that Ni_xO_y and $Ni(OH)_2$ were

formed after electroplating (data not shown). In addition, Ni NPs could also have been oxidized by residual oxygen inside the quartz tube during the CVD process. **Fig. 5(b)** shows a cycle of the galvanostatic charge-discharge curves at the current of 5 mA. In contrast to the symmetrical triangular shape of a typical electric double-layer capacitor, the discharge curves show nonlinearities, indicating an occurrence of faradaic reaction in the active electrode material and substantiating the results from the CV curves. The specific capacitance calculated from the CV curve at a scan rate of 5 mVs^{-1} was approximately 53 Fg^{-1}.

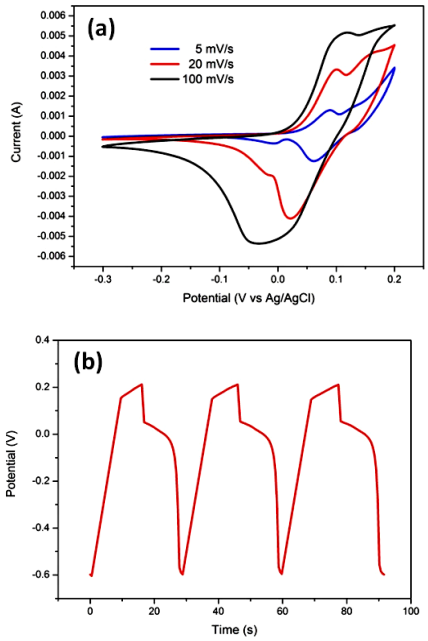

Fig. 5. (a) Cyclic voltammetry curves of Ni1.5-CNTs with different scan rate and (b) galvanostatic charge-discharge curves.

All of these preliminary results signified that facile growth of CNTs by Ni NPs catalyst, deposited using DC electroplating method was fully achieved. The synthesized CNTs showed a real potential for supercapacitor electrode application. However, further work and optimization are still necessary.

Conclusion

Novel CNTs synthesis method that is simple and low cost was proposed. This method uses controllable electroplated Ni NPs as catalyst and ethanol as carbon source for CVD process. The electroplating voltage directly affected the size of Ni NPs, which, in turn, affecting the morphology and structure of the synthesized CNTs. By selecting the appropriate voltage, graphitic layers of CNTs can be made parallel to the tube axis with a narrow distribution of tube diameters at 60±5 nm. The synthesized CNTs showed a real potential as supercapacitor with a specific capacitance of 53 Fg^{-1} at a scan rate of 5 mVs^{-1}. Further optimization of the amount ratio of oxidized Ni NPs and CNTs should improve the supercapacitor performance.

Acknowledgements

We acknowledge support from the Thailand Research Fund (DBG5580005) and from the National Nanotechnology Center (NANOTEC), NSTDA, Ministry of Science and Technology, Thailand, through its program of Center of Excellence Network and the Thailand Center of Excellence in Physics (ThEP).

Reference

1. Park, S.; Vosquerichian, M.; Bao, Z., *Nanoscale* **2013**, *5*. **DOI:** 10.1039/C3NR33560G
2. Karakaya, M.; Zhu, J.; Raghavendra, A.J.; Podila, R.; Parler Jr., S.G.; Kaplan, J.P.; Rao A.M.; *Appl. Phys. Lett.* **2014**, *105*, 263103. **DOI:** 10.1063/1.4905153
3. Esser, B.; Schnorr, J.M.; Swager, T.M.; *Angew. Chtm. Int. Ed.* **2012**, *51*, 5752. **DOI:** 10.1002/anie.201201042
4. Lee, C.J.; Park, J.; Yu, J.A., *Chem. Phys. Lett.* **2002**, *360*, 250. **DOI:** 10.1016/S0009-2614(02)00831-X
5. Muangrat, M.; Porntheeraphat, S.; Wongwiriyapan, W., *Engineering Journal* **2013**, *17*, 35. **DOI:** 10.4186/ej.2013.17.5
6. Zhang, R.Y.; Amlani, I.; Basker J.; Tresek, J. and Tsui, T.K, *Nano Lett.* **2003**, *3*, 731. **DOI:** 10.1021/nl034154z
7. Hata, K.; Futaba, D.N.; Mizuno, K.; Namai, T.; Yumura, M.; Iijima, S., *Science* **2004**, *306*, 1362. **DOI:** 10.1126/science.1104962
8. Teblum, E.; Noked, M.; Grinblat, J.; Kremen, A.; Muallem, M.; Fleger, Y.; Tischler, Y.R.; Aurbach, D.; Nessim, G.D.; *J. Phys. Chem. C* **2014**, *118*(33), 19345. **DOI:** 10.1021/jp5015719
9. Park, K.H.; Lee, S.; Koh, K.H., *Diamond & Related Materials* **2005**, *14*, 2094. **DOI:** 10.1016/j.diamond.2005.06.013
10. Singh, M.K.; Singh, P.P.; Titus, E.; Misra, D.S.; LeNormand, F., *Chem. Phys. Lett.* **2002**, *354*, 331. **DOI:** 10.1016/S0009-2614(02)00133-1
11. Sung, W.Y.; Kim, W.J.; Lee, H.Y.; Kim, Y.H.; *Vacuum* **2008**, *82*, 551. **DOI:** 10.1016/j.vacuum.2007.07.051
12. Chen, W.; Fan, Z.; Gu, L.; Bao, X.; Wang, C., *Chem. Commun.* **2010**, *46*, 3905. **DOI:** 10.1039/C000517G
13. Kataura, H.; Kumazawa, Y.; Maniwa, Y.; Umezu, I.; Suzuke, S.; Ohtsuka, Y.; Achiba, Y., *Synthetic Metals* **1999**, *103*, 2555. **DOI:** 10.1016/S0379-6779(98)00278-1
14. Li, H.B.; Yu, M.H.; Wang, F.X.; Liu, P.; Liang, Y.; Xiao, J.; Wang, C.X.; Tong, Y.X.; Yang, G.W., *Nature Communications* **2013**, *4*, 1. **DOI:** 10.1038/ncomms2932

THAI JOURNAL OF PHYSICS, SERIES 10, (2014)

Facile growth of carbon nanotube by electroplated Ni catalyst

Visittapong Yordsri[1],Winadda Wongwiriyapan[1-3]*, Wirat Jarernboon[1-3] and Chanchana Thanachayanont[4]

[1]*College of Nanotechnology, King Mongkut's Institute of Technology Ladkrabang,Chalongkrung Rd., Lardkrabang, Bangkok 10520, Thailand*

[2]*Nanotec-KMITL Center of Excellence on Nanoelectronic Device, Chalongkrung Rd., Ladkrabang, Bangkok, 10520 Thailand*

[3]*Thailand Center of Excellence in Physics, CHE, Si Ayutthaya Rd., Bangkok, 10400, Thailand*

[4]*National Metal and Materials Technology Center, 114 Thailand Science Park, Paholyothin Rd., Klong 1, Klong Luang, Pathumthani 12120, Thailand*

A facile growth of carbon nanotube (CNT) by electroplated Ni as catalyst was proposed. Ni catalyst layers were deposited on Cu sheet by direct-current electroplating technique. Electroplated voltages were varied at 1.0, 1.5 and 2.0 V. CNTs were synthesized on electroplated Ni by chemical vapor deposition (CVD) using ethanol as carbon source. Atomic force microscopy (AFM), scanning electron microscopy (SEM), transmission electron microscopy (TEM) and Raman spectroscopy were utilized for characterization of electroplated Ni catalyst and synthesized CNTs. Electroplated Ni at 1.0, 1.5, 2.0 V had particle sizes of 78, 75 and 113 nm, respectively. CNTs with a uniform diameter of approximately 54 nm with graphene layers being parallel to CNT axis, corresponding to multi-wall CNTs, were obtained by using electroplated Ni at 1.5 V. Electroplated Ni at 1.0 V produced CNTs with graphitic layers making an angle to CNT axis, while electroplated Ni at 2.0 V produced curly CNTs with a wide diameter distribution. These results show that electroplated voltage directly affects morphology and structure of Ni layers and Ni catalyst with a smaller size and uniform diameter is a key for uniform CNT synthesis

Keywords: Electroplating, Carbon nanotube, Chemical vapor deposition

1. INTRODUCTION

Carbon nanotube (CNT) is well-known as the promising materials in recent nanotechnology due to its great mechanical property, electrical property and the large effective surface area. These useful properties make CNT be suitable material for many applications such as electronics devices, energy storage devices and sensors [1,2]. Many researches study on techniques for CNT synthesis. Arc discharge and laser ablation [3,4] are generally used for CNT synthesis but these techniques are time-consuming process and high cost. Chemical vapor deposition (CVD) technique is one of the main methods for CNT synthesis with advantages of simple, low cost and no need vacuum in process. For CNT synthesis by CVD technique, metal catalyst is an essential ingredient for CNT nucleation growth [5,6]. Normally, evaporation and sputtering techniques are utilized for catalyst film preparation. However, these techniques are time-consuming process and high cost. Recently, high density of multiwalled CNTs was synthesized on Ni electroplated Cu substrates by microwave plasma CVD [7]. K. H Park *et al*. also proposed growth of carbon nanofiber films with electroplated Ni catalyst using methane (CH_4) as carbon source [8]. In this study, a facile growth of CNT was proposed by using direct-current (DC) electroplating for Ni film preparation and CNTs was synthesized by CVD using ethanol as carbon source. Effect of electroplated voltage on morphology and structure of CNTs was investigated. It was found that electroplated voltage directly affect yield, purity, diameter distribution and graphitic layer structure of CNTs.

*Corresponding author. *E-mail*: kwwinadd@kmitl.ac.th

2. EXPERIMENT

For the preparation of the Ni catalyst layers, direct-current electroplating technique was used. A commercial Ni electroplating bath for jewelry coating was used as electrolyte in an electroplating process. Ni ingot and Cu sheet (Nilaco Corporation, Japan) was connected to the cathode and the anode of the circuit, respectively. The applied voltages were varied at 1.0, 1.5 and 2.0 V. Distance between both electrodes, temperature and time were fixed at 10 cm, 45ºC and 5 min, respectively. Morphology and grain size of the deposited Ni catalysts on Cu sheets were characterized by atomic force microscopy (AFM; SEIKO SPA400) technique.

Next, Ni catalyst-electroplated Cu sheet was set into a quartz tube reactor for chemical vapor deposition (CVD) process. Firstly, the quartz tube was filled with Ar gas at a flow rate of 500 sccm for 30 min to eliminate oxygen and air. Next, Ni catalyst-electroplated Cu sheet was heated to 800ºC and ethanol (AR grade, Labscan) was vaporized and switched into the quartz tube by Ar bubbling at a flow rate of 300 sccm for 20 min for CNT growth. The synthesized CNTs were cooled down to room temperature under Ar ambient before taken out from the quartz tube. Morphology, diameter and structure of graphitic layer, and crystallinity of the synthesized CNTs were characterized by scanning electron microscopy (SEM; Hitachi S-3400N),

transmission electron microscopy (TEM; JEOL JEM-2010) and Raman spectroscopy (Thermal Scientific; DXR™ SmartRaman Spectrometer), respectively.

3. RESULTS AND DISCUSSIONS

Figs. 1(a)-1(c) show AFM images of the Ni catalyst layer on Cu sheets obtained from electroplated voltages of 1.0, 1.5 and 2.0 V, respectively. Ni nanoparticles were formed by all electroplated voltages. The average particle sizes formed at electroplated voltages of 1.0, 1.5 and 2.0 V were approximately 78±3 nm, 75±16 nm and 113±10 nm, respectively. Thus, under the controlled electroplating condition, Ni nanoparticles with controllable size for use as catalyst in CNT synthesis can be formed.

After CVD process, Cu sheet surface was wholly covered with a black powder by visual. The detailed morphology was observed by SEM. Figs. 2(a)-2(c) show SEM images of CNTs synthesized from electroplated voltages of 1.0, 1.5 and 2.0 V, respectively. Tubular structures were observed for all electroplated voltages but morphologies and structures were different. For electroplated voltages of 1.0 and 1.5 V, synthesized CNTs were straight with high aspect ratio while CNTs synthesized from electroplated voltage of 2.0 V were curly and agglomerated in cluster.

For TEM characterization, typically, magnification in a range of X20000 to X500000 was used for observation. The higher resolution in TEM images could precisely identify the graphitic layers of CNTs synthesized from different electroplated voltages. Figs. 3(a)-3(c) show TEM images of CNTs synthesized from electroplated voltages of 1.0, 1.5 and 2.0 V, respectively. Insets are TEM images of graphitic layer at high resolution. At electroplated voltages of 1.0 V and 1.5 V, the CNTs were in the same tubular shape with the diameter range of approximately 36 nm and 54 nm, respectively, at low resolution. However, at high resolution, it was found that their graphitic layers were completely different. Inset of Fig. 3(a) shows that graphitic layers of the CNTs were angle to the tube axis wall for electroplated voltage of 1.0 V, while inset of Fig. 3(b) shows clearly that graphitic layers of the CNTs were parallel to the tube axis. At electroplated voltage of 2.0 V, the structures of the synthesized resultants were completely different from those of 1.0 and 1.5 V. The resultants were largely curly with Ni catalyst inside with wide tube diameter distribution (Fig.3(c)).

Next, the synthesized CNTs were characterized by Raman spectroscopy. Generally, in carbon materials characterization, Raman spectra can identify the existence of graphitic carbon (*G*-band) and disordered carbon (*D*-band). Fig. 4 shows the Raman spectra of CNTs obtained from different electroplated voltages of (a) 1.0 V, (b) 1.5 V and (c) 2.0 V. The excited light was Ar ion laser with a wavelength of 532 nm (2.33 eV) Two sharp peaks at Raman shift of approximately 1350 cm^{-1} (*D*-band) and 1590 cm^{-1} (*G*-band) were observed from all samples. The ratio of *G*-band and D-band (I_G/I_D) can be used to evaluate the crystallinity of the CNTs. A higher I_G/I_D ratio indicates a higher degree of structural ordering and purity of the CNTs [9]. It was found that I_G/I_D of the CNTs obtained from the electroplated voltage of 1.0, 1.5 and 2.0V were 0.53, 1.77 and 1.06, respectively. The CNTs obtained from electroplated voltage of 1.5V had the highest I_G/I_D. These results correspond to the SEM and TEM results, showing that the CNTs obtained from electroplated voltage of 1.5 V were relatively higher purity and/or had lower defects

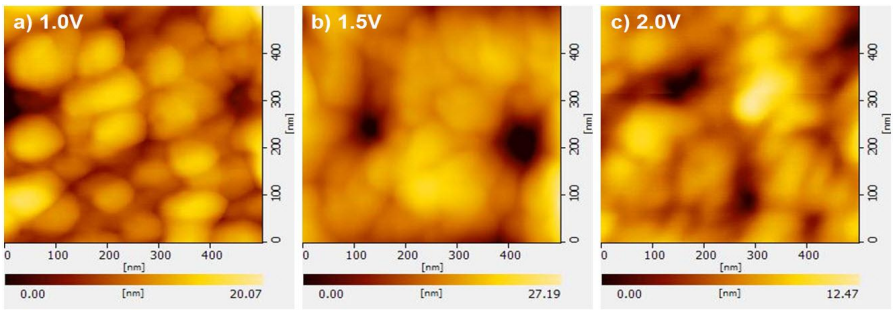

FIGURE 1. AFM images of Ni catalyst layer formed at electroplated voltages of (a) 1.0 V, (b) 1.5 V and (c) 2.0 V.

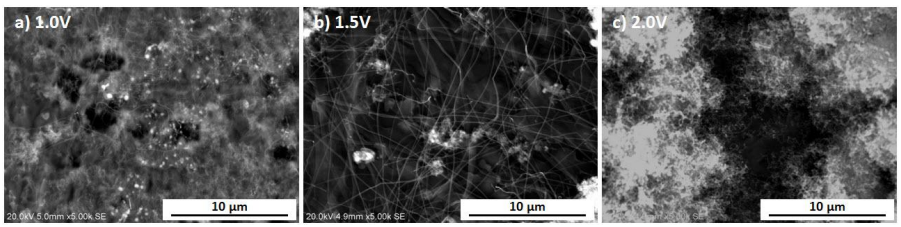

FIGURE 2. SEM images of CNTs obtained from different electroplated voltages of (a) 1.0 V, (b) 1.5 V and (c) 2.0 V.

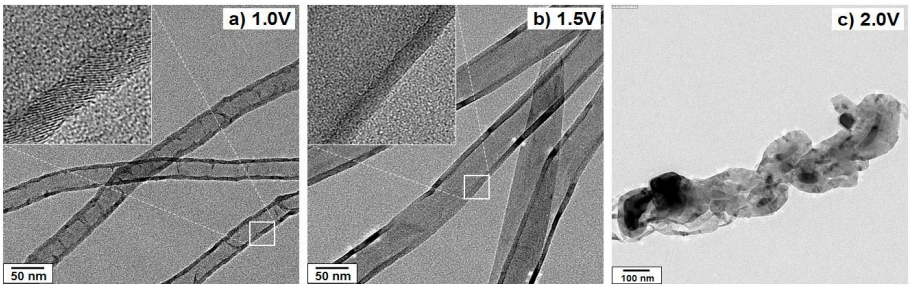

FIGURE 3. TEM micrographs with additional high resolution of CNTs obtained from different electroplated voltages of (a) 1.0 V, (b) 1.5 V and (c) 2.0 V.

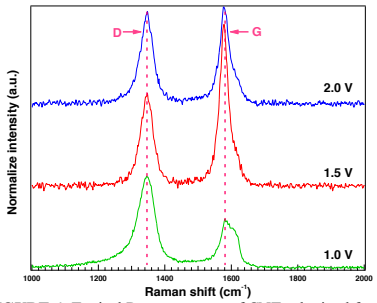

FIGURE 4. Typical Raman spectra of CNTs obtained from different electroplated voltages of (a) 1.0 V, (b) 1.5 V and (c) 2.0 V.

inside the parallel graphitic layers. These results show that electroplated voltage directly affects morphology and structure of Ni layers and Ni catalyst with a smaller size and uniform diameter is a key for uniform CNT synthesis

4. CONCLUSION

Novel synthesis of CNTs with simple and low cost method was proposed by the use of controllable electroplated Ni as catalyst and the use of ethanol as carbon source during CVD process. The electroplated voltages for Ni catalyst formation directly affect the morphology and structure of CNTs. The graphitic layers of CNTs can be selectively parallel or angle to the tube axis with a narrow tube diameter distribution of 54 nm. By the different CNTs structures obtained by controllable Ni catalyst, it could lead to further research with the mechanical property and electrical conductivity characterization in order to optimum suitable properties for devices and applications.

ACKNOWLEDGMENTS

This work is financially supported by the Thailand Research Fund (DBG5580005), the National Nanotechnology Center (NANOTEC), NSTDA, Ministry of Science and Technology, Thailand, through its program of Center of Excellence Network and the Thailand Center of Excellence in Physics (ThEP). We acknowledge facility support from National Metal and Materials Technology Center (MTEC).

1. Steve, P., Michael, V., Zhenan, Bao., A review of fabrication and applications of carbon nanotube film-based flexible electronics, Nanoscale, Issue 5. 2013
2. Yu, J., Hongyuan, C., Minghai, C., et al., Graphene-patched CNT/MnO2 nanocomposite papers for the electrode of high-performance flexible asymmetric supercapacitors, Applied Materials & Interfaces, Vol. 5, pp. 3408-3416. 2013
3. Ando, Y., Zhao, X., Hataura, H., et. al., Multiwalled carbon nanotubes prepared by hydrogen arc, Diamond and Related Materials, Vol. 9, pp. 847-851. 2000
4. Shiang-Kuo, C., Jeng-Rong, H., John, C., Fabrication of transparent double-walled carbon nanotubes flexible matrix touch panel by laser alation technique, Optics & Laser Technology, Vol. 43, pp. 1371-1376. 2011
5. Lee, C.J., Park, J., Yu, J.A., Catalyst effect on carbon nanotubes synthesized by thermal chemical vapor deposition, Chemical Physics Letters, vol. 360, pp. 250-255. 2002
6. Worawut, M., Supanit, P., Winadda, W., Effect of Metal Catalysts on Synthesis of Carbon Nanomaterials by Alcohol Catalytic Chemical Vapor Deposition, Engineering Journal, Vol. 17, Issue 5, pp. 35-39. 2013
7. Singh, M.K., Singh, P.P., Titus, E., et al., High density of multiwalled carbon nanotubes observed on nickel electroplated copper substrates by microwave plasma chemical vapor deposition, Chemical Physics Letters, Vol. 354, pp. 331-336. 2002
8. Kyung, H.P., Soonil, L., Ken, H.K., Growth and high current field emission of carbon nanofiber films with electroplated Ni catalyst, Diamond & Related Materials, Vol. 14, pp. 2094-2098. 2005
9. Kataura, H., Kumazawa, Y., Maniwa, Y., et al., Optical properties of single-wall carbon nanotubes, Synthetic Metals, Vol. 103, pp. 2555-2558. 1999